Implications of Human LRRK2 Protein on the Regulation of Cytoskeleton Dynamics in Parkinson's Disease

Dissertation

zur Erlangung des Grades eines

Doktors der Naturwissenschaften

der Mathematisch-Naturwissenschaftlichen Fakultät

und

der Medizinischen Fakultät

der Eberhard-Karls-Universität Tübingen

vorgelegt

von

Marta Garcia Miralles

aus

Sant Cugat del Vallès, Catalunya (Spain)

October 2013

Tag der mündlichen Prüfung:	16 October 2013.....
Dekan der Math.-Nat. Fakultät:	Prof. Dr. W. Rosenstiel
Dekan der Medizinischen Fakultät:	Prof. Dr. I. B. Autenrieth
1. Berichterstatter:	Prof. Dr. Thomas Gasser.
2. Berichterstatter:	Prof. Dr. Peter Heutink
Prüfungskommission:	Prof. Dr. Thomas Gasser
	Prof. Dr. Peter Heutink
	Prof. Dr. Olaf Riess
	Prof. Dr. Thilo Stehle

I hereby declare that I have produced the work entitled: ***"Implications of human LRRK2 protein on the regulation of cytoskeleton dynamics in Parkinson's disease"***,

submitted for the award of a doctorate, on my own (without external help), have used only the sources and aids indicated and have marked passages included from other works, whether verbatim or in content, as such. I swear upon oath that these statements are true and that I have not concealed anything. I am aware that making a false declaration under oath is punishable by a term of imprisonment of up to three years or by a fine.

Tübingen, _____ _____

I CONTENTS

II LIST OF FIGURES AND TABLES

LIST OF FIGURES

LIST OF TABLES

III ABBREVIATIONS

°C	degree celcius
4E-BP	4E-binding protein
aa	amino acid
AD	Alzheimer's disease
AD	autosomal-dominant
ALS	amyotrophic lateral sclerosis
ANK	ankyrin
APS	ammonium persulfate
AR	autosomal-recessive
ARM	armadillo
ATP	adenine triphosphate
BDC	ß-catenin destruction complex
Bp	base pair
BS	brainstem
BSA	bovine serum albumin
Ca^{2+}	calcium
C. elegans	*Caenorhabditis elegans*
Cdc42	cell division cycle protein 42
CHIP	C-terminus of HSP70-interacting protein
CNS	central nervous system
COR	C-terminal of ROC

CPNE8	Copine 8
Ctrl	control
Ctx	cortex
dd	*double-distilled*
D. melanogaster	*Drosophila melanogaster*
DA	dopaminergic, dopamine
DAT	dopamine transporter
DBS	deep brain stimulation
DIV	day in vitro
DJ-1	Daisuke-Junko-1
DLB	dementia with lewy bodies
DMSO	dimethylsulfoxide
DNA	deoxyribonucleic acid
DOPA	3,4-dihydrosyphenylalanine
DVL1/2/3	disheveled family of proteins 1/2/3
E	embryonic day
EF1A	elongation factor 1α
EndoA	endophilinA
ES	embryonic stem
ERK	extracellular-signal-regulated kinase 1/2
ERM	ezrin/radixin/moesin
F-actin	filament actin

Fwd	forward
g	gram
GAP	GTPase activating protein
GBA	glucocerebrosidase
GDIs	GDP-dissociation inhibitors
GDP	guanosine diphosphate
GEF	nucleotide exchange factor
GS	G2019S LRRK2 mutation
GSK3ß	glycogen synthase kinase 3ß
GST	glutathione S-transferase
GTP	guanosine triphosphate
GWAS	genome wide association studies
h	hour
HEK293	human embryonal kidney cells
HEPES	4-(2-hydroxyethyl)-1-piperazineethanesulfonic acid
Hip	hippocampus
HRP	horseradish-peroxidase
HS	healthy subject
Hsp	heat shock protein
hWT	human wild type
IP	immunoprecipitation
iPSCs	induced pluripotent stem cells

IT	I2020T LRRK2 mutation
JIP	c-Jun N-terminal kinase-interacting protein
Kb	kilobase
KD	knock down
kD	kilodalton
KI	knock-in
KO	knock out
L	liter
LB/LBs	lewy body/lewy bodies
L-Dopa	L-3, 4-dihydroxyphenylalanine
LRR	leucine-rich repeat
LRRK2/1	leucine-rich repeat kinase 2/1
LN/LNs	lewy neurite/lewy neurites
m	milli
M	molar
MAPK	mitogen activated protein kinase
MAPKKK	mitogen activated protein kinase kinase kinase
MAPT	microtubule association protein tau
MB	midbrain
MBP	maltose binding protein
mDA	midbrain dopaminergic neurons
Min	minute

MKK	mitogen-activated kinase kinase
MPP+	1-methyl-4-phenylpyridinium
MPTP	1-methyl-4-phenyl, 1, 2, 3, 6-tetrahydropyridine
mRNA	messenger ribonucleic acid
MSA	multiple system atrophy
n	nano
NGS	normal goat serum
non-tg	non-transgenic
n.s	not significant
NS	N1437S LRRK2 mutation
P	postnatal day
PAGE	polyacrylamide gelelectrophoresis
Paraquat	N,N'-dimethyl-4,4'-bipyridinium dichlorid
PBS	phosphate buffered saline
PCR	polymerase chain reaction
PD	Parkinson's disease
PDGF-ß	platelet-derived growth factor B chain promoter
PINK1	phosphatase and tensin [PTEN] homolog-induced putative kinase1
Rev	reverse
RC	R1441C LRRK2 mutation
RIP1	receptor-interacting protein 1
RNA	ribonucleic acid

ROC	Ras of complex proteins
ROCO	ROC-COR
rpm	rotations per minute
RT	room temperature
RT-PCR	reverse transcription PCR
sec	seconds
SDS	sodium dodecyl sulfate
SH-SY5Y	human neuroblastoma cell line
siRNA	small interfering RNA
SN	substantia nigra
SNCA	α-synuclein
SNpc	substantia nigra pars compacta
Stm	striatum
STN	subthalamic nucleus
TEMED	N, N, N', N'-tetramethylethylenediamine
Tg	transgenic
TH	tyrosine hydroxylase
TRADD	tumor necrosis factor receptor type 1-associated death domain protein
U	units
WT	wild type
VTA	ventral tegmental area
α-syn	alpha-synuclein

ßFGF	beta fibroblasts growth factor
µ	micro
µM	micro meter

Amino acids:

Ala, A: alanin; Arg, R: arginin; Asn, N: aparagin; Asp, D: aspartat; Cys, C: cystein; Gln, Q: glutaimin; Glu, E: glutamat; Gly, G: glycin; His, H: histidin; Ile, I:isoleucin; Leu, L: leucin; Lys, K: lysin; Met, M: methionin; Phe, F: phenylalanin; Pro, P: prolin; Ser, S: serin; Thr, T: threonin; Trp, W: tryptophan; Tyr, Y: tyrosin; Val, V: valin.

IV. SUMMARY

Parkinson's disease (PD) is the most common neurodegenerative movement disorder in the ageing population. Although the vast majority of cases are considered sporadic, around 10-20% is caused by pathogenic missense mutations in PD-associated genes. Among these, mutations in the *LRRK2* gene are the most frequent cause of late-onset autosomal-dominant familial but interestingly also sporadic PD. In recent years, over 40 missense variants have been reported in the *LRRK2* gene. Of these, only seven have been demonstrated to be pathogenic based upon clear segregation with disease in *LRRK2*-linked families including N1437H, R1441C/G/H, Y1699C, G2019S, and I2020T. The most prevalent mutation is the G2019S contributing up to 1-2% of sporadic and 7% of familial PD case in Caucasians, and up to 20% of total PD cases in Ashkenazy Jews, or 40% in North African Berbers. Recently, mutations in the *LRRK2* gene have been implicated in the dysfunction of several cellular pathways, but still the pathophysiological function of the gene remains unknown.

In the present work, a novel LRRK2 transgenic mouse model was generated and characterized in an attempt to elucidate the pathophysiological function of LRRK2. The LRRK2 transgenic mouse model expressed either human wild-type or G2019S LRRK2 protein under the neuron specific Thy1.2 promoter resulting in almost physiological levels of LRRK2 (~2-fold increased protein levels). The characterization of Thy1-2-LRRK2 transgenic mouse model showed expression of LRRK2 protein in affected-PD in brain regions such as cortex, midbrain, and hippocampus. However, the mice did not recapitulate the selective loss of dopaminergic (DA) neurons in *substantia nigra pars compacta* (SNpc), a major hallmark of postmortem brain from PD patients, suggesting that human LRRK2 protein overexpression, at least at physiological levels, is not sufficient to elicit PD-associated neuropathology. Nevertheless, the current proposed role of LRRK2 acting at the molecular level of different cellular processes suggests the use of Thy1.2-LRRK2 transgenic mouse model as a valuable tool to study the pathophysiological function of human LRRK2 and pathogenic-LRRK2 mutations in those cellular processes.

One specific question addressed in the present work was to further explore the role of human LRRK2 protein regulating actin cytoskeleton dynamics in neurite outgrowth in Thy1.2-LRRK2 transgenic mice, and cellular adhesion and locomotion in human fibroblasts. Previous evidence suggested a potential role of LRRK2 regulating actin and microtubule cytoskeleton dynamics as a mechanism underlying LRRK2-associated PD pathology. In this study, primary hippocampal cultures derived from Thy1.2-LRRK2 transgenic mice exhibited reduced neurite outgrowth and arborization in human WT LRRK2 neurons whereas no alterations were observed in G2019S LRRK2 compared to non-transgenic neurons, suggesting that two different regulatory mechanisms may be involved regulating neurite outgrowth and arborization. In addition, primary human skin fibroblasts derived from LRRK2-PD patients and healthy subjects were analyzed for cellular adhesion and locomotion, however, no alterations were observed in LRRK2-PD fibroblasts compared to WT LRRK2 fibroblasts. To investigate the role of LRRK2 kinase activity regulating actin cytoskeleton dynamics in those processes, cells were treated with the specific LRRK2 kinase inhibitor LRRK2-IN-1. Inhibition of LRRK2 kinase activity resulted in increased neurite outgrowth and arborization only in G2019S-LRRK2 neurons, and in alterations in cellular adhesion in fibroblast, but not in cellular locomotion, except in I2020T-LRRK2 fibroblasts. These results suggest that interaction between mutated LRRK2 kinase and LRRK2-IN-1 may be different to WT LRRK2 possible by altering interaction partner or changing LRRK2 properties.

In summary, the present study supports the involvement of physiological expression levels of human LRRK2 in the regulation of actin cytoskeleton arrangements and dynamics in neurite outgrowth but not in cellular adhesion and locomotion. This work also shows that inhibition of LRRK2 kinase activity modulates actin cytoskeleton dynamics in neurite outgrowth and cellular adhesion only in cells carrying the G2019S and I2020T LRRK2 kinase mutations. Altogether, these results suggest a physiological function of LRRK2 in the regulation of actin cytoskeleton arrangements and/or dynamics that dependents on LRRK2 kinase activity.

1 INTRODUCTION

1.1 Parkinson's Disease

In 1817 James Parkinson published "*An Essay on the Shaking Palsy*", a detailed report describing the clinical features of six patients with a neurological disorder consisting of resting tremor, lessened muscular power, abnormal truncal posture, and propulsive gait which he termed *paralysis agitans* (Parkinson 1817, reprinted in (Parkinson, 2002)). In the mid-1800, Jean-Martin Charcot identified the main clinical cardinal features of the neurological disorder described by James Parkinson as resting tremor, rigidity, postural instability, and bradykinesia. Also, on behalf of his discoverer, he suggested renaming the neurologic disorder known as *paralysis agitans* to Parkinson's disease (PD) (Fahn, 2003; Gandhi and Wood, 2005; Savitt et al., 2006). In the early 1900, the loss of neurons in the substantia nigra pars compacta (SNpc), and the presence of neuronal deposits (Lewy bodies) in surviving nigral neurons were described as the main pathological features of PD by Constantin Trétiakoff (Fahn, 2003; Parent and Parent, 2010). Fifty years later, in 1958, the neurotransmitter dopamine (DA) was discovered in the mammalian brain, finding that led to identify DA deficiencies in corpus striatum and substantia nigra (SN) in PD patients. In the same year, it was also discovered that neurons from SNpc conform the nigrostriatal dopaminergic pathway. All these findings brought to unveil that the loss of neurons in SNpc results in DA deficiency in the striatum being responsible for the appearance of the major symptoms of PD (Dauer and Przedborski, 2003; Parent and Parent, 2010; Savitt et al., 2006). These advances in the understanding of PD pathology culminated in 1960 with the discovery of L-dopa (L-3,4-dihydroxyphenylalanine), a DA precursor used as therapy to alleviate some of the motor symptoms of PD, discovery that changed the scenario in the treatment of PD. Since then, other therapies have been used to treat PD, but still the most potent antiparkinsonian drug used throughout the disease course is L-dopa (Dauer and Przedborski, 2003; Fahn, 2008a; Parent and Parent, 2010; Samii et al., 2004). Nowadays, L-dopa is administrated in combination with carbidopa or benserazide, two peripheral dopa

decarboxylase inhibitors that block the conversion of L-dopa to dopamine in the peripheral system, therefore allowing L-dopa to penetrate the blood-brain barrier. Once L-dopa is in the brain, it is converted to dopamine, thereby increasing the effectiveness of the therapy (Fahn, 2008a; Lees et al., 2009; Samii et al., 2004; Savitt et al., 2006). Although motor symptoms improve by 20-70% initially, long-term treatment with L-dopa leads to complicated motor fluctuations and dyskinesia over the years, which are difficult to control with medical treatment in some advanced PD patients (Fahn, 2008b; Lees et al., 2009; Parent and Parent, 2010; Samii et al., 2004). In those patients, deep brain stimulation (DBS) is the most widely surgical procedure used as therapeutic approach. DBS consists in the implantation of electrodes in different basal ganglia altered in PD such as the subthalamic nucleus (STN), in order to stimulate them electrically. For instance, the electric stimulation of STN disrupts/inhibits its excessive neuronal activity resulting in the final activation of the cortical motor system, consequently improving the motor symptoms of PD (Fahn, 2008b; Fasano et al., 2012; Lang and Lozano, 1998).

Despite all the advances in the understanding of PD pathology, and the improvement in the therapeutic strategies, Parkinson's disease is still a chronic, progressive, and incurable neurological disorder affecting about 1% of the population over the age of 65 years. The percentage of affected population rises steeply with the age, affecting about 4% of the population over 85 years (Alves et al., 2008; Bekris et al., 2010; Samii et al., 2004) .Even though PD can affect all ethnic populations, the prevalence of the disease varies geographically, increasing in industrialized countries were the population lives longer (Alves et al., 2008; Bekris et al., 2010; Samii et al., 2004). Therefore, major efforts need to be done to elucidate the pathogenesis of PD in order to finally find a therapeutic treatment that not only is able to control the motor and non-motor symptoms of PD, but also stops the progression of the disease.

1.1.1 Clinical Features of PD

"Parkinsonism" refers to a neurological syndrome defined by the combination of six motor symptoms including tremor at rest, bradykinesia, rigidity, postural instability, flexed posture, and freezing phenomenon. In order to diagnose a patient with parkinsonism, at least two of these symptoms have to be present being tremor at rest or bradykinesia one of them (Fahn, 2003). Parkinsonism can be classified into primary or secondary causes. In the first group, the classification includes degenerative diseases of unknown or genetic origin that cause primary parkinsonism such as multiple system atrophy (MSA), dementia with Lewy bodies (DLB), or Parkinson's disease (PD) which accounts up to 80% of the cases (Dauer and Przedborski, 2003). In the second group, the classification includes acquired or symptomatic parkinsonism as a consequence of drug intake, toxins, infection, vascular multi-infarct syndrome, or trauma (Bohlhalter and Kaegi, 2011).

Clinically, PD is characterized by the presence of several motor symptoms even though various non-motor symptoms can be observed through the course of the disease. The main cardinal features of PD are rigidity (muscle stiffness), bradykinesia (slowness of movement), tremor at rest, and postural instability (impaired balance). However, other non-motor symptoms including autonomic, cognitive, and psychiatric problems can appear together with the main cardinal features (Thomas and Beal, 2007). PD symptoms are gradual, being almost unnoticeable at the beginning, and worsening over time. Most of patients manifest rest tremor or bradykinesia as a first symptom, followed by the appearance of rigidity. Those symptoms can be treated with L-dopa since they are the result of DA deficiency in striatum. As the disease progresses, other symptoms not related to DA develop such as flexed posture, freezing phenomenon, and loss of postural reflexes (Fahn, 2003). After several years of L-dopa treatment, patients no longer respond to the treatment, resulting in the re-appearance of some of the early motor symptoms which may lead to immobility, and balance disabilities (Fahn, 2003). Finally, non-motor features appear such as

autonomic symptoms, sleep problems, sensory symptoms, behavioral and mental alterations, and declining in cognition (Fahn, 2003).

1.1.2 Neuropathological Features of PD

The main pathological hallmarks of PD are the loss of nigrostriatal dopaminergic, neuromelanin-containing neurons in the *substantia nigra pars compacta* (SNpc), together with the presence of intracytoplasmic protein aggregates termed Lewy Bodies (LBs) or Lewy Neurites (LNs) (Dauer and Przedborski, 2003; Savitt et al., 2006).

The pathological feature of PD mainly related to the characteristic motor symptoms of the disease is the loss of dopaminergic neurons in the SNpc (Figure 1.1). As mentioned above, dopaminergic neurons contain high levels of neuromelanin which confers the characteristic dark-brown pigmentation of the SNpc. In brains of PD patients, loss of dopaminergic neurons can be anatomically observed as a depigmentation of the SNpc. (Dauer and Przedborski, 2003). Nigrostriatal dopaminergic neurons have the cell body in the SNpc and synapse in the putamen nucleus of the striatum where they release the neurotransmitter dopamine (DA). At the onset of the symptoms, 60% of neurons are already lost causing about 80% of DA depletion in the putamen (Dauer and Przedborski, 2003; Samii et al., 2004). In less extend, mesolimbic dopaminergic neurons from the ventral tegmental area (VTA) with projection into the caudate nucleus of the striatum are also affected.

PD has a characteristic pattern of neurodegeneration, being the dopaminergic nerve terminals in the striatum the first target of the degenerative process followed by the cell body loss in the ventrolateral and caudal portions of the SNpc, suggesting a “dying back” process of neuronal death (Dauer and Przedborski, 2003). Not only dopamine neurons are affected, it has been reported that approximately 30-50% of nondopamine cells including monoaminergic cells, cholinergic cells, and hypocretin cells are lost at the end stage of PD which might be involved in the mechanism underlying the non-motor symptoms of the disease (Obeso et al., 2010).

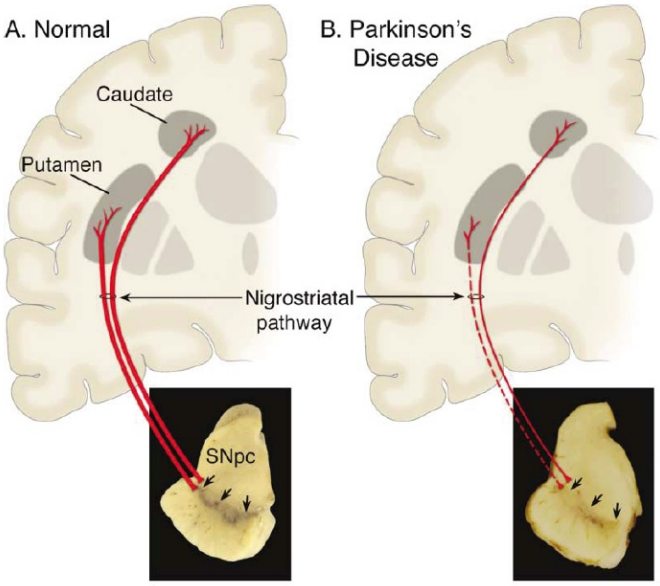

Figure 1.1 Schematic representation of the nigrostriatal dopaminergic pathway in Normal (A) or in Parkinson's disease (B) (Modified from (Dauer and Przedborski, 2003))**. (A)** Dopaminergic neurons in SNpc project and synapse in the Striatum (putamen and caudate nucleus) composing the nigrostriatal pathway (thick solid red line) where they releasing the DA neurotransmitter. SNpc presents a dark-brown pigmentation as a result of high neuromelanin content in dopaminergic neurons (black arrows). **(B)** In Parkinson's disease, the nigrostriatal pathway degenerates as a result of massive loss of dopaminergic neurons in SNpc that project and synapse in the putamen nucleus (dashed red line) and a modest loss of dopaminergic neurons that project and synapse in the caudate nucleus (thin solid red line). In PD, SNpc presents a reduced dark-brown pigmentation as a result of dopaminergic neuronal loss (black arrows).

The other pathological feature of PD is the presence of spherical eosinophilic protein aggregates in the soma of the neurons known as Lewy Bodies (LBs) (Figure 1.2), or in the neuronal cell processes known as Lewy Neurites (LNs) (Braak et al., 2004; Wakabayashi et al., 2012). The major component of LBs is a misfolded form of α-synuclein which tends to self-aggregate with other altered forms of α-synuclein. In addition, immunohistochemical studies have revealed that LBs contain more than 90 components such as synphilin-1, phosphorylated neurofilaments, ubiquitin, and tau, among others. (Braak et al., 2004; Wakabayashi et al., 2012).

LBs are subdivided into classical (brainstem) or cortical types based on their morphology. The classical type of LBs are spherical or elongated structures with a dense inner core and a peripheral halo whereas the cortical type are irregular in shape and lack both the inner core and the peripheral halo (Lees et al., 2009; Wakabayashi et al., 2012).

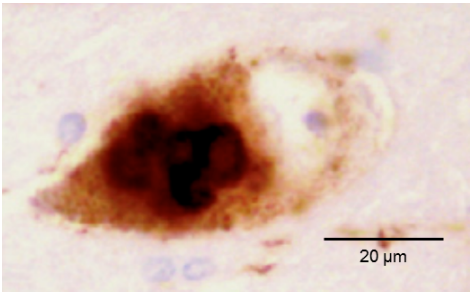

Figure 1.2 Lewy Body (LB) in a neuron in the substantia nigra from a Parkinson's disease patient (modified from (Lees et al., 2009))**.** Light microscopy image of α-synuclein immunoreactivity.Lewy body in a surviving neuron.

The distribution of LBs and LNs throughout the brain during the course of PD results in the subdivision of the disease into a presymptomatic, and a symptomatic phase. In the presymptomatic phase, LBs and LNs appear in specific brain areas of asymptomatic PD patients whereas in the symptomatic phase, LBs and LNs are widespread throughout the brain following a concrete pattern (Braak et al., 2004). This pathological pattern of progression for PD was first proposed by Braak et al. and consists in six neuropathological stages (Braak et al., 2004; Wakabayashi et al., 2012). This staging system describes LBs and LNs progression from the dorsal motor nucleus (stage 1), through the pontine tegmentum (stage 2), into the SN and amygdala (stage 3), then the mesocortex and thalamus (stage 4), and finally through the neocortex (stage 5 and 6) (Figure 1.3) (Braak et al., 2004; Wakabayashi et al., 2012). Braak PD stages 1-2 correspond to the asymptomatic phase of PD, stages 3-4 relate to the manifestation of the characteristic motor symptoms, and stages 5-6 correspond to the appearance of non-motor symptoms and cognitive impairment (Braak et al., 2004; Wakabayashi et al., 2012). LBs and LNs are not a unique characteristic of PD, they can be found in Alzheimer's disease (AD) in a condition called dementia with LB disease (DLB). In a lesser extent, LBs can be observed in people of advance age as an incidental pathologic finding (Dauer and Przedborski, 2003).

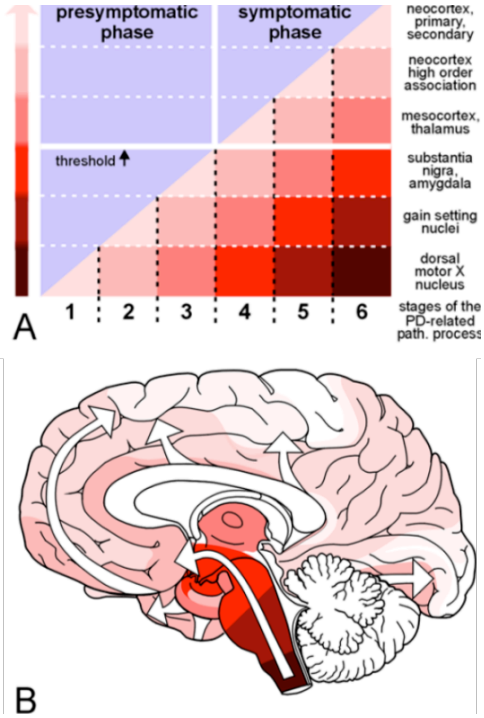

Figure 1.3 Neuropathological stages of Parkinson's disease progression (modified from (Braak et al., 2004))**. (A)** LBs and LNs appear in the presymptomatic phase of asymptomatic persons in vulnerable brain regions. In the symptomatic phase, LBs and LNs spread throughout the brain in a concrete manner (right) in 6 neuropathological stages. The severity of the disease (colored shading areas under the diagonal) grows at the same time that the disease progresses (the severity is indicated by the darker degrees in the colored arrow). **(B)** Diagram showing the ascending order (white arrows) of the pathological process (colored shading areas represent severity of the pathology corresponding to that in A).

1.1.3 Epidemiology of PD

In the past decades, major efforts have been done in order to determine the cause of PD. Despite considerably advances have been made in this area of research, the etiology of PD remains still unclear. It was largely considered that PD was a sporadic non-genetic disorder, however, in the past decades genetic studies of PD families and advances in molecular genetics have strengthened the hypothesis that PD is a disorder with a complex, multifactorial etiology likely arising from the elaborated combination of environmental, genetic factors, and gene-environment interactions, all of them acting directly on the aging brain (Alves et al., 2008; Bekris et al., 2010; Klein and Westenberger, 2012; Samii et al., 2004).

1.1.3.1. Environmental Factors

Although modern genetics revealed important genetic basis in familial PD accounting up to 10%-20% of PD cases, the majority of PD cases are sporadic and idiopathic. The discovery in 1983 that people intoxicated with MPTP (1-methyl-4-phenyl-1,2,3-tetrahydropyridine), a toxic side product in the synthesis of a pethidine analogue, developed parkinsonism clinically indistinguishable from PD, resulted in the first evidence that environmental exposure could be a potential cause for PD (Bekris et al., 2010; Gao and Hong, 2011; Langston et al., 1983;

Samii et al., 2004). MTPT can cross the blood-brain barrier, and once in the brain is converted by the enzyme monoamine oxidase B to MPP+ (1-methyl-4-phenylpyrdinium ion), the active metabolite. Released MPP+ is selectively taken up by the dopamine transporter in dopaminergic neurons where it accumulates and inhibits the mitochondrial complex I of the respiratory chain (Dauer and Przedborski, 2003; Gao and Hong, 2011; Samii et al., 2004). This finding led to the hypothesis that exposure to other chemicals similar to MPP+ such as paraquat (a common herbicide) or inhibitors of the mitochondrial chain such as rotenone (a pesticide) could be related to the development of PD (Dauer and Przedborski, 2003; Gao and Hong, 2011; Samii et al., 2004).

In addition, some epidemiologic studies suggested that early-life brain inflammation due to brain injury, or infectious agents may develop to post-encephalitic parkinsonism, but recent studies revealed that this type of parkinsonism is clinically distinct from PD (Gao and Hong, 2011). Interestingly, other environmental influences have been suggested to be neuroprotective reducing the risk of developing PD such as cigarette smoking and caffeine intake, however, this association needs still further investigation (Schapira and Jenner, 2011) (Dauer and Przedborski, 2003; Gao and Hong, 2011; Samii et al., 2004).

1.1.3.2. Genetic Factors

PD was originally considered a disorder of sporadic non-genetic origin, but recent advances in molecular genetics have revealed that 5-20% of PD patients have monogenic forms of the disease; changing the view on the etiology of PD (Gao and Hong, 2011). In the past fifteen years, 18 chromosomal loci known as *PARK loci* have been described in inherited PD patients and families (Bekris et al., 2010; Gao and Hong, 2011). However, the causative gene has not yet been identified for most of these loci. At the same time, not all the genes described until now contain a disease-causing mutation; instead, they contain some polymorphisms that have been associated to genetic risk factors for PD (Bekris et al., 2010; Klein and Westenberger, 2012).

To date, only at 6 of the 18 *PARK* loci, genes have been identified to carry mutations linked to familiar monogenic forms of PD accounting for about 30% of familial PD cases. Mutations in *SNCA (PARK1* and *4)*, and *LRRK2 (PARK8)* are known to cause autosomal-dominant (AD) PD forms whereas mutations in *Parkin (PARK2)*, *PINK (PARK6)*, *DJ-1 (PARK7)*, and *ATP13A2 (PARK9)* are responsible for autosomal-recessive (AR) PD forms of inheritance. Moreover, mutations in the exact same genes have been reported to account for about 3-5% of the sporadic PD cases. All the *PARK* PD-related loci, its chromosomal localization, form of inheritance, and the PD-causative gene, if identified, are listed in Table 1 (Bekris et al., 2010; Gao and Hong, 2011; Klein and Westenberger, 2012; Samii et al., 2004). In addition, common variants (polymorphisms) in 2 *PARK*-designated genes (*SNCA* and *LRRK2*) and in the microtubule association protein tau (*MAPT*) gene, and loss-of-function mutations in the glucocerebrosidase (*GBA*) gene have been well described to be risk factors for PD (Bekris et al., 2010; Farrer, 2006; Klein and Westenberger, 2012).

More recently, Genome Wide Association Studies (GWAS) have tried finding loci in which common variability could contribute to the risk of a disease. Using this approach, 3 new putative loci for PD, *PARK16-18*, have been identified and suggested as susceptibility loci for PD, however, further confirmation needs to be done (Bekris et al., 2010; Farrer, 2006; Gasser et al., 2011; Klein and Westenberger, 2012; Satake et al., 2009; Simon-Sanchez et al., 2009).

1.1.3.3. Gene-Environment Interaction

In the last decades few human association studies have investigated the interaction between genes-environment and its effect on PD susceptibility, describing some positive associations. Just to mention one example, high exposure to pesticides or paraquat in subjects with genetic variants in the dopamine transporter (DAT) has revealed increased susceptibility for PD. However, results must be interpreted carefully since only few studies with small amount of exposed subjects have been done (Gao and Hong, 2011).

Nomenclature	Gene Locus	Gene	Inheritance	Disorder
PARK1	4q21-22	SNCA	AD	EOPD
PARK2	6q25.2-q27	Parkins	AR	EOPD
PARK3	2p13	Unknown	AD	Classical PD
PARK4	4q21-q23	SNCA	AD	EOPD
PARK5	4p13	UCHL1	AD	Classical PD
PARK6	1p35-p36	PINK1	AR	EOPD
PARK7	1p36	DJ-1	AR	EOPD
PARK8	12q12	LRRK2	AD	Classical PD
PARK9	1p36	ATP32A2	AR	Kufor-Rakeb syndrome; atypical PD with dementia, spasticity, and supranuclear gaze palsy
PARK10	1p32	Unknown	Risk Factor	Classical PD
PARK11	2q36-27	Unknown; not GIGYF2	AD	Late-onse PD
PARK12	Xq21-q25	Unknown	Risk Factor	Classical PD
PARK13	2p12	HTRA2	AD or risk factor	Classical PD
PARK14	22q13.1	PLA2G6	AR	Early-onset dystonia-parkinsonism
PARK15	22q12-q13	FBX07	AR	Early-onset parkinsonian-pyramidal syndrome
PARK16	1q32	Unknown	Risk Factor	Classical PD
PARK17	16q11.2	VPS35	AD	Classical PD
PARK18	3q27.1	EIF4GI	AD	Classical PD

AD, autosomal dominant; AR, autosomal recessive; EOPD, early-onset PD

Table 1 PARK PD-related loci (modified from (Klein and Westenberger, 2012))**.**

1.2 PARK8: Leucine-Rich Repeat Kinase 2 (LRRK2)

In 2002, Funayama et al. identified a new locus for Parkinson's disease in a Japanese family with autosomal-dominant parkinsonism mapping on the chromosome 12p.11.2-q13.1. The new locus was termed *PARK8* following the nomenclature used to assign genetic loci linked to PD (see Table 1) (Funayama et al., 2002). Two years later, mutations in the *Leucine-Rich Repeat Kinase 2 (LRRK2)* gene were identified in two independent groups as the cause of autosomal-dominant PARK8-linked parkinsonism (Paisan-Ruiz et al., 2004; Zimprich et al., 2004). Most of the LRRK2 affected families displayed the typical cardinal features of PD with positive response to L-dopa, however, pathologically they presented a wide range of phenotypes including typical LB PD pathology, widespread LB pathology, nigral degeneration without LB pathology, and tau and ubiquitin pathology (Funayama et al., 2002; Paisan-Ruiz et al., 2004; Zimprich et al., 2004).

1.2.1 Structure of LRRK2

The *LRRK2* gene contains 51 exons encoding an extremely large protein of 2527 amino acids (aa) which comprises several independent domains (Zimprich et al., 2004). The LRRK2 protein, also referred to as Dardarin, belongs to the ROCO family of proteins characterized by the presence of a supradomain composed by a Ras of Complex (ROC) GTPase domain, with high sequence similarity to Ras small GTPases, linked to a C-terminal of ROC (COR) domain (Marin et al., 2008). Interestingly, LRRK2 protein holds another enzymatic domain, a serine/threonine kinase. In addition, several protein-protein interaction domains have been identified in the LRRK2 protein including an armadillo (ARM), ankyrin (ANK), leucine-rich repeat (LRR), and a WD40 domain which may act as a scaffold for assembly of different protein complexes resulting in the final activation of a wide variety of signaling cascades (Figure 1.4) (Mata et al., 2006; Zimprich et al., 2004).

The active form of LRRK2 consists of a dimeric structure composed by the self-interaction of LRRK2 through the ROC and the N-terminus domain (Berger et al., 2010; Deng et al., 2008; Gloeckner et al., 2006; Greggio et al., 2008). Also, the presence of the WD40 domain has been described to contribute in the self-interaction of LRRK2, reinforcing the interaction as shown by GST-pull down and co-immunoprecipitation assays (Greggio et al., 2008). Several reports have suggested that the LRRK2 kinase activity of the protein is also required to stabilize the formation of dimeric structures, since its inactivation results in the inability of LRRK2 to assembly in dimeric-LRRK2 structures (Greggio et al., 2008; Sen et al., 2009).

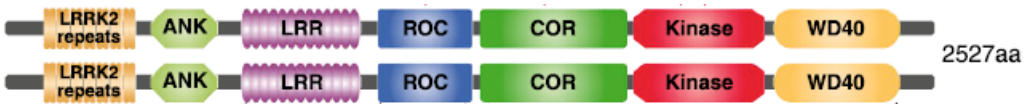

Figure 1.4 Schematic representation of the domain structure of LRRK2 (modified from (Tsika and Moore, 2012)). LRRK2 is a dimeric protein that consists of several protein-protein interactor domains (LRRK2 repeats; ANK, ankyrin domain; LRR, leucine-rich repeat domains; WD40 domain) and a catalytic core (Roc-COR-Kinase).

1.2.2 Cellular Localization of LRRK2

LRRK2 mRNA and protein has been reported to be expressed in anatomic regions and specific neuronal populations important to the pathogenesis of PD, but also in peripheral tissues in both rodent and human brain tissue (Biskup et al., 2006; Galter et al., 2006; Han et al., 2008; Higashi et al., 2007a; Higashi et al., 2007b; Westerlund et al., 2008). The temporal expression profile and the localization pattern of endogenous LRRK2 have been extensively analyzed in rat and mouse models. These studies have described earliest detection of LRRK2 mRNA at embryonic day 17 (E17), showing a dramatic increment at postnatal day 7 (P7), to finally reach mature expression pattern 1 month after birth (Biskup et al., 2007; Higashi et al., 2007b; Westerlund et al., 2008). Also, LRRK2 mRNA and protein was observed to be widely distributed throughout the brain of adult rodents, being expressed in

pyramidal neurons in the cerebral cortex, medium-size spiny neurons and interneurons in the caudate-putamen (striatum), large neuronal cells in the brainstem, Purkinje cells in cerebellum, CA1-3 and granule neurons from dentate gyrus in the hippocampal formation, olfactory bulb, and dopaminergic neurons in the substantia nigra pars compacta (Biskup et al., 2006; Higashi et al., 2007b; Melrose et al., 2007; Westerlund et al., 2008). Moreover, LRRK2 in rodents is also expressed in peripheral tissues including lung, kidney, heart, spleen, and lymph nodes (Biskup et al., 2007; Westerlund et al., 2008).

In postmortem human brains, endogenous LRRK2 protein expression has been observed in pyramidal neurons in the cortex, melanin-containing dopaminergic neurons in the substantia nigra, and GABAergic and cholinergic neurons in the caudate-putamen in the striatum (Biskup et al., 2006; Westerlund et al., 2008). Also, LRRK2 protein was detected in peripheral tissues including kidney, and fetal thymus (Westerlund et al., 2008).

At a subcellular level, LRRK2 protein is localized throughout the cytoplasm of neuronal soma and dendritic processes in punctate structures where it is associated to microtubule network, mitochondria, and membranous structures including Golgi, endoplasmic reticulum, and synaptic vesicles (Biskup et al., 2006).

1.2.3 Enzymatic Activities of LRRK2

As mentioned above, LRRK2 is a very interesting and unusual protein since it encodes within a single polypeptide chain two distinct enzymatic domains: a kinase domain and a Roc-Cor GTPase domain. Moreover, the presence of several protein-protein interaction domains suggests a possible function as a scaffolding protein (Anand and Braithwaite, 2009; Berwick and Harvey, 2011; Mata et al., 2006).

1.2.3.1. Kinase Activity

The LRRK2 kinase domain shares high sequence homology to mixed-lineage kinases (MLKs), a subclass of the mitogen-activated protein kinase kinase kinase (MAPKKK) family, which have both serine (Ser)/threonine (Thr), and tyrosine (Tyr) kinase activity (Gloeckner et al., 2009; Tsika and Moore, 2012; West et al., 2007; Zimprich et al., 2004). The function of protein kinases consists in catalyzing the transfer of the γ-phosphate of ATP to protein substrates (phosphorylation) or within the kinase protein (autophosphorylation) (Hubbard and Till, 2000; Zimprich et al., 2004).

In vitro experiments have assessed that LRRK2 has kinase activity (Figure 1.5 A), having the ability to autophosphorylate and phosphorylate the myelin basic protein (MBP), a generic kinase substrate (Gloeckner et al., 2009; Greggio et al., 2006; Luzon-Toro et al., 2007; West et al., 2007), as well as the LRRKtide and Nictide, two synthetic substrate peptides using *in vitro* kinase assays (Jaleel et al., 2007; Nichols et al., 2009). So far, there is lack of evidence that LRRK2 holds kinase activity in mammalian cells or tissue *in vivo*, since those systems present insufficient levels of protein to perform biochemical and enzymological assays (Anand and Braithwaite, 2009; Tsika and Moore, 2012).

Like other protein kinases, LRRK2 kinase activity is regulated by phosphorylation of the activation loop. The LRRK2 activation appears to be regulated by intermolecular autophosphorylation of two sites, the residues T2031 and S2032 within the activation loop, and depends on basal activity. Another residue, the T2035 also in the activation loop is important for the catalytic activity of LRRK2, although it is not a phosphate acceptor (Luzon-Toro et al., 2007). Some studies have suggested that the C-terminal WD40 domain or just the seven C-terminal amino acids of the LRRK2 protein are required for LRRK2 kinase activity since deletion of these fragments results in an inactive form of the LRRK2 protein unable to autophosphorylate or phosphorylate any substrate (Jaleel et al., 2007).

1.2.3.2. GTPase Activity

The LRRK2 Roc domain shares sequence homology with all five subfamilies of the Ras-related small GTPase superfamily including Ras, Rho, Rab, Sar/Arf, and Ran. It also contains conserved motifs necessary for GTP binding and intrinsic hydrolysis of GTP, both necessary for GTPase activity (Guo et al., 2007; Zimprich et al., 2004). The LRRK2 Roc domain is demonstrated to be an authentic and functional GTPase with ability to bind GTP through its guanine nucleotide phosphatase-binding (p-loop) motif, and possesses low intrinsic GTPase hydrolysis as observed by *in vitro* GTP binding and hydrolysis assays (Figure 1.5 B) (Deng et al., 2008; Guo et al., 2007; Li et al., 2007; Smith et al., 2006; Taymans et al., 2011; Tsika and Moore, 2012; West et al., 2007). Ras-related small GTPases act as molecular switches to regulate a wide range of cellular functions. They cycle between a GDP-bound (inactive) state to a GTP-bound (active) state (Guo et al., 2007; Wennerberg et al., 2005). This cycling between both states is controlled by three classes of regulatory proteins. The first class is the guanine nucleotide exchange factors (GEFs) which facilitate the binding of GTP by exchanging GDP to GTP to promote the formation of the GTP-bound (active) form. The second class is the GTPase activating proteins (GAPs) which increase the intrinsic GTPase hydrolysis promoting the GDP-bound (inactive) form and therefore, inactivating the GTPase protein. Finally, the third class of regulatory proteins is the GDP-dissociation inhibitors (GDIs) which stabilize an inactive GDP-bound pool of the protein (Guo et al., 2007; Wennerberg et al., 2005).

Recently, two regulatory proteins have been identified to control the LRRK2 Roc GTPase activity cycling between the GDP-bound (inactive) state to the GTP-bound (active) state (Figure 1.5 B). The Rho guanine nucleotide exchange factor 7, ARHGEF7, was first identified as a putative GEF in a LRRK2 microarray expression analysis performed in SH-SY5Y cells. Repression of LRRK2 by interference RNA (iRNA) resulted in upregulation of the *ARHGEF7* gene (Habig et al., 2008). Further experiments demonstrated that LRRK2 interacts with ARHGEF7 *in vitro* in mammalian cells and *in vivo* in rodent brain tissue. More

importantly, ARHGEF7 influences the GTP exchange capacity of LRRK2 and enhances the GTP hydrolysis of LRRK2 *in vitro*, suggesting that ARHGEF7 acts as a GEF for LRRK2 at least in *in vitro* studies (Haebig et al., 2010). Later on, the ADP-ribosylation factor (Arf) GTPase activating protein, ArfGAP1, was identified as a putative GAP for LRRK2 in a genetic modifier screen in yeast. Following studies showed that LRRK2 interacts with ArfGAP1 *in vitro* in mammalian cells and *in vivo* in rodent brain tissue and not only ArfGAP1 showed preference to interact with GTP-bound LRRK2 but also promoted the GTPase hydrolysis activity of LRRK2, supporting a role for ArfGAP1 as a GAP for LRRK2 (Stafa et al., 2012). The identification of the novel ARHGEF7 and ArfGAP1 as a GEF and GAP, respectively, of LRRK2 may explain the poor GTPase activity exhibited by LRRK2 in previous *in vitro* experiments (Tsika and Moore, 2012; West et al., 2007)

1.2.3.3. Potential Intrinsic Regulatory Mechanism of LRRK2

The presence of both a functional MAPKKK domain, and a GTPase (Roc) domain within the LRRK2 protein postulated the possibility that LRRK2 has an intramolecular mechanism to regulate its activity. Several *in vitro* studies have shown that LRRK2 deficient GTP-binding mutant proteins, i.e. K1347A and T1348N, present ablation of kinase activity. Also, addition of GDP in the cell lysate during immunoprecipitation (IP) studies resulted in decreased kinase activity of LRRK2 WT protein whereas addition of GTPγS, a non-hydrolysable nucleotide, resulted in increased kinase activity .These results led to suggest that the LRRK2 kinase activity is dependent on the existence of a functional GTPase domain, prompting to hypothesize the possibility that the LRRK2 kinase domain is a direct downstream effectors of the Roc GTPase domain (Guo et al., 2007; Li et al., 2007; Taymans et al., 2011; West et al., 2007). However, a more recent report proposed that LRRK2 kinase activity is not dependent on a specific GTP/GDP bound state of the GTPase domain, since binding of GTP or GDP did not affect the kinase activity of the protein, but instead, it is dependent on the capacity for GTP binding. Therefore, these evidences suggest that LRRK2 kinase activity is not a direct effector of the Roc GTPase domain (Taymans et al., 2011). Interestingly, when the GTP-

binding ability was tested in a kinase-inactive LRRK2 protein, no alterations were observed (West et al., 2007), suggesting that the GTPase activity can function independently of the kinase domain.

The identification of the Roc GTPase domain as main autophosphorylation target of the LRRK2 kinase activity prompted to hypothesize that the kinase domain might be a modulator of the Roc GTPase function, however, this mechanism still remains to be elucidated. (Anand and Braithwaite, 2009; Gloeckner et al., 2010; Greggio et al., 2009; Taymans et al., 2011; Tsika and Moore, 2012 ; Webber et al., 2011; West et al., 2007). Altogether, these evidences seem to indicate that LRRK2 has a complex and poorly understood bidirectional relationship between the GTPase and kinase domain that needs further investigation.

1.2.3.4. LRRK2 Protein as Scaffold

The presence of several protein-protein interaction domains such as leucine-rich repeats (LRR), ankyrin (ANK), and WD40 domain suggests that LRRK2 might serve as a scaffolding protein to assemble several signaling complexes (Mata et al., 2006; Zimprich et al., 2004). The formation of different complexes could depend on specific upstream signals and subcellular localization as it has been observed in MAPK scaffolding proteins (Berwick and Harvey, 2011; Mata et al., 2006). Recently, LRRK2 has been described for the first time to participate as scaffold in the canonical Wnt signaling cascade. In basal conditions LRRK2 functions as scaffold in the cytoplasmic multi-protein complex known as ß-catenin destruction complex (BDC) which is recruited to the membrane after signal activation. LRRK2 not only interacts with key Wnt signaling proteins, but also bridges membrane and cytosolic components of Wnt signaling. Pathogenic LRRK2 mutations have shown to disrupt the interaction of LRRK2 with proteins of the complex, and also to weaken the activation of the canonical Wnt signaling pathway, mechanism that might underlie the neurodegeneration observed in PD (Berwick and Harvey, 2012).

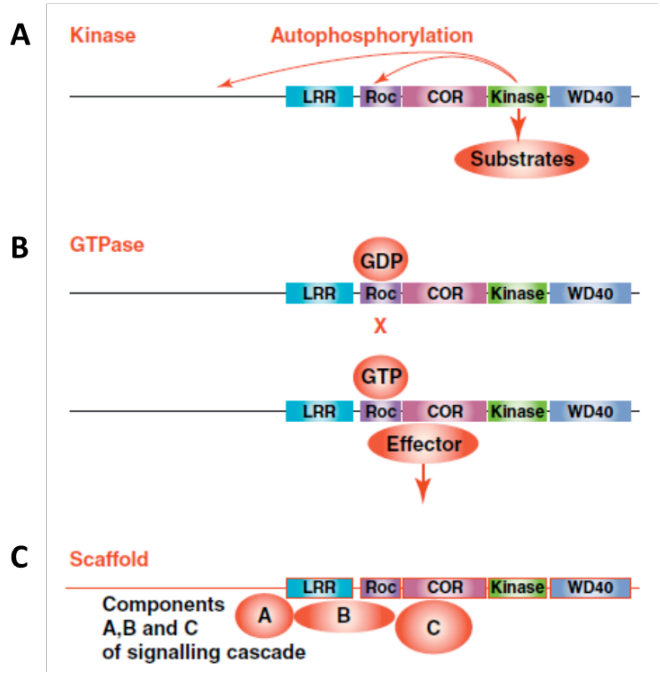

Figure 1.5 Schematic representation of possible mechanisms of LRRK2 action (modified from (Berwick and Harvey, 2011). **(A)** LRRK2 could function as a kinase, phosphorylating substrates and most probably presents autophosphorylation as a mechanism of self-regulation. **(B)** LRRK2 could functions as a small GTPase cycling between a GDP-bound inactive state (upper panel) to a GTP-bound active state (upper panel). Only bind to GTP LRRK2 would be able to stimulate downstream effectors. **(C)** LRRK2 could function as a scaffolding protein to assemble different signaling complexes. These three mechanisms are not mutually exclusive.

1.2.4 Pathogenic LRRK2 Mutations

Mutations in the LRRK2 gene are the most frequent cause of late-onset autosomal-dominant familial and sporadic Parkinson's disease (PD). In recent years, over 40 missense mutations have been reported in the *LRRK2* gene; however, the pathogenicity of most of these variants remains inconclusive. To date, only seven of these LRRK2 variants have been convincingly described to be pathogenic including N1437H, R1441C/G/H, Y1699C, G2019S, and I2020T (Figure 1.7) (Bekris et al., 2010; Ross et al., 2011). The G2019S missense mutation is the most prevalent contributing up to 1-2% of sporadic and up to 7% of familial PD cases in Caucasian populations (Bekris et al., 2010; Ross et al., 2011). However, its prevalence varies between populations, ranging from 15%-20% in total PD cases in Ashkenazi Jews (Ozelius et al., 2006) to approximately 40% in North African Arabs (Lesage et al., 2006). In contrast, this variant is less frequent in Asian populations. In addition, the G2019S variant exhibits reduced penetrance and is age dependent, increasing from 17% at age 50 years to 85% at age 70 years (Bekris et al., 2010; Farrer, 2006; Gasser et al., 2011; Ross et al., 2011). The next most frequent mutation, R1441G, owing to a founder effect, has a

prevalence up to 8% in Basques and is highly penetrant, being estimated 95% at the age of 75 years (Klein and Westenberger, 2012; Ross et al., 2011). Two common LRRK2 variants, G2385R and R1628P, are found in 3%-4% of Chinese descent and are well-validated risk factors for PD (Bekris et al., 2010; Gasser et al., 2011; Ross et al., 2011).

1.2.4.1. Effect on Enzymatic Activity

The majority of familial disease-associated LRRK2 mutations are localized mainly in the Roc-COR-Kinase region of LRRK2, also known as catalytic core (Tsika and Moore, 2012), suggesting that pathogenic-LRRK2 mutations may affect the different LRRK2 enzymatic activities.

(i) Mutations in the kinase domain of LRRK2

The G2019S and I2020T mutations are located within a high conserved region critical for substrate access, the activation loop of the kinase domain (Figure 1.6). Whereas the G2019S present a clear enhanced kinase activity *in vitro*, there is controversial data regarding the effect of the I2020T LRRK2 mutation on kinase activity, with some studies supporting an increased kinase activity (Gloeckner et al., 2006; West et al., 2007) while others have reported a decreased kinase activity (Anand et al., 2009; Jaleel et al., 2007).

It has been proposed that the G2019S mutation may lead to a conformational change in the activation loop, mimicking the constitutively active form of the protein. As mentioned above (see Introduction part 1.2.3), the T2035 residue in the activation loop is important for the catalytic activity of the protein. Alanine substitution in this residue in the G2019S LRRK2 protein (G2019S/T2035A) resulted to be as hyper active as the G2019S protein whereas the addition of a second alanine substitution in the G2019 residue, therefore creating a double mutant protein (G2019A/T2035A), resulted in a protein catalytically dead (Luzon-Toro et al., 2007).

In vitro binding assays have demonstrated that the differences in kinase activity between the G2019S and I2020T mutations are partially attributed to altered ATP affinity. Whereas the G2019S mutant exhibits 2-fold lower ATP affinity than the wild-type LRRK2, the I2020T mutation exhibits 6-fold higher ATP affinity thus, suggesting that these differences in ATP affinity could have an effect on enzymatic properties of LRRK2 protein (Reichling and Riddle, 2009).

(ii) Mutations in the Roc GTPase domain of LRRK2

The R1441C/G/H mutations are located outside the GTP binding pocket of the GTPase domain, a non-conserved region through various GTPase families (Figure 1.6). Their localization suggests that they are quite unlikely to directly alter the GTPase activity of LRRK2 (Lewis et al., 2007). The R1441C and R1441G exhibit intrinsic GTP hydrolysis although presenting a significantly slower rate of GTP-GDP hydrolysis than the WT LRRK2 protein. These observations suggests that the R1441C/G LRRK2 protein exhibit a slower inactivation process than WT LRRK2 protein therefore, prolonging the time that LRRK2 spends in an active GTP-bound state (Anand and Braithwaite, 2009; Guo et al., 2007; Lewis et al., 2007; Li et al., 2007; West et al., 2007). At the present, it is not clear whether the reduced GTP hydrolysis with no or minor effects on GTP binding capacity observed in these LRRK2 mutant proteins enhance the kinase activity of the LRRK2 protein (Anand and Braithwaite, 2009; Guo et al., 2007; Lewis et al., 2007; Li et al., 2007; West et al., 2007).

The N1437H mutation is located in the Roc GTPase domain of the LRRK2 protein, and has been recently identified to be pathogenic. Since it is a new variant, its GTPase activity has not yet been determined, however, it has been already tested that N1437H LRRK2 protein exhibits increased GTP binding capacity and also increased kinase activity, which would be consistent with decreased GTPase activity (Rudenko et al., 2012).

(iii) Mutations in the COR domain of LRRK2

The Y1699C mutation is located in the COR domain of the LRRK2 protein (Figure 1.6). The evidences regarding the effect of the Y1699C mutation on the enzymatic activities of LRRK2 protein suggest that this mutant protein exhibits decreased GTPase activity. There is less consistent data regarding its GTP binding capacity, some reports observed an slightly increased whereas others observed no alterations in GTP binding capacity. Overall, most of the evidences point to an enhanced kinase activity exhibited by the Y1699C LRRK2 mutation (Daniels et al., 2011b; Rudenko et al., 2012; West et al., 2007).

1.2.4.2. Effect on Self-Interaction and Dimerization

LRRK2 self-interaction has been suggested throughout a different number of assays and techniques. This self-interaction of LRRK2 has been described to take place through different LRRK2 domains leading to the formation of LRRK2 species consistent with a dimer-sized complex (Greggio et al., 2008; Sen et al., 2009).

Some pathogenic and artificial LRRK2 mutations have been observed to alter the ability of LRRK2 to stabilize the formation of dimer-sized complexes. The G2019S and I2020T LRRK2 mutations have been suggested to stabilize the formation of dimer-sized structures whereas the introduction of the artificial kinase activity ablating mutation D1994A reduces the ability to form dimers (Sen et al., 2009). Also, it has been described that LRRK2 self-interacts through the Roc domain. The R1441 residue located in the Roc domain stabilizes the LRRK2 dimer formation at the Roc:Roc GTPase tandem domain through the generation of hydrogen bonds therefore, any mutation in this residue, i.e. R1441C, would disrupt the Roc:Roc GTPase tandem domain interaction resulting in the destabilization of the LRRK2 dimeric GTPase domain(Deng et al., 2008). However, when using full-length R1441C LRRK2 protein, no differences in the formation of dimer-sized complexes were observed compared to WT LRRK2 (Sen et al., 2009). The artificial GTP binding ablating K1347A mutation in the GTPase domain also results in reduction of LRRK2 dimer formation (Sen et al., 2009). Finally, the Y1699C mutation is located in the intra-molecular Roc:COR interface

strengthening the intra-molecular interaction thus, resulting in the destabilization of the LRRK2 dimer formation at the Roc:COR tandem domain (Daniels et al., 2011b). Altogether, these evidences suggest that LRRK2 dimer formation is kinase activity dependent (Daniels et al., 2011b; Deng et al., 2008; Greggio et al., 2008; Sen et al., 2009).

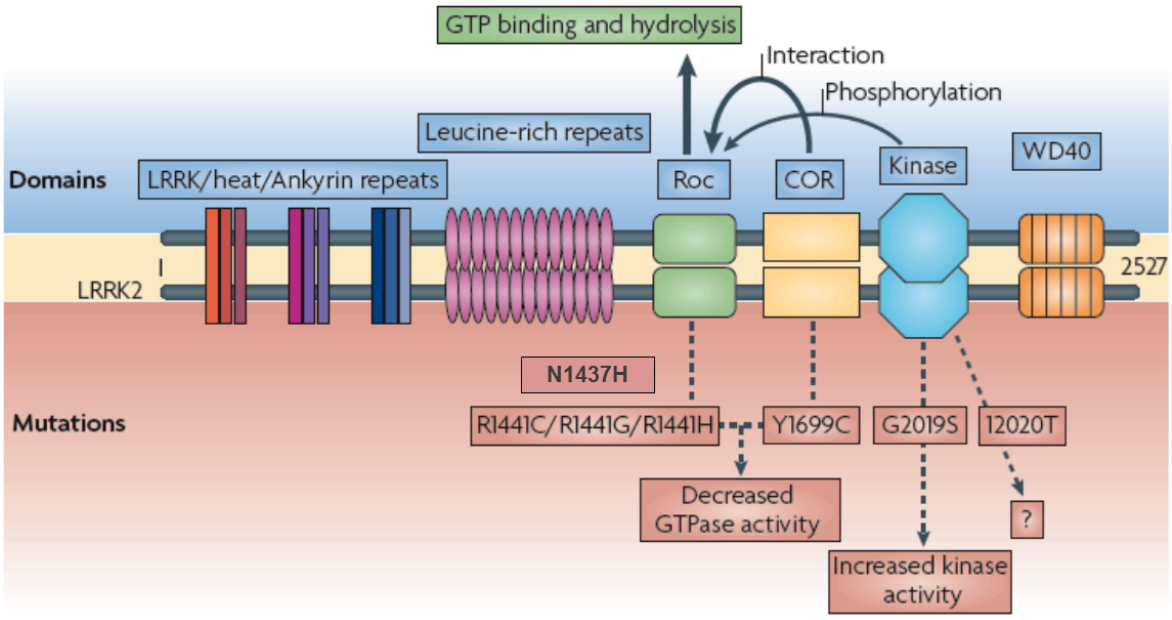

Figure 1.6 Localization of pathogenic LRRK2 mutations and its effect on enzymatic activities of LRRK2 protein (modified from (Cookson, 2010))**.** LRRK2 is schematically represented as a dimer. The different domains and proposed enzymatic activities and intramolecular interactions proposed are listed above. The 7 known LRRK2 pathogenic mutations and its effect on enzymatic activities are listed below. The N1437H, R1441C7G/H and Y1699C decrease GTPase activity, whereas G2019S increases kinase activity. The effect of I2020T mutation in kinase activity is inconsistent among studies. The kinase and GTPase domain may be related since the Roc domain is autophosphorylated in different sites by the kinase domain (above in blue). The COR domain has been shown to interact with the Roc domain in the LRRK2 dimer conformation.

1.2.5 Putative Physiological and Pathological Functions of LRRK2

Despite all the genetic evidence that link mutations in the *LRRK2* gene as a cause for PD, and all the information collected over the past 10 years regarding the LRRK2 protein, i.e. structure, localization, and enzymatic activities, still there is a lack of reliable cellular and molecular evidence regarding the physiological function of LRRK2 as well as its role in the pathology of PD (Anand and Braithwaite, 2009; Daniels et al., 2011a). Critical for the understanding of the biochemical and functional role of LRRK2 is the identification of its true substrates and interactors. In the past years, investigations in this direction have been carried out in the LRRK2 field (Anand and Braithwaite, 2009; Daniels et al., 2011a).

1.2.5.1. Substrates and Interactors of LRRK2

Several LRRK2 substrates and interactors have been suggested over the past years from evidence obtained from *in vitro*, cellular, and biochemical studies, however, the relevance of these proteins as physiological or pathological substrates and interactors need further confirmation in cells and *in vivo* models (Anand and Braithwaite, 2009).

The LRRK2 protein holds two enzymatic domains with GTPase and a kinase activity. The data published until the present support the idea that these enzymatic activities are important for the LRRK2-related pathology, and the identification of putative physiological substrates would bring further insights about the function of LRRK2. The first described LRRK2 substrate identified through *in vitro* biochemical assays was moesin, showing that LRRK2 phosphorylates moesin at threonine (Thr) 558 (Jaleel et al., 2007). Moesin together with ezrin and radixin belong to the moesin/ezrin/radixin (ERM) protein family known to link the actin cytoskeleton to the plasma membrane (Parisiadou and Cai, 2010). In the same study, LRRK2 was shown to phosphorylate ezrin and radixin which share the same amino acid sequence surrounding the Thr-558 site of phosphorylation in moesin. The identification of moesin as a LRRK2 substrate suggested for the first time a potential role of LRRK2 in actin cytoskeleton dynamics (Jaleel et al., 2007; Parisiadou and Cai, 2010). Other LRRK2 substrates involved in cytoskeleton dynamics are ß-tubulin (Daniels et al., 2011a; Gillardon,

2009) and glycogen synthase kinase 3ß (GSK3ß) (Daniels et al., 2011a; Lin et al., 2010). Also, LRRK2 was found to phosphorylate *in vitro* mitogen-activated kinase kinase (MKK) 3/6 and 4/7 involved in cellular stress response (Daniels et al., 2011a; Gloeckner et al., 2009; Hsu et al., 2010), the eukaryotic initiation factor 4E-binding protein (4E-BP) involved in protein translation (Daniels et al., 2011a; Imai et al., 2008), the GTPase-activating protein ArfGAP1 (Daniels et al., 2011a; Stafa et al., 2012), and more recently endophilinA (EndoA) which is involved in synaptic endocytosis (Matta et al., 2012).

In addition, LRRK2 contains several protein-protein interaction domains and therefore, it has been suggested to act as a scaffold for assembly of different protein complexes. Using different techniques such as mass spectrometry, yeast two-hybrid screening, and protein pull-down assays several proteins have been identified to interact with LRRK2 (Anand and Braithwaite, 2009). The different LRRK2 interactors can be grouped in several cellular processes including chaperone machinery (Hsp90, the Hsp90 co-chaperone $p50^{CDC37}$ and the C-terminus of Hsp70-interacting protein (CHIP)) (Daniels et al., 2011a; Ding and Goldberg, 2009; Ko et al., 2009; Parisiadou et al., 2009; Sen et al., 2009), cytoskeleton dynamics (α and ß-tubulin, actin- associated proteins, GSK3ß, EF1A and disheveled family of proteins (DVL1/2/3)) (Daniels et al., 2011a; Gandhi et al., 2008; Gillardon, 2009; Gloeckner et al., 2006; Lin et al., 2010; Meixner et al., 2011; Sancho et al., 2009), apoptosis (FADD, TRADD and RIP1) (Daniels et al., 2011a; Ho et al., 2009), synaptic vesicle endocytosis (Rab5) (Daniels et al., 2011a; Shin et al., 2008), MAPK signaling (MKK3/6 , MKK4/7, JIP1-3 and JIP4) (Daniels et al., 2011a; Gloeckner et al., 2009; Hsu et al., 2010; Jaleel et al., 2007), and finally in cell signaling (14-3-3 isoforms proteins) (Daniels et al., 2011a; Dzamko et al., 2010; Nichols et al., 2010).

A clear substrate and interactor of LRRK2 is LRRK2 itself, which presents autophosphorylation and has been shown to be active as a dimer (Anand and Braithwaite, 2009; Deng et al., 2008; Greggio et al., 2008; Sen et al., 2009; Smith et al., 2006; West et al., 2007).

1.2.5.2. Molecular and Cellular Pathways Implicated in LRRK2-mediated Neurodegeneration

The identification of putative substrates and interactor partners of LRRK2 has provided potential clues regarding the physiological function of LRRK2. Also, the use of pathogenic LRRK2 mutations in cellular, molecular, and biochemical assays has given some evidence of the pathogenic mechanisms of LRRK2-mediate neurodegeneration (Anand and Braithwaite, 2009; Daniels et al., 2011a; Tsika and Moore, 2012). To date, several cellular functions and molecular pathways have been suggested to be regulated by LRRK2 such as vesicular trafficking, neurite outgrowth, cytoskeletal regulation, autophagy-lysosomal pathway, mitochondrial function, apoptosis, DA neurotransmission, and protein translational and degradation control, all leading to neuronal damage (Figure 1.7) (Anand and Braithwaite, 2009; Berwick and Harvey, 2011; Tsika and Moore, 2012).

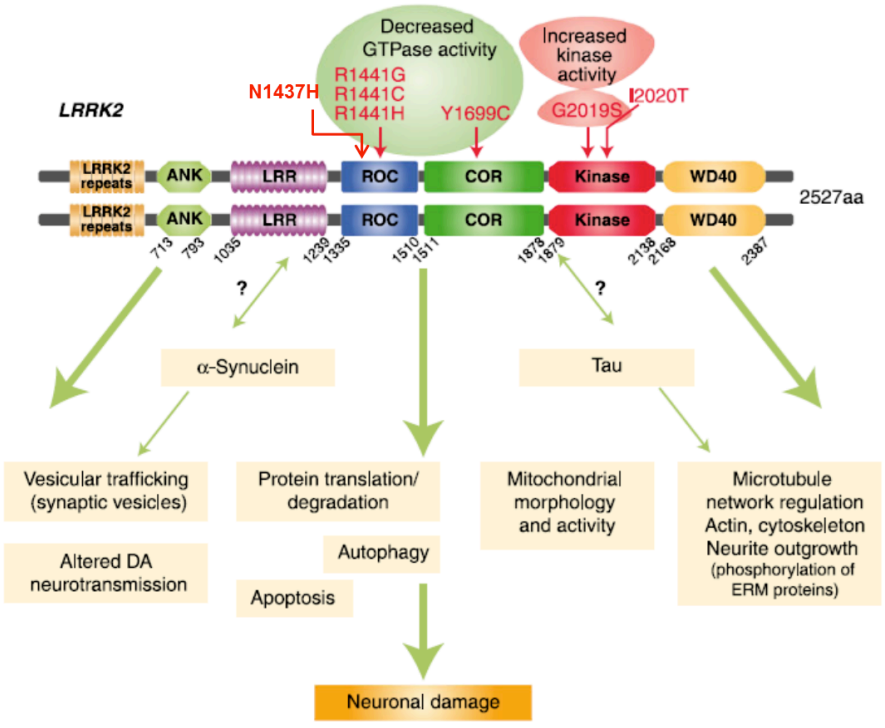

Figure 1.7 LRRK2-related cellular functions and molecular pathways (modified from (Tsika and Moore, 2012). LRRK2 has been implicated in regulating several molecular pathways that could potentially underlie neuronal damage from data obtained from cellular and animal models. Further understanding is needed about the LRRK2 interaction with α-synuclein and tau and the pathogenic-LRRK2 molecular mechanisms leading to neurodegeneration. (ERM, ezrin/radixin/moesin).

(i) Function of LRRK2 Regulating Actin Cytoskeleton Arrangements and/or Dynamics in Neurite Outgrowth and Branching Complexity.

LRRK2 has been suggested to be involved in the regulation of neurite outgrowth maintenance and branching complexity (Figure 1.8). Several studies performed in primary neuronal cultures and differentiated SH-SY5Y cells have reported that overexpression of the pathogenic G2019S and I2020T LRRK2 mutations led to a reduction in neurite outgrowth maintenance and branching complexity (Dachsel et al., 2010; MacLeod et al., 2006; Plowey et al., 2008; Ramonet et al., 2011; Sanchez-Danes et al., 2012; Winner et al., 2011). On the contrary, ablation of LRRK2 protein expression led to observe an increment of neurite outgrowth maintenance and branching complexity. Altogether, these results suggested that the regulation of neurite outgrowth and branching complexity by LRRK2 is kinase activity dependent (Dachsel et al., 2010; MacLeod et al., 2006; Ramonet et al., 2011; Winner et al., 2011).

The first mechanisms that has been suggested to be involved in the regulation of neurite outgrowth and branching complexity by LRRK2 is through the phosphorylation of Ezrin/Radixin/Moesin (ERM) family of proteins, previously described as putative LRRK2 substrates (Jaleel et al., 2007). Primary neuronal cultures overexpressing the G2019S LRRK2 protein presented an increased number of phosphorylated (P)-ERM positive and accumulation of filament (F)-actin in filopodia, resulting in the reduction of neurite outgrowth and branching complexity. On the contrary, ablation of LRRK2 protein resulted in a decreased number of p-ERM proteins and reduced accumulation of F-actin rescuing the reduced neurite outgrowth and branching complexity phenotype observed by the overexpression of G2019S LRRK2 protein. This same effect was observed after the inhibition of p-ERM and F-actin accumulation (Parisiadou and Cai, 2010; Parisiadou et al., 2009). These data provided the first model by which the G2019S LRRK2 mutation causes a gain-of-function effect that leads to a neurite sprouting disruption critical for neuronal morphology (Parisiadou et al., 2009).

Later, with the identification of the small Rho GTPase family proteins as interactors of LRRK2 and also known for its role in actin cytoskeleton remodeling (Chan et al., 2011; Haebig et al., 2010), a second molecular mechanism underlying the regulation of neurite outgrowth and branching by LRRK2 was proposed. The small Rho family GTPase Rac1 was shown to interact with LRRK2, and overexpression of both proteins resulted in increased GTP bound active state of Rac1 and redistribution of LRRK2 localization to the membrane. The G2019S neurite outgrowth shortening observed in G2019S overexpressed SH-SY5Y differentiated cells was rescued by the overexpression of Rac1, suggesting that LRRK2 increases Rac1 active state and this stimulates actin cytoskeleton remodeling resulting in neurite processes outgrowth (Chan et al., 2011).

Recently, a third mechanism underlying the regulation of neurite outgrowth and branching complexity by LRRK2 has been proposed involving the newly identified GTPase-activating protein ArfGAP1 protein. The ArfGAP1 protein has been suggested to interact with and increase the GTPase and kinase activity of LRRK2. Primary cortical neurons overexpressing G2019S LRRK2 protein and ArfGAP1 synergistically promoted reduced neurite outgrowth phenotype whereas silencing of ArfGAP1 protein resulted in the rescue of the G2019S-induced neurite outgrowth shortening (Stafa et al., 2012). At the same time, ArfGAP1-induced neurite outgrowth phenotype is partially rescued by silencing LRRK2 protein. Altogether these data suggests that ArfGAP1 regulates GTP hydrolysis of LRRK2 resulting in reduced LRRK2 neurite outgrowth, and at the same time LRRK2 phosphorylates ArfGAP1 resulting in reduced ArfGAP1 neurite outgrowth (Stafa et al., 2012).

Besides the role of LRRK2 in the regulation of actin cytoskeleton dynamics in neurite outgrowth and branching complexity, a recent analysis of the LRRK2 interactome has provided the identification of new LRRK2 interactors all related to actin cytoskeleton dynamics. Some of the revealed proteins are actin isoforms as well as proteins associated to actin filament assembly, organization, rearrangement, and maintenance (Meixner et al., 2011).

1.2.6 Animal Models of LRRK2

Given the complexity of the LRRK2 protein, the understanding of its physiological function and its pathological role in PD has been a difficult task. To overcome this problem, the development of LRRK2 animal models has become a critical tool to dissect the mechanisms underlying the pathogenic pathway of a disease as well as to develop new therapeutic treatments (Xu et al., 2012). At the present, several LRRK2 *in vivo* models have been produced in yeast, *C.elegans*, *D.melanogaster*, and rodent models. This section focuses and summarizes the most common characteristics observed in the different LRRK2 transgenic mouse models published until now (Xu et al., 2012), although a list with detailed information regarding each LRRK2 transgenic mouse model is provided in Table 2.

A good LRRK2 transgenic mouse model should recapitulate the clinical and neuropathological characteristics of the human disease avoiding any phenotype not related to it (Xu et al., 2012). To date, several LRRK2 transgenic mouse models overexpressing the human or murine WT, G2019S, I2020T, or R1441C/G LRRK2 protein in cDNA or BAC clones have been published (Li et al., 2010; Li et al., 2009; Lin et al., 2009; Maekawa et al., 2012; Melrose et al., 2010; Melrose et al., 2007; Ramonet et al., 2011; Tong et al., 2009; Wang et al., 2008), however, at the moment it is difficult to draw comparisons among them since they have been generated by different groups and methods, and characterized by different laboratories using distinct techniques and protocols (Xu et al., 2012).

Still, analysis of the LRRK2 transgenic mouse models available until now has revealed the presence of several common features allowing some comparisons between them (Xu et al., 2012). It is consistent that most of these LRRK2 transgenic mouse models do not recapitulate the two main neuropathological hallmarks of PD, age-dependent loss of DA neurons in SNpc, and the presence of Lewy bodies (Daniels et al., 2011a; Li et al., 2011; Xu et al., 2012). However, in some it is possible to observe the presence of abnormalities in the DA system, such as stimulated DA neurotransmission, decreased DA levels, or behavioral deficits which are important features of PD, especially in early stages of the disease (Daniels et al., 2011a; Li et al., 2011; Xu et al., 2012). These observations suggest that LRRK2 may be involved in the regulation of specific functions in the nigrostriatal dopaminergic pathway instead of being a critical determinant of the development and survival of DA neurons (Daniels et al., 2011a; Li et al., 2011). Also, axonal degeneration can be commonly observed in some of these LRRK2 transgenic mouse models, supporting the "dying back" mechanism as a likely step in PD development (Daniels et al., 2011a; Xu et al., 2012). Finally, another observation that appears to be consistent in these LRRK2 transgenic mice carrying different mutations is a dosage dependence effect where stronger PD-like phenotypes are correlated with higher levels of transgene expression (Xu et al., 2012).

In summary, the generation of more robust LRRK2 animal models will greatly aid the *in vivo* validation of research hypothesis, the genetic dissection of pathogenic pathways, and the formulation of new therapeutic treatments for PD.

Table 2 LRRK2 transgenic mouse models (modified from (Xu et al., 2012))

Group	LRRK2 genetic construction	Pathologic LRRK2-PD mutation and expression over murine (fold)	Motor activities and age onset	Loss of TH+ neurons in SN	Striatal DA neurotransmission	Phospho-tau species
(Melrose, Kent et al. 2007; Melrose, Dachsel et al. 2010)	Human BAC with vector in FVB	WT (~20 fold)	Not changed at 7 months	Not changed at 2 years	↓ without pharmacological manipulation at 9 months	ND
		G2019S (~14 fold)	Not changed at 7 months	Not changed at 2 years	↓ without pharmacological manipulation at 9 months	↑ aged
(Li, Liu et al. 2009)	Human BAC without pBACe3.6 vector in FVB	WT	Not changed	Not changed	ND	Not changed
		R1441G (~5-10 fold)	↓ at 6 months L-dopa responsive	Not changed, but had signs of ↓ neurite density and cell size at 9 months	↓ at 12 months	↑ at 9 months
(Li, Patel et al. 2010)	Mouse BAC FLAG-tagged LRRK2 in C57BL6	WT (~6 fold)	Hyperactive at 6 months	Not changed at 18 months	Not changed at 12 months	↓ at 18 months
		G2019S (~6 fold)	Not changed at 12 months	Not changed at 12 months	↓ at 12 months	Not changed at 18 months
(Ramonet, Daher et al. 2011)	CMVE-PDGFß promoter driven, Myc-tagged human LRRK2 in C57BL6J+C3H/HeJ	WT (~3-5 fold)	ND	Not changed as lack of expression	Not changed	ND
		G2019S (~3-5 fold)	Not changed at 15 months	↓ at 19 months, ↓ neurite density	Not changed at 15 months	Not changed
		R1441C (~3-5 fold)	↓ at 15 months	Not changed as lack of expression	Not changed in striatum ↓ in cerebral cortex at 15 months	ND
(Tong, Pisani et al. 2009)	Knockin in C57BL6+129	R1441C (endogenous)	↓ in response to AMPH	Not changed	Not changed at 24 months	Not changed
(Wang, Xie et al. 2008)	Human HA-tagged LRRK2 G2019S expression was suppressed by doxycycline to >90% after 4 weeks in tetO-G2019S/CaMKII-tTA in forebrain in C57BL6	G2019S (ND)	ND	ND	ND	ND
(Lin, Parisiadou et al. 2009)	Human HA-tagged LRRK2 in 3 sets of lines:	tetO-WT/CamKII-tTA (~8-16 fold)	↑ at 12 months	ND	ND	ND
		tetO-G2019S/CamKII-tTA (~8-16 fold)	ND	ND	ND	ND
	Deletion of Kinase domain 1887-2102 aa	tetO-KD/CamKII-tTA (<1 fold)	ND	ND	ND	ND
(Lee, Shin et al. 2010)	Herpes simples virus (HSV) amplicon-based untagged constructs applied in C57BL6	WT	ND	Not changed	ND	ND
		G2019S	ND	↓	ND	ND
		G2019S/D1994A (KD)	ND	Not changed	ND	ND
(Maekawa, Mori et al. 2012)	CMV promoter driven, V5-tagged human LRRK2 in C57BL/6J+C3H	I2020T (~1.2-1.5 fold)	Beam test ↓ at 43 weeks but not changed at 73 weeks Rotarod Test ↓ at 34 weeks but not changed at 42-59 weeks	Not changed at 18 months	↓ at 10 weeks	
(Chen, Weng et al. 2012)	CMVE-PDGFß promoter driven, HA-tagged human LRRK2 in FVB/N	WT (10 copies transgene)	Not changed at 12-16 months	Not changed	Not changed	Not changed
		G2019S (10 copies transgene)	↓ at 12-16 months L-Dopa responsive	↓ at 12-16 months	↓ at 12 months	↑ at 12 months

↑, increased; ↓, decreased; AMPH, amphetamine; BAC, bacterial artificial chromosome; HA, hemagglutinin; KD, kinase-dead; ND, not determined; WT, wild-type; SN, substantia nigra; DA, dopamine; PD, Parkinson's disease

1.3 Objectives

Genetic evidence has linked mutations in the LRRK2 gene as the most frequent cause of PD. However, the physiological function of LRRK2 and its role in the pathology of PD still remain unknown. In the past years, several studies have tried to identify the true physiologic substrate and interactor partners of LRRK2 as well as to develop new *in vivo* animal models able to recapitulate the clinical and neuropathological features of PD in order to bring further understanding of the LRRK2-related pathogenicity in PD. The results obtained from these studies have suggested the implication of LRRK2 in several molecular signaling pathways that could lead to neuronal damage, and therefore, could be involved in the mechanisms underlying PD neuropathology.

The present study attempted to elucidate the pathophysiological function of LRRK2 in the pathogenesis of PD by generating and characterizing a novel Thy1.2-LRRK2 transgenic mouse model and also by exploring the potential role of human LRRK2 in the regulation of actin cytoskeleton arrangements and/or dynamics in mouse and human cell models. Thereby, (I) the Thy1.2-LRRK2 transgenic mouse model was generated expressing either WT or G2019S LRRK2 protein at physiological levels. Then, (II) the temporal expression profile and localization pattern of LRRK2 transgene was investigated in regions important for the pathology of PD in the brain of Thy1.2-LRRK2 transgenic mice, and PD-associated neuropathology was analyzed in SNpc. In addition, (II) neurite outgrowth and branching complexity analysis was performed in primary hippocampal cultures derived from Thy1.2-LRRK2 transgenic mice, and (III) the processes of cellular adhesion and locomotion were investigated in primary human skin fibroblasts derived from healthy-subjects and LRRK2 PD patients in order to explore the implications of human LRRK2 protein regulating actin cytoskeleton dynamics. Finally, (IV) the specific LRRK2 kinase inhibitor, LRRK2-IN-1, was tested in both mouse and human cellular models to investigate the involvement of LRRK2 kinase activity in the regulation of actin cytoskeleton arrangement and/or dynamics.

In summary, the purpose of this work was to investigate the LRRK2-related pathology of PD in a novel Thy1.2-LRRK2 transgenic mouse model, and to explore the role of human LRRK2 protein and the involvement of LRRK2 kinase activity regulating actin cytoskeleton arrangements and/or dynamics in mouse and human cellular models.

2 RESULTS

2.1 Generation and Characterization of Thy1.2-LRRK2 Transgenic Mouse Model

The lack of a good LRRK2 transgenic mouse model able to recapitulate the main neuropathological hallmarks of PD, and the need to further investigate and understand the *in vivo* role of LRRK2 protein in both physiological conditions and the pathophysiology of PD, brought the laboratory of Prof. Dr. Jucker (Department of Cellular Neurology at the Hertie Institute for Clinical Brain Research in Tübingen;Garcia-Miralles, et al. unpublished) to generate a novel LRRK2 transgenic mouse model expressing human wild-type (hWT) or G2019S LRRK2 protein. To further characterize the Thy1.2-LRRK2 transgenic mice, temporal expression profile and localization pattern of human *LRRK2* transgene was determined in brain tissue, and PD-associated neuropathology was investigated in *substantia nigra pars compact* (SNpc).

2.1.1 Generation of Thy1.2-LRRK2 Transgenic Mouse Model

To generate the transgenic mice, the cDNA comprising the 51 exons encoding the human full-length LRRK2 protein, wild-type or G2019S, was subcloned into the murine Thy-1.2 promoter expression cassette (Figure 2.1 A). The murine Thy-1.2 gene belongs to the immunoglobulin-like supergene family, and comprises 4 exons that encode for a glycoprotein expressed in both, the immune and the nervous system (Giguere et al., 1985). This tissue-specific pattern of expression depends on the activation of two different enhancer elements, the thymus and the neural enhancer (Gordon et al., 1987; Vidal et al., 1990). The Thy1.2 promoter cassette lacks the codifying sequence of the murine Thy-1.2 gene (3' end of the second exon, third exon and 5' end of the fourth exon), and the thymus enhancer localized at the third intron, but maintains the neural enhancer element localized at the 3' end of the first intron, driving in the mice neuronal-specific LRRK2 transgene expression (Figure 2.1 A). Final expression constructs were microinjected into C57BL/6 oocytes in order to produce the Thy1.2-LRRK2 transgenic mice.

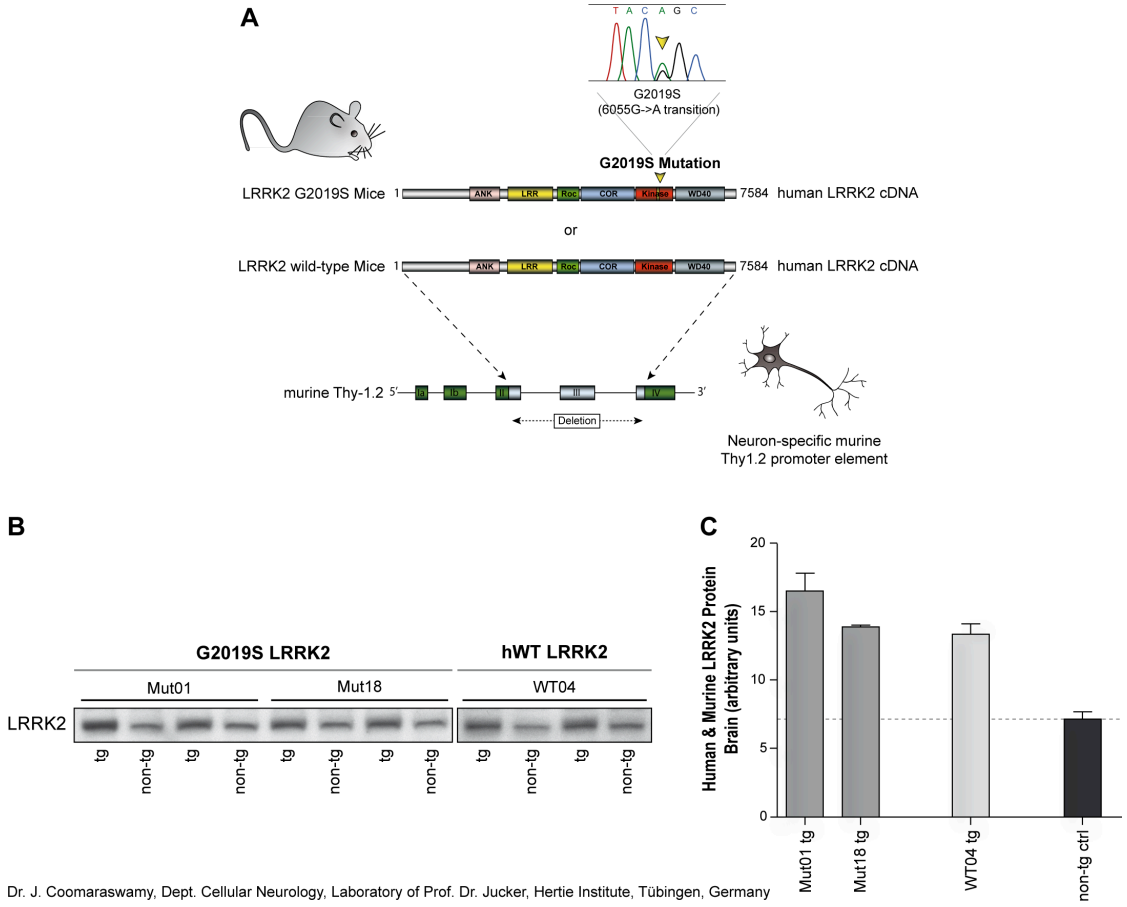

Figure 2.1 Thy1.2-LRRK2 transgenic mouse generation (modified from (Garcia-Miralles, et al. unpublished). **(A)** Human full length wild-type or G2019S mutant LRRK2 cDNA were subcloned into the murine Thy-1.2 promoter element driving neuronal-specific transgene expression. (**B)** Western blot analysis of LRRK2 protein expression in brain lysates from hWT (WT04) and G2019S (Mut01 and Mut18) LRRK2 transgenic mouse and non-transgenic littermate controls. (**C)** Densitometry quantitation revealed two-fold overexpression of human LRRK2 protein levels in LRRK2 transgenic mice (WT04, Mut01 and Mut18 lines) compared to murine LRRK2 protein levels from the non-transgenic controls. (tg, transgenic; non-tg, non-transgenic). **(A, B, C)** Experiments performed by Dr. J. Coomaraswamy, Department of Cellular Neurology, Laboratory of Prof. Dr. Jucker, Hertie Institute for Clinical Brain Research, Tübingen, Germany).

Of all initial transgenic mice obtained, four wild-type LRRK2 founders (WT04, WT23, WT26, WT29), and four G2019S mutant LRRK2 founders (mut01, mut05, mut16, mut18) were identified and bred with C57BL/6 mice to transmit the transgene to the progeny. Three transgenic lines, WT04 (wild-type LRRK2 line), Mut01 and Mut18 (G2019S mutant LRRK2 line) revealed significantly higher transgene expression levels and produced positive offspring, being then selected to further quantify levels of human LRRK2 protein in brain tissue from F2 generation mice at 4 months by immunoblotting (Figure 2.1 B). The MID antibody (Klein et al., 2009) directed against the middle region (amino acids 801-1000) of both human and murine LRRK2 protein was used to detect LRRK2 protein. Densitometry quantitation of total human and murine LRRK2 protein levels in each transgenic line showed a two-fold overexpression of human LRRK2 protein compared to murine Lrrk2 from non-transgenic controls (Figure 2.1 C), suggesting that the Thy1.2-LRRK2 transgenic mouse model expresses LRRK2 protein levels resembling the physiological/endogenous murine Lrrk2 protein levels. (Experiments shown in Figure 2.1 were performed by Dr. J. Coomaraswamy, Department of Cellular Neurology, Laboratory of Prof. Dr. Jucker, Hertie Institute for Clinical Brain Research, Tübingen, Germany).

2.1.2 hLRRK2 mRNA and Protein Analysis in the Brain of Transgenic Mice

To assess temporal expression profile of human LRRK2 mRNA in brain tissue, semi-quantitative RT-PCR was performed at different stages of the development, starting at embryonic day 14 (E14) and following at postnatal days (P) 2, 7, 10, 15, and 21 in hWT (WT04) and G2019S (Mut01 and Mut18) Thy1.2-LRRK2 transgenic lines. Early detection of human LRRK2 mRNA transgene was observed at P2 in all transgenic lines, starting with low expression levels at E14, the earliest time point of the embryonic development analyzed (Figure 2.2. A). An increment of LRRK2 mRNA expression levels was observed at P7 which was sustained over time until the latest time point analyzed, P21 (Figure 2.2. A).

In order to investigate whether human LRRK2 transgene is expressed in areas of the brain important for the pathology of PD, the specific localization pattern of the transgene was analyzed by *in situ* hybridization and immunoblotting. *In situ* hybridization of LRRK2 mRNA was performed using two different human specific LRRK2 oligonucleotides probe sets directed against exon 30-31 (LRRK2 Roc domain), and exon 35-36 (LRRK2 COR domain) (performed by Dr. D. Galter, Department of Neuroscience, Karolinska Institutet, Stockholm, Sweden). Comparable expression levels of human LRRK2 mRNA were observed in hippocampus and cortex of 11 month old hWT (WT04) and G2019S (Mut01 and Mut18) LRRK2 transgenic mice, but no signal was detected in non-transgenic (non-tg) littermate controls. Moreover, a mouse α-synuclein oligonucleotide probe set was used as positive control (Figure 2.2.B).

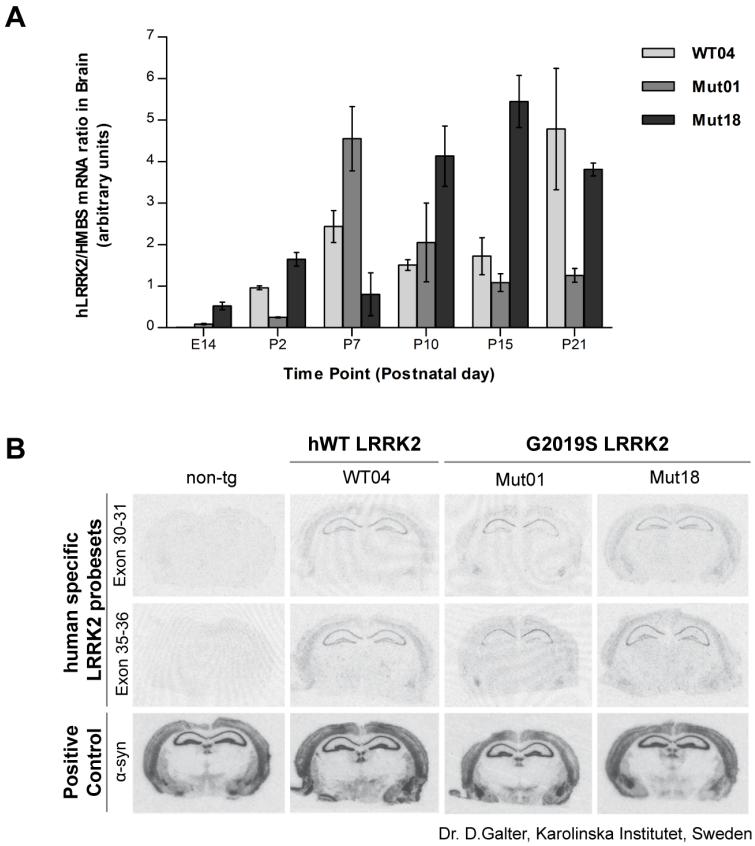

Figure 2.2 hLRRK2 mRNA analysis in the brain of Thy1.2-LRRK2 transgenic mice. (A) Semi-quantitative RT-PCR of human LRRK2 mRNA expression in whole brain at different time points of the development showed early detection of the transgene at postnatal day 2 (P2) in all transgenic lines. Data represents mean ± SEM; n=3-5 per group. (**B)** In-situ hybridization analysis (Dr. D. Galter, Dept. of Neuroscience, Karolinska Institutet, Stockholm, Sweden) with two human specific LRRK2 probesets (Exon 30-31 and Exon 35-36) at 11 month old mice. Comparable expression levels of human LRRK2 transgene could be observed in hippocampus and cortex from hWT (WT04) and G2019S (Mut01 and Mut18) LRRK2 transgenic mice. Mouse α-synuclein oligonucleotide probe set was used as positive control.

In addition, human LRRK2 protein expression pattern was assessed in protein lysates from different regions of the brain obtained from 10 months old hWT and G2019S LRRK2 transgenic mice by immunoblotting with a human LRRK2 specific antibody (Novus-267 or MJFF5). Consistent with mRNA results, human LRRK2 protein was detected in hippocampus (Hip) and cortex (Ctx) (Figure 2.3 B), and in other regions of the brain including brainstem (BS) and midbrain (MB) (Figure 2.3 A) in both hWT (WT04) and G2019S (Mut01 and Mut18) Thy1.2-LRRK2 transgenic mice but not in non-tg littermate controls (Figure 2.3.A). Expression of human LRRK2 protein was not detectable in striatum from *LRRK2* transgenic mice compared to non-tg littermate controls (Figure 2.3 A). Thus, human LRRK2 protein was detectable in different regions of the brain including, hippocampus, cortex, brainstem, and midbrain by *in situ* hybridization and immunoblotting, corresponding to anatomic regions important for the neuropathology of PD (Biskup et al., 2006; Biskup et al., 2007; Westerlund et al., 2008).

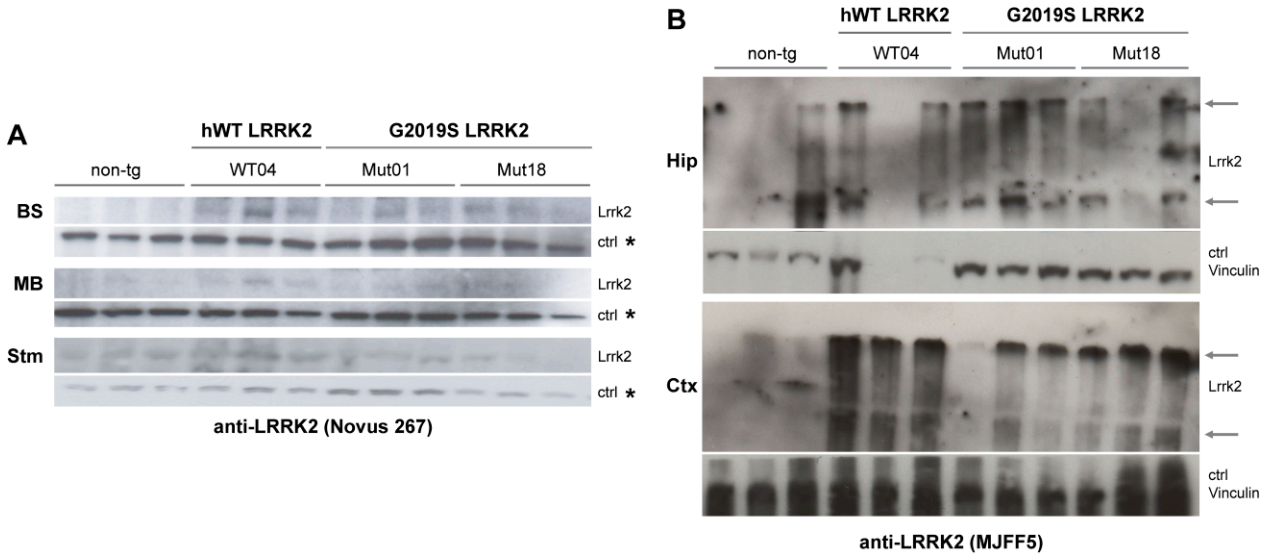

Figure 2.3 LRRK2 protein analysis in the brain of Thy1.2-LRRK2 transgenic mice. (A-B) Western blot analysis of LRRK2 protein expression in different brain regions at 10 months. (A) LRRK2 protein was detected in brainstem (BS) and midbrain (MB) with a human-specific LRRK2 antibody (NB300-267) but not in striatum (Stm).(*) A non-specific band was used as loading control (ctrl). (B) LRRK2 protein was detected in hippocampus (Hip) and cortex (Ctx) with a human-specific LRRK2 antibody (MJFF5). Arrows show LRRK2 protein expression. Anti-vinculin antibody was used as loading control. For each line n=3 mice, except in hippocampus n=2 mice in WT04 line.

Based on the results obtained by immunoblotting analysis (Figure 2.1 B) and by *In situ* hybridization (Figure 2.2 B), the Mut18 line from G2019S Thy1.2-LRRK2 transgenic mice presented the most similar levels of human LRRK2 protein (Figure 2.1 B, C) and mRNA expression in the brain as the WT04 line from hWT Thy1.2-LRRK2 transgenic mouse (Figure 2.2 B). For this reason, the Mut18 line was selected to further characterize the novel Thy1.2-LRRK2 transgenic mouse model, and to perform future experiments.

2.1.3 Analysis of Parkinson's Disease Associated Loss of Dopaminergic Neurons in the Thy1.2-LRRK2 Transgenic Mice

To determine whether overexpression of human LRRK2 protein in the LRRK2 transgenic mice causes PD-associated neuropathology, analysis of dopaminergic (DA) neurons in substantia nigra pars compacta (SNpc) was performed. Coronal brain sections from hWT (WT04) and G2019S (Mut18) Thy1.2-LRRK2 transgenic mice at 12-13 months and age-matched non-tg controls were stained with tyrosine hydroxylase (TH), a dopaminergic neuronal marker, using an immunoperoxidase stain system, and Nissl counterstain as nuclear neuronal marker (Figure 2.4 A). No differences were observed in estimated total number of TH-positive and Nissl-positive neurons in Thy1.2-LRRK2 transgenic mice compared to non-tg age matched controls (*n.s p>0.05*, one-way ANOVA, Tukey's *post hoc* analysis) (Figure 2.4 B). These results suggest that overexpression of human LRRK2 protein in this particular transgenic mouse model is not sufficient to cause either loss and/or neurodegeneration of DA neurons, nor loss of nigral neurons in SNpc.

The fact that no PD-associated neuropathology was observed in the Thy1.2-LRRK2 transgenic mouse model was expected, considering the low overexpression of the human LRRK2 transgene (only two-fold higher than the murine Lrrk2 protein) observed in the Thy1.2-LRRK2 transgenic mice. Consistent with these findings, other LRRK2 transgenic mouse models overexpressing G2019S, R1441C, or I2020T LRRK2 protein at low or higher expression levels also fail to reveal loss of DA neurons in SNpc in aged mice (Li et al., 2010; Maekawa et al., 2012; Melrose et al., 2010; Melrose et al., 2007; Ramonet et al., 2011). This

suggests that overexpression of LRRK2 protein and aging of the mice is not sufficient to cause neurodegeneration of DA neurons in SNpc. Another possible explanation for the lack of PD-associated neuropathology could be the absence of human LRRK2 mRNA or protein expression in SNpc in the Thy1.2-LRRK2 transgenic mice.

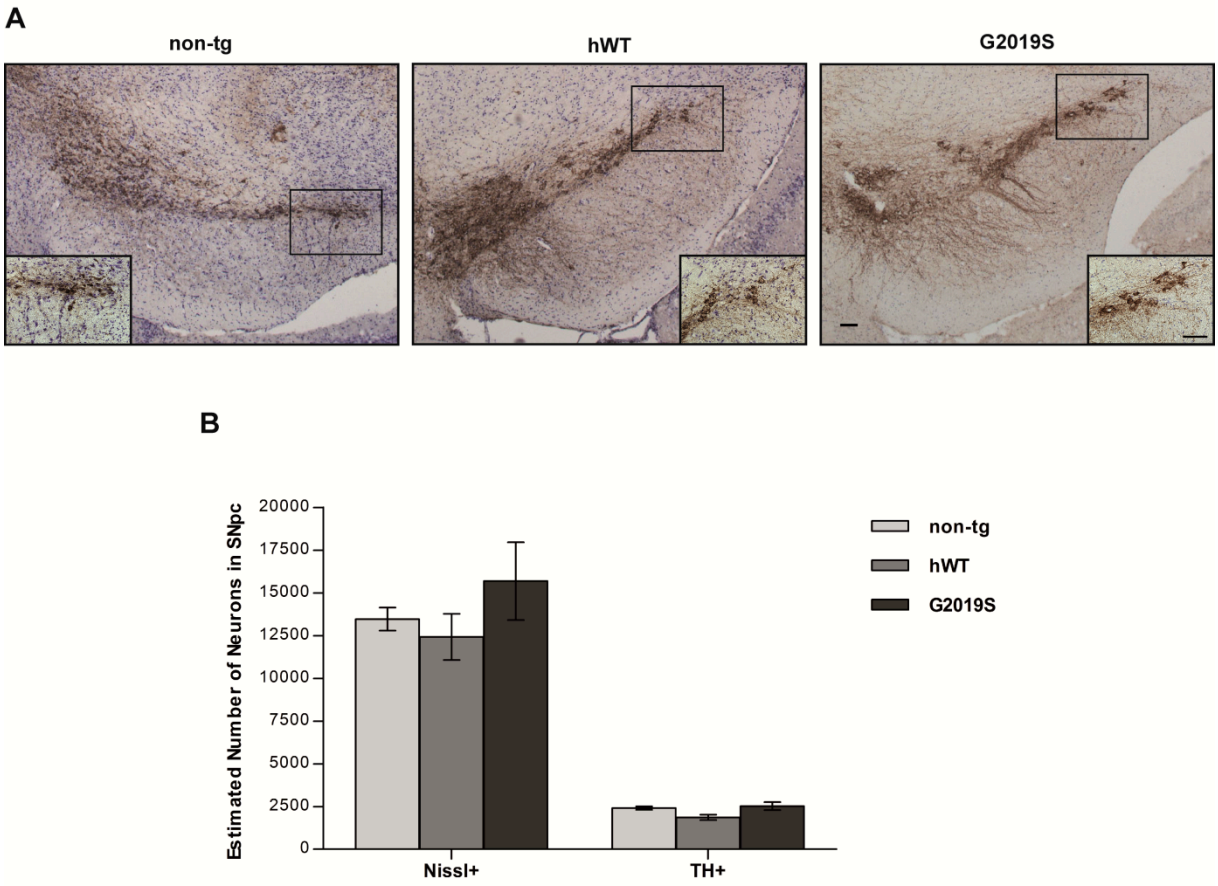

Figure 2.4 PD associated neuropathology analysis in Thy1.2-LRRK2 transgenic mice. (A) Representative coronal section of the SNpc following tyrosine hydroxylase (TH) immunoperoxidase stain and Nissl counterstain from non-tg, hWT and G2019S transgenic mice at 12-13 month. (Scale bars: 100µm). (**B)** Stereologic counts of TH+ and Nissl+ neurons in SNpc from non-tg, hWT and G2019S LRRK2 transgenic mice at 12-13 month. No significant differences could be observed between groups. Data represent mean ± SEM; n= 2 for hWT and G2019S, n=3 for non-tg. *n.s p>0.05*, one-way ANOVA, Tukey's *post hoc* analysis.

2.2 Role of LRRK2 in the Regulation of Cytoskeleton Dynamics

In vitro and *in vivo* studies have implicated LRRK2 in a variety of cellular functions and molecular pathways such as actin cytoskeleton dynamics and neurite outgrowth, suggesting a role of LRRK2 in its regulation (Kett and Dauer, 2012; Kumar and Cookson, 2011; Parisiadou and Cai, 2010; Tsika and Moore, 2012; Yue and Lachenmayer, 2011). To bring further insights into this potential function of LRRK2, the implications of physiological expression levels of human LRRK2 protein in the regulation of actin cytoskeleton arrangements and/or dynamics were explored in two different cellular models. Primary hippocampal cultures obtained from the Thy1.2-LRRK2 transgenic mice were used to study neurite outgrowth, and primary human skin fibroblasts derived from LRRK2-PD patients were used to study cell adhesion and cell locomotion dynamics.

2.2.1 Role of LRRK2 Regulating Actin Cytoskeleton Dynamics in Neurite Outgrowth

Recent studies have involved LRRK2 in the regulation of neurite outgrowth and showed that overexpression of G2019S LRRK2 protein in primary neuronal cultures reduces neurite outgrowth and branching, whereas partial or total deletion of LRRK2 protein produces the opposite effect, an increment in neurite outgrowth and branching complexity (Dachsel et al., 2010; MacLeod et al., 2006; Winner et al., 2011, Ramonet, 2011 #52). Interestingly, no effect has been observed when human wild-type LRRK2 protein is overexpressed, suggesting a potential role of LRRK2 kinase activity in the regulation of neurite outgrowth (Dachsel et al., 2010; MacLeod et al., 2006; Ramonet et al., 2011; Winner et al., 2011). Moreover, it is important to mention that most of these studies have been performed in overexpressed LRRK2 systems, but none of these studies published so far has focused on the implication of physiological expression levels of human LRRK2 protein in the regulation of neurite outgrowth. To examine whether the Thy1.2-LRRK2 transgenic mouse model can recapitulate the neurite outgrowth and branching phenotype as observed in other studies (Dachsel et al., 2010; MacLeod et al., 2006; Ramonet et al., 2011; Winner et al., 2011), primary hippocampal

cultures dissociated from hWT (WT04) and G2019S (Mut18) Thy1-2-LRRK2 transgenic mice, and non-tg littermate controls were cultured and analyzed for different parameters associated to neurite outgrowth and branching complexity. In addition, to better understand the role of LRRK2 kinase domain in the regulation of neurite outgrowth, hippocampal neuronal cultures were treated with the specific LRRK2 kinase inhibitor LRRK2-IN-1 (Deng et al., 2011) in order to investigate whether the potential role of LRRK2 regulating neurite outgrowth is kinase activity dependent or not.

Primary hippocampal neurons were selected to perform these experiments due to higher expression levels of human LRRK2 transgene in this particular region compared to other brain regions as observed by *in situ* hybridization (Figure 2.2 B). Therefore, hippocampal neurons dissociated at P0 from Thy1-2-LRRK2 transgenic mice hippocampus, both hWT (WT04) and G2019S (Mut18), and non-tg littermate controls were cultured for 3, 7, and 14 days in vitro (DIV) with the presence of DMSO-control (vehicle) or 0.1µM LRRK2-IN-1 (Figure 2.5) (Deng et al., 2011).

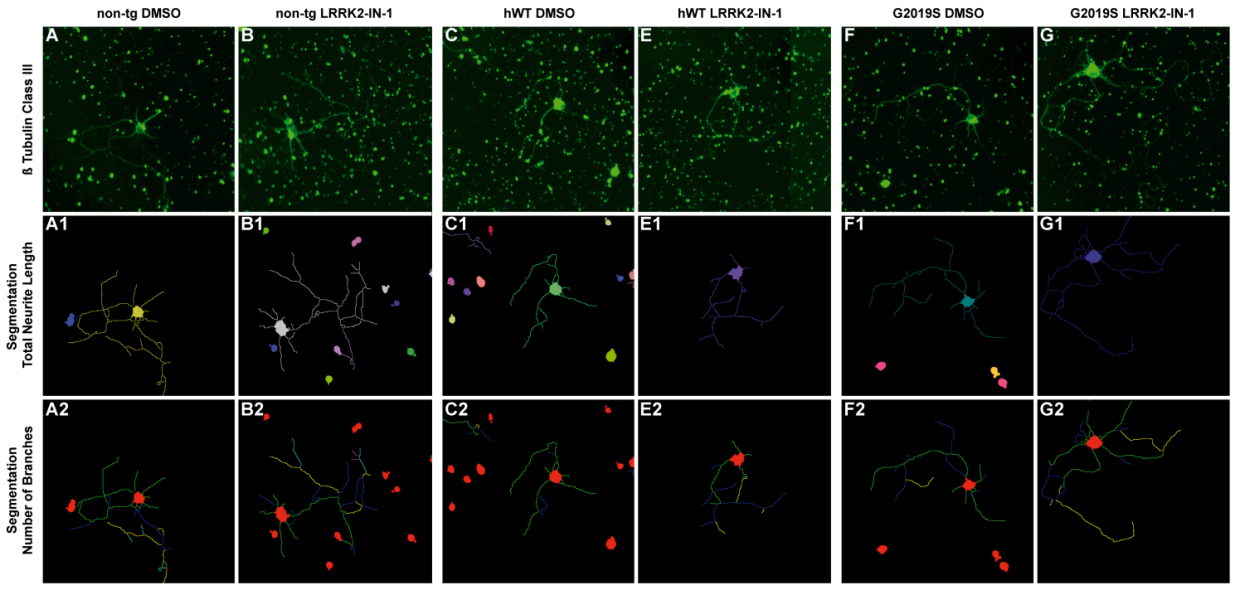

Figure 2.5 Morphology of primary hippocampal neurons derived from Thy1.2-LRRK2 transgenic mice. (A-G) ß-Tubulin Class III staining in non-tg, hWT and G2019S LRRK2 hippocampal neurons at DIV7 treated with DMSO or 0.1µM LRRK2-IN-1 obtained with the BD Pathway 855 high content Bioimager. (A1-G1) Segmentation images obtained from Attovision Software showing total neurite length and number of branches (A2-G2) from non-tg, hWT and G2019S LRRK2 hippocampal neurons with DMSO or 0.1µM LRRK2-IN-1 corresponding to ß-tubulin III staining images (A-G).

Interestingly, at DIV7 hippocampal neurons expressing hWT LRRK2 protein (n=1697, 5 independent experiments) showed a slight but significant decrease in total neurite length and number of branches compared to non-tg littermate controls (n=1339, 5 independent experiments) in DMSO condition (*p<0.05, independent *t*-test) (Figure 2.6 B, E)(Figure 2.7 A, B). However, it is worth mentioning that at DIV3 no significant differences in total neurite length and number of branches were observed, whereas at DIV14 a tendency towards an increment in total neurite length and number of branches was observed, although it was not significant (Figure 2.6 A, C, D, F))(Figure 2.7 A, B). In contrast, at DIV7 hippocampal neurons expressing G2019S LRRK2 protein (n=1526, 4 independent experiments) did not present differences in total neurite length and number of branches compared to non-tg littermate controls (n=1268, 4 independent experiments; *n.s p>0.05*, independent *t*-test) in DMSO condition (Figure 2.6 B, E) (Figure 2.7 A, B). Also, no differences in total neurite length and number of branches were observed at DIV3 and 14 (Figure 2.6 A, C, D, F) (Figure 2.7 A, B). Taken all together, these results suggest that primary hippocampal neurons expressing G2019S LRRK2 protein obtained from the Thy1.2-LRRK2 transgenic mice did not recapitulate the reduced neurite outgrowth and branching phenotype observed by other groups using different cellular and mouse models (Dachsel et al., 2010; MacLeod et al., 2006; Ramonet et al., 2011; Winner et al., 2011). This result is not totally unexpected taking into account that human LRRK2 protein levels exceed endogenous murine LRRK2 protein by two-fold in the Thy1.2-LRRK2 transgenic mouse model (Figure 2.1 B, C) which could explain the lack of phenotype. These observations are in agreement with a recently published study which suggested that endogenous expression levels of LRRK2 protein did not compromise neurite outgrowth and branching complexity in experiments carried out in a G2019S mutant LRRK2 knock-in mouse model (Dachsel et al., 2010). In addition, the slight reduction of neurite outgrowth and branching complexity observed in hWT LRRK2 hippocampal cultures suggests that LRRK2 is indeed involved in the regulation of neurite outgrowth.

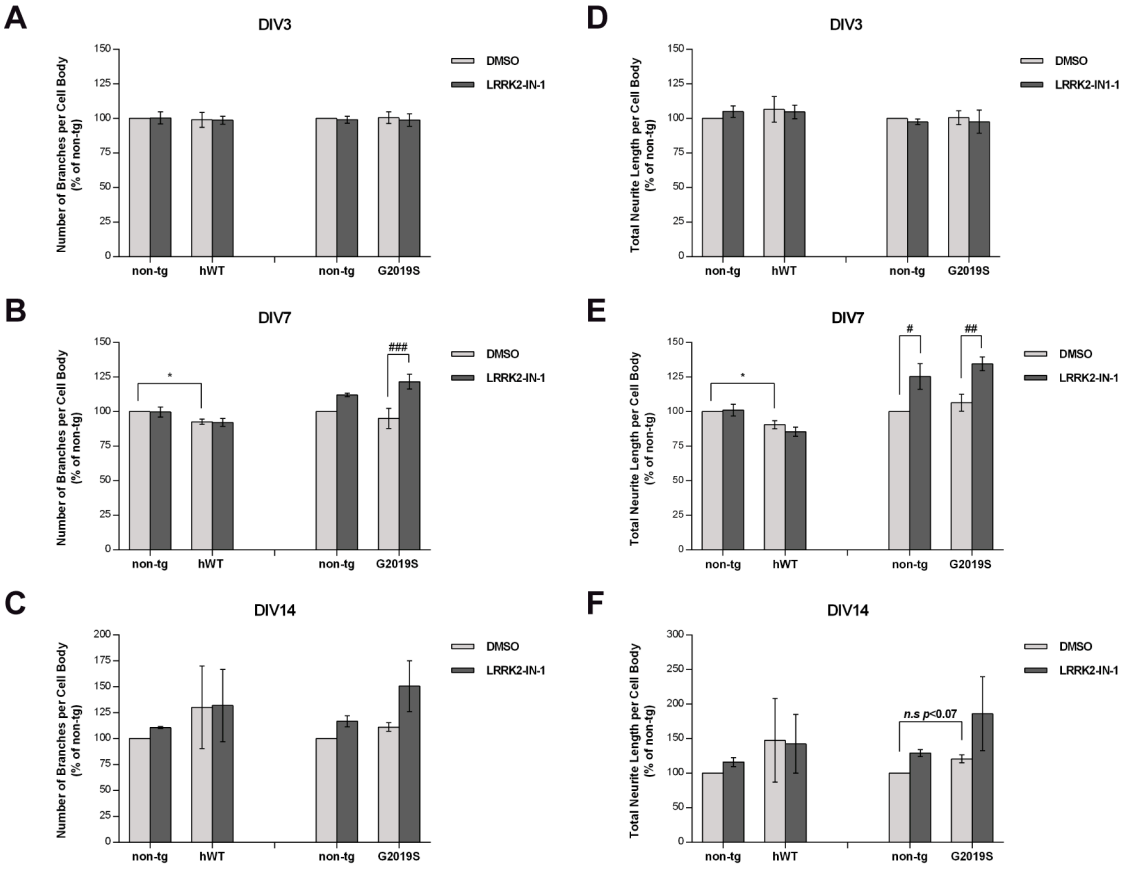

Figure 2.6 Neurite outgrowth analysis in primary hippocampal neurons from LRRK2 transgenic mice. (A-C) Number of branches **(D-F),** and total neurite length in primary hippocampal neurons from Thy1.2-LRRK2 transgenic mice at DIV3, 7, and 14 after DMSO or 0.1μM LRRK2-IN-1 treatment. hWT LRRK2 neurons displayed a slight reduction in number of branches (B), and total neurite length (E) at DIV7 compared to non-tg neurons with DMSO treatment, but no differences were observed at DIV3 and 14 (A, C, D, F), and after LRRK2-IN-1 treatment (B, E). No differences in number of branches (B), and total neurite length (E) were observed in G2019S LRRK2 neurons with DMSO treatment at DIV3, 7, and 14 compared to non-tg littermate neurons but an increased neurite outgrowth and branching complexity phenotype was observed with LRRK2-IN-1 treatment at DIV7 and DIV14 (B-F). Non-tg littermate neurons displayed only increased total neurite length with LRRK2-IN-1 treatment at DIV7 (F). Data represent mean ± SEM; Number of neurons analyzed: non-tg DMSO=1339, non-tg LRRK2-IN-1=1609, hWT DMSO=1697, hWT LRRK2-IN-1=1542, n=4 independent experiments; non-tg DMSO=1268, non-tg LRRK2-IN-1=1522, G2019S DMSO=1526, G2019S LRRK2-IN-1=1844, n=5 independent experiments; *$*p<0.05$, $***p<0.001$* independent *t*-test (effect of genotype in each treatment condition); *$^{\#}p<0.05$, $^{\#\#}p<0.01$, $^{\#\#\#}p<0.01$* two-way ANOVA, Tukey's *post hoc* analysis (effect between treatment conditions in each genotype).

In order to understand whether the kinase activity of LRRK2 protein plays a role in the regulation of neurite outgrowth, primary hippocampal neurons were cultured with the presence of the specific LRRK2 kinase inhibitor, LRRK2-IN-1. In this condition, a significant increment in total neurite length and number of branches could be observed in murine WT LRRK2 (non-tg) neurons (n=1522, 4 independent experiments) or G2019S LRRK2 neurons (n=1844, 4 independent experiments) treated with 0.1μM LRRK2-IN-1 at DIV 7 compared to neurons treated with DMSO-control (Figure 2.6 B, E) (Figure 2.7 C,D) ($^{\#}p<0.05$, $^{\#\#}p<0.01$, $^{\#\#\#}p<0.01$ two-way ANOVA, Tukey's *post-hoc* analysis). In contrast, the presence of LRRK2-IN-1 in neurons overexpressing hWT LRRK2 protein (n=1542, 5 independent experiments) had no effect in total neurite length and number of branches at DIV7 compared to neurons cultured with the presence of DMSO-control (Figure 2.6 B, E) (Figure 2.7 C,D) (*n.s p>0.05*, two-way ANOVA, Tukey's *post-hoc* analysis). No significant differences could be observed at DIV3 in hWT and G2019S LRRK2 neurons treated with 0.1μM LRRK2-IN-1compared to DMSO-control treated neurons (*n.s p>0.05*, two-way ANOVA, Tukey's *post-hoc* analysis), suggesting a lack of effect of the specific LRRK2 kinase inhibitor at this time point (Figure 2.6 A, D) (Figure 2.7 C, D). In contrast, at DIV14, hWT and G2019S LRRK2 neurons displayed a trend towards an increment in total neurite length and number of branches with the presence of the LRRK2-IN-1 (Figure 2.6 C, F) (Figure 2.7 C,D). Taken all together, these data points towards a general increment in total neurite length and branching complexity at DIV7 and DIV14 in primary hippocampal neurons treated with LRRK2-IN-1 in comparison to neurons treated with DMSO-control (Figure 2.7 A-D). Consistent with these findings, other studies reported the same increased neurite outgrowth phenotype when the LRRK2 kinase activity was abolished by knocking-down/out the LRRK2 protein or overexpressing the K1906M kinase-dead LRRK2 protein (Dachsel et al., 2010; MacLeod et al., 2006; Plowey et al., 2008). These results suggest that specific inhibition of LRRK2 kinase activity by LRRK2-IN-1 affects the regulation of neurite outgrowth and branching complexity, especially in neurons expressing G2019S LRRK2 protein, indicating a potential function of human LRRK2 protein regulating actin cytoskeleton dynamics in a kinase-dependent manner.

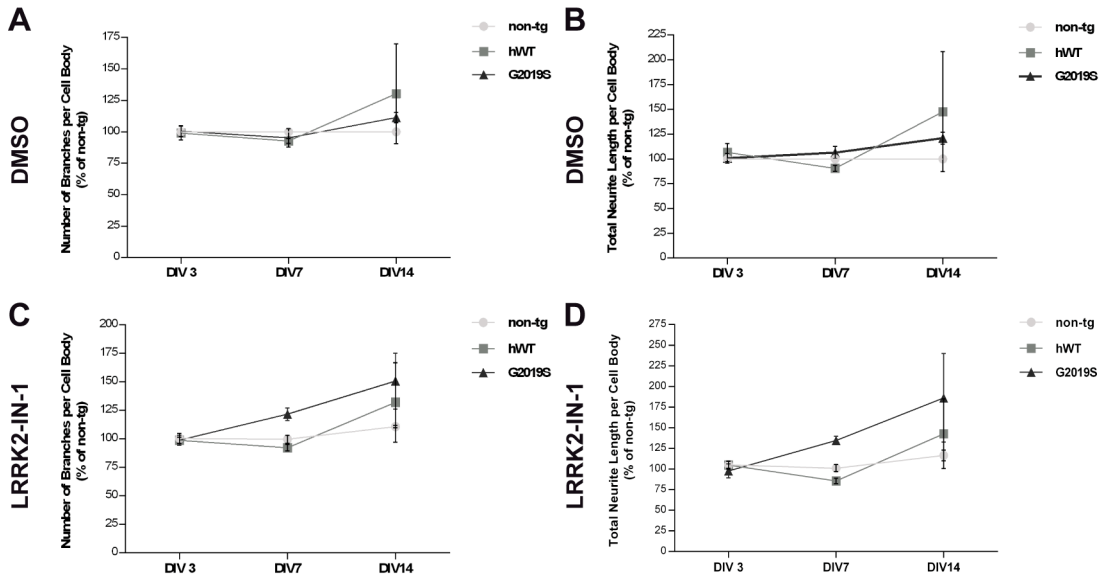

Figure 2.7 Over time neurite outgrowth analysis in primary hippocampal neurons from LRRK2 transgenic mice. (A-C) Number of branches and **(B-D)** total neurite length analysis in primary hippocampal neurons from Thy1.2-LRRK2 transgenic mice at DIV3, 7 and 14 after DMSO (vehicle) or 0.1μM LRRK2-IN-1 treatment over time. Data represent mean ± SEM; Number of neurons analyzed: non-tg DMSO=1339, non-tg LRRK2-IN-1=1609, hWT DMSO=1697, hWT LRRK2-IN-1=1542, n=4 independent experiments; non-tg DMSO=1268, non-tg LRRK2-IN-1=1522, G2019S DMSO=1526, G2019S LRRK2-IN-1=1844, n=5 independent experiments; *$*p<0.05$, ***$p<0.001$* independent *t*-test (effect of genotype in each treatment condition); $^{\#}p<0.05$, $^{\#\#}p<0.01$, $^{\#\#\#}p<0.01$ two-way ANOVA, Tukey's *post hoc* analysis (effect between treatment conditions in each genotype).

In conclusion, the results obtained from the Thy1.2-LRRK2 transgenic mouse model show that hippocampal neurons expressing hWT LRRK2 protein at physiological levels display a reduction in total neurite length and number of branches whereas the G2019S LRRK2 neurons in DMSO-control conditions do not display any differences (Figure 2.6 D, I). These results bring further insight into the role of human LRRK2 protein expressed at physiological levels regulating neurite outgrowth and branching complexity. However, other groups reported lack of neurite outgrowth and branching complexity in hWT overexpressed neuronal cultures and reduction in neurite outgrowth and branching complexity in G2019S overexpressed neuronal cultures (Chan et al., 2011; Dachsel et al., 2010; MacLeod et al., 2006; Plowey et al., 2008; Ramonet et al., 2011; Sanchez-Danes et al., 2012). These

differences reported between models could be explained by the high levels of overexpressed LRRK2 protein observed in other cellular and mouse models (Dachsel et al., 2010; MacLeod et al., 2006; Parisiadou et al., 2009; Plowey et al., 2008) compared to the low expression levels observed in the Thy1.2-LRRK2 transgenic mice. Also, differences in expression conditions and neuronal systems used, i.e. differentiated SH-SY5Y cells versus primary neuronal cultures (cortical, hippocampal or brainstem), could influence the results observed. Treatment of hWT and G2019S LRRK2 expressing hippocampal neurons with the specific kinase inhibitor LRRK2-IN-1, resulted in a general increment in number of branches and total neurite length at DIV7 and DIV14 (Figure 2.7 C, D), especially in G2019S LRRK2 neurons, as observed in other reported studies after abolishing the LRRK2 kinase activity (Chan et al., 2011; Dachsel et al., 2010; MacLeod et al., 2006; Plowey et al., 2008; Ramonet et al., 2011; Sanchez-Danes et al., 2012), suggesting that neurite outgrowth and branching complexity regulation by LRRK2 is kinase activity dependent.

2.2.2 Role of LRRK2 Regulating Actin Cytoskeleton Dynamics in Cell Adhesion and Cell Locomotion in Primary Human Skin Fibroblasts.

It has been shown that LRRK2 protein is involved in neurite outgrowth, has a potential role in the regulation of cytoskeleton arrangements and/or dynamics, and interacts with members of the Rho family small GTPases (Chan et al., 2011; Haebig et al., 2010). Also, the fact that Rho family small GTPases are the main regulators of actin cytoskeleton (Lambrechts et al., 2004; Mackay and Hall, 1998) prompted to hypothesize a potential function of LRRK2 in the regulation of cell adhesion and locomotion dynamics, two cellular processes that require actin cytoskeleton arrangements and/or dynamics in order to take place (Lambrechts et al., 2004). To address this question, primary human skin fibroblasts derived from LRRK2-PD patients and healthy-control subjects were used since they express endogenous levels of LRRK2 protein. In total, seven fibroblast lines bearing different pathogenic-LRRK2 PD mutations located either in the kinase or Roc GTPase domain of the LRRK2 protein (G2019S, I2020T, N1437S (Haebig et al., 2010) and R1441C) (Table 3, Figure 2.8), and 4 lines of age-matched healthy-control fibroblasts (Table 3) were used.

	Identification Number	Sex	Age at biopsy	Age onset	Mutation	Protein Domain
Healthy Subjects	ID16423	F	77	-	-	-
	ID16424	M	62	-	-	-
	ID16425	F	80	-	-	-
	ID16392	M	61	-	-	-
LRRK2-PD Patients	DNA13287	M	58	55	G2019S	Kinase Domain
	DNA14694	F	62	53	G2019S	Kinase Domain
	DNA12098	F	77	70	G2019S	Kinase Domain
	DNA8743	F	63	57	I2020T	Kinase Domain
	DNA9236	F	61	39	R1441C	GTPase Domain
	DNA10688	M	42	38	N1437S	GTPase Domain
	DNA10689	M	68	48	N1437S	GTPase Domain

(F, female; M, male)

Table 3 List of primary human skin fibroblast lines

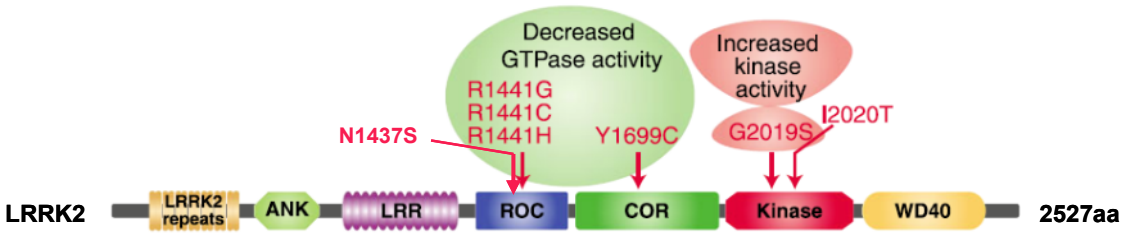

Figures 2.8 Location of the most common LRRK2 pathogenic mutations in the LRRK2 protein (modified from (Tsika and Moore, 2012)). Primary human skin fibroblast lines derived from LRRK2-PD patients expressing the G2019S and I2020T mutation in the kinase domain and N1437S and R1441C in the Roc GTPase domain were used to study the role of LRRK2 in the regulations of actin cytoskeleton arrangements and/or dynamics.

Fibroblasts carrying either the G2019S or the I2020T pathogenic mutation in the kinase domain were selected for this study since activated Rho family of small GTPases can interact with and activate different downstream effectors and proteins in order to stimulate a wide range of cellular processes, including actin cytoskeleton dynamics (Heasman and Ridley, 2008; Mackay and Hall, 1998). It has been already published that the Rho family small GTPases interact with LRRK2 (Chan et al., 2011; Haebig et al., 2010) and could most likely activate the LRRK2 kinase domain which in turn may activate downstream effectors involved in the regulation of actin cytoskeleton. Also, fibroblasts bearing either the N1437S or the R1441C pathogenic mutation in the Roc GTPase domain were included in this study. It has been reported that the Roc GTPase domain shares sequence homology with all 5 subfamilies of the Ras-related small GTPases superfamily (Guo et al., 2007), which includes the Rho small GTPase subfamily, acting most probably as a GTPase. (Guo et al., 2007; Ito et al., 2007; Lewis et al., 2007; Li et al., 2007; Smith et al., 2006). In addition, a possible intrinsic activation of the LRRK2 kinase activity by the LRRK2 GTPase domain has been postulated (Anand and Braithwaite, 2009). Taking these data altogether, it is then likely that the Roc GTPase domain, via activation of the LRRK2 kinase activity, could either directly or indirectly trigger the activation of downstream effectors involved in the regulation of cytoskeleton dynamics.

Cell adhesion and cell locomotion assays were used as the final outcome to test whether LRRK2 is involved in actin cytoskeleton arrangements and/or dynamics. Experiments using fibroblasts from healthy-control subjects (WT LRRK2) and LRRK2-PD patients carrying mutations in the kinase or GTPase domain were performed to understand whether endogenous WT LRRK2 protein or the different pathogenic LRRK2 variants play a role in this regulation. We also used the specific LRRK2 inhibitor, LRRK2-IN-1, in order to inhibit the kinase activity of the LRRK2 protein and understand whether the regulation of actin cytoskeleton arrangements and/or dynamics by LRRK2 is kinase activity dependent or not.

First of all, expression of endogenous LRRK2 protein in primary skin fibroblasts was assessed in basal condition and after treatment with the specific LRRK2 kinase inhibitor LRRK2-IN-1 by immunoblotting analysis prior to performing cell adhesion and cell locomotion assays. A representative fibroblast line of healthy-control subjects (WT LRRK2) and one fibroblast line from each pathogenic-LRRK2 PD mutation, G2019S and I2020T in the kinase domain, and N1437S and R1441C in the GTPase domain were used for this specific experiment. Immunoblotting results with the anti-LRRK2 antibody (MJFF2) showed a ~280 kDa band corresponding to the molecular weight of the LRRK2 protein demonstrating expression of endogenous LRRK2 protein in all fibroblast lines analyzed in basal (DMSO-control) and LRRK2-IN-1 treatment condition (Figure 2.9 A, B).

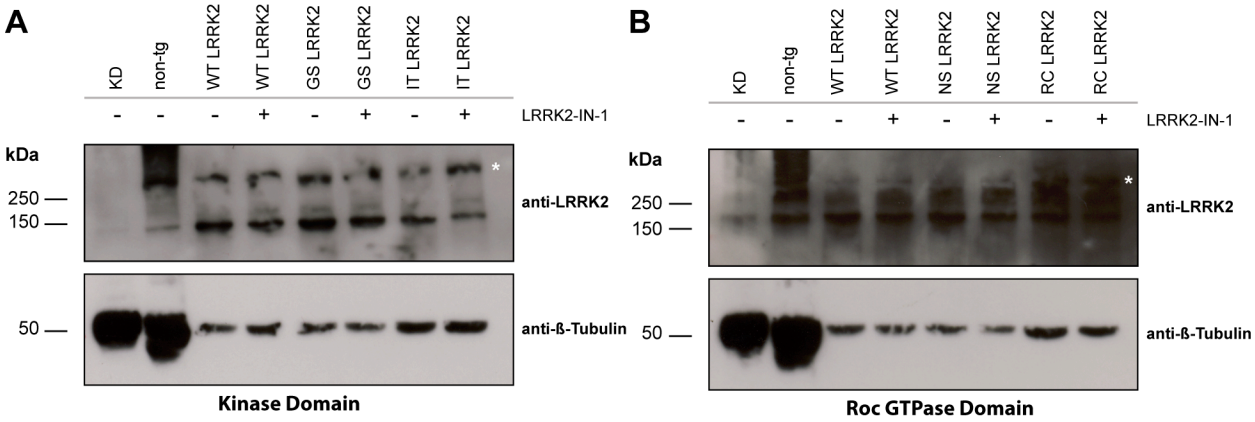

Figure 2.9 LRRK2 protein expression in primary human skin fibroblasts derived from WT LRRK2 (healthy-control subjects) or LRRK2-PD patients. (A-B) Western blot analysis of LRRK2 protein expression in primary human skin fibroblasts derived from healthy-control subjects (WT LRRK2) and LRRK2 PD-patients with mutations in the kinase domain (A) and ROC GTPase domain (B) after treatment with DMSO (vehicle) or 0.1μM of LRRK2 IN-1 inhibitor with the anti-LRRK2 antibody (MJFF2). Brain lysate from LRRK2 knock-down mouse (KD) and brain cortex lysates from non-tg mouse were used as negative and positive control, respectively. One fibroblast line was used from healthy-subjects (HS, ID16425), G2019S LRRK2 (GS, DNA13287), I2020T LRRK2 (IT, DNA8743), N1437S LRRK2 (NS, DNA10688) and R1441C LRRK2 (RC, DNA9236) (Table 3). (* LRRK2 protein).

To study cellular adhesion at basal conditions, primary skin fibroblasts at the same passage were seeded and then fixed at different time points (10min, 30min, 1h, 2h or 3h). No significant differences in cellular adhesion were observed in fibroblasts derived from WT LRRK2 (healthy-control) compared to fibroblasts carrying mutations in the LRRK2 kinase domain (*n.s p>0.05,* two-way ANOVA with Repeated Measures with Tukey's *post hoc* analysis) (Figure 2.10 A) or LRRK2 GTPase domain in the different time points analyzed (*n.s p>0.05,* two-way ANOVA with Repeated Measures with Tukey's *post hoc* analysis) (Figure 2.10 B). These results suggest that pathogenic-LRRK2 mutations in both domains, kinase and GTPase, do not alter the regulation of actin cytoskeleton arrangements and/or dynamics.

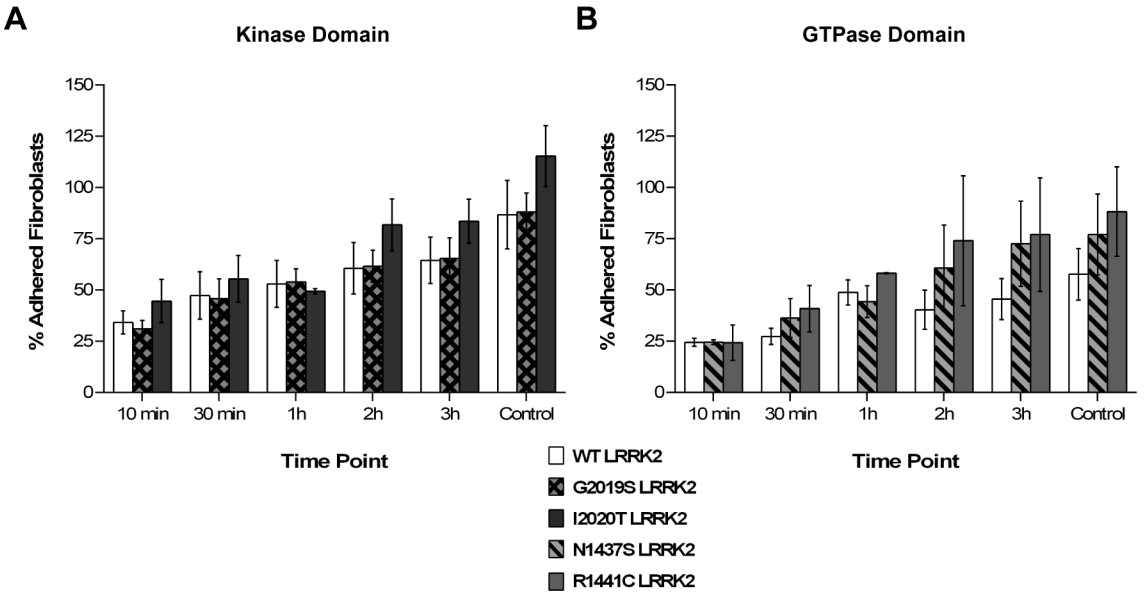

Figure 2.10 Cell adhesion assay in primary human skin fibroblasts from WT LRRK2 (healthy-control subjects) and LRRK2 PD patients over time. (A-B) Percentage of adhered fibroblasst with mutations in the LRRK2 kinase domain (A) and LRRK2 ROC GTPase domain (B) different times points. No significant differences in adhesion capacity were observed between lines. Data represent mean ± SEM; n=4 independent experiments (A) and n=3 independent experiments (B); WT LRRK2 (Healthy-control Subjects) = 4 fibroblast lines; G2019S LRRK2 = 3 fibroblast lines; I2020T LRRK2 = 1 fibroblast line; N1437S-LRRK2 = 2 fibroblast lines; R1441C-LRRK2 = 1 fibroblast line. *n.s* two-way ANOVA with Repeated Measures with Tukey's *post hoc* analysis.

Nevertheless, the fact that WT LRRK2 and different pathogenic-LRRK2 PD mutations are not involved in the regulation of actin cytoskeleton dynamics in cellular adhesion, does not invalidate the possibility that human LRRK2 protein could still play a role in this regulation through its kinase activity. To address this question, further cellular adhesion assays were performed in primary human skin fibroblasts treated with 0 (DMSO-control), 0.1 or 1μM of the specific LRRK2 kinase inhibitor, LRRK2-IN-1, for 30 min and 2 hours. Fibroblasts carrying the I2020T LRRK2 kinase mutation, but not other mutants, treated for 30 min with 1μM of LRRK1-IN-1 exhibited a significant trend towards an enhanced percentage of cell adhesion properties compared to I2020T LRRK2 fibroblasts treated with 0μM LRRK2-IN-1, WT LRRK2 treated with 0 or 1μM LRRK2-IN-1, and G2019S LRRK2 fibroblasts treated with 1μM LRRK2-IN-1. However, differences were not sustained after 2 hours (*$p<0.05$*, *$p<0.01$* two-way

ANOVA with Tukey's *post hoc* analysis) (Figure 2.11 A). No significant differences in cell adhesion were observed in WT LRRK2 (healthy-control) fibroblasts and G2019S-LRRK2 fibroblast after treatment with the LRRK2-IN-1 inhibitor for 30 min or 2h compared to non-treated conditions (*n.s* two-way ANOVA with Tukey's *post hoc* analysis). However, decreased cell adhesion in WT LRRK2 (healthy-control subjects) and G2019S-LRRK2 fibroblasts can be observed after treatment with 1μM LRRK2-IN-1 compared to 0μM treatment (DMSO-control) at 30 min, suggesting at least a weak inhibitory effect. Fibroblasts carrying the N1437S or the R1441C LRRK2 mutation in the ROC GTPase domain and treated with the LRRK2-IN-1 for 30 min or 2 hours did not exhibit any significant alterations in cellular adhesion properties compared to non-treated conditions (Figure 2.11 B).

It is intriguing to observe that inhibition of the LRRK2 kinase activity only in I2020T LRRK2 fibroblasts has an effect in cellular adhesion properties but a negligible or very weak effect was observed in WT LRRK2 (healthy-control subjects) or G2019S LRRK2 fibroblast lines, questioning whether the LRRK2-IN-1 has only a specific inhibitory effect on the I2020T LRRK2 kinase activity or on the contrary, the specific LRRK2 kinase inhibitor has no effect on the I2020T LRRK2 mutation. To address this issue, the results from the 4 independent experiments obtained at 30 min with or without LRRK2-IN-1 treatment in I2020T LRRK2 fibroblasts (Figure 2.11 C) were statistically analyzed. A test to identify possible outliers (Grubb's test), and another to analyze normal distribution of the sample (D'Agostino's K^2 test) were performed since only one fibroblast line carrying the I2020T LRRK2 mutation was used in the assay and therefore, the results presented some variability. The statistical analysis undertaken confirmed the significance of the alterations observed in cellular adhesion properties in fibroblasts in this assay. Taking all together, these results indicate that only I2020T LRRK2 fibroblasts treated with the specific LRRK2 kinase inhibitor exhibit enhanced cellular adhesion, suggesting that specific inhibition of LRRK2 kinase activity modulates the regulation of actin cytoskeleton dynamics in cellular adhesion mainly in I2020T-LRRK2 fibroblasts.

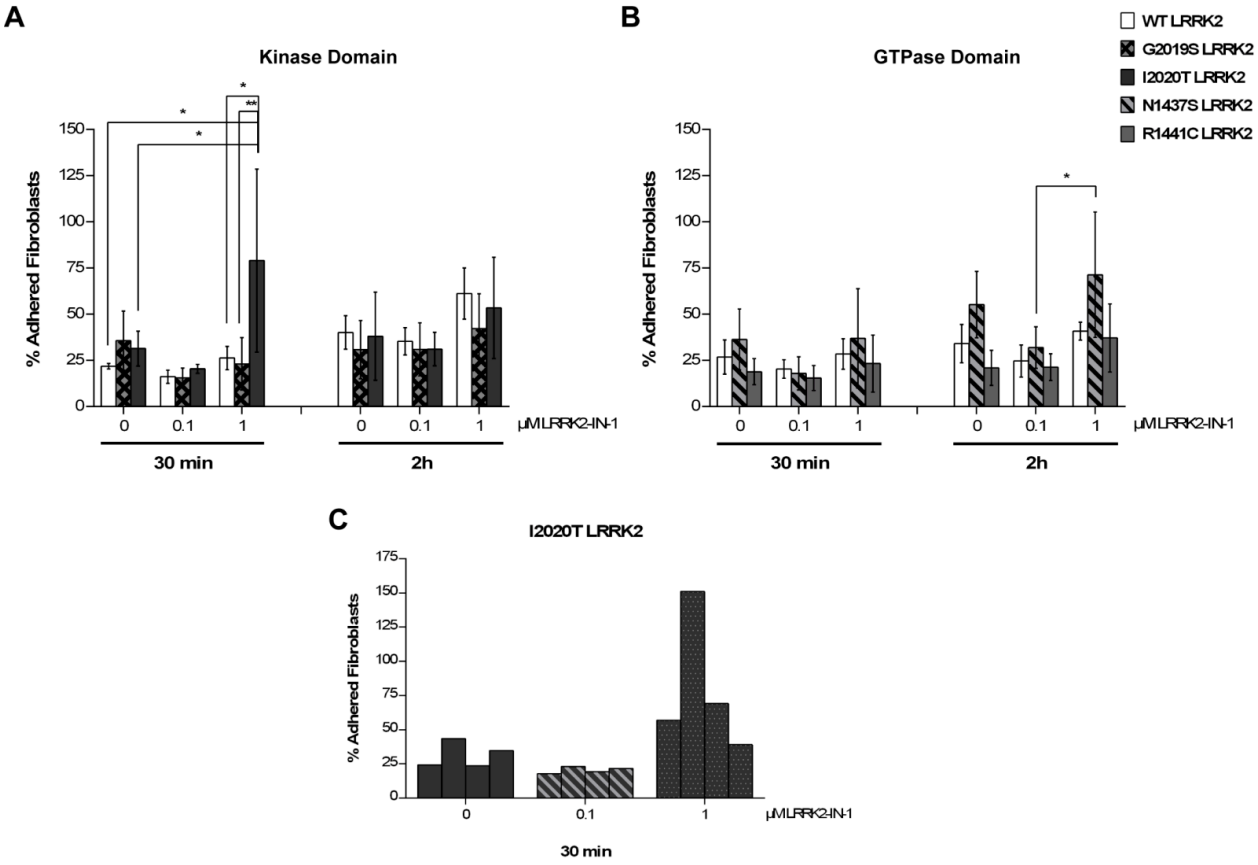

Figure 2.11 Cell adhesion assay in primary human skin fibroblasts from WT LRRK2 (healthy-control subjects) and LRRK2 PD patients after treatment with the specific LRRK2 inhibitor, LRRK2-IN-1. (A-C) Percentage of adhered fibroblasts with mutations in the LRRK2 kinase domain (A) and LRRK2 ROC GTPase domain (C) after treatment with 0 (DMSO-control), 0.1µM and 1µM LRRK2 IN-1 inhibitor for 30 min and 2 hours. Primary skin fibroblasts expressing the I2020T LRRK2 pathogenic mutation exhibited enhanced adhesion after 30 min with the presence of 1µM LRRK2-IN-1 inhibitor compared to I2020T LRRK2 fibroblasts treated with 0µM LRRK2-IN-1, WT LRRK2 treated with 0 and 1µM LRRK2-IN-1 and G2019S LRRK2 treated with 1µM LRRK2-IN-1 (A). No differences could be observed in fibroblasts with pathogenic LRRK2 mutations in the ROC domain (C). **(B)** Percentage of adhered fibroblasts with the I2020T LRRK2 mutation obtained in each independent experiments after 0, 0.1µM and 1µM LRRK2-IN-1 treatment. No outliers were identified after Grubb's test analysis with Graphpad Prism 6 and due to small sample size D'Agostion's K^2 test to analyze normal distribution was unable to be performed by Graphpad Prism 6. Data represent mean ± SEM; n=4 independent experiments (A) and n=3 independent experiments (C). WT LRRK2 (Healthy-control Subjects) = 4 fibroblast lines; G2019S LRRK2 = 3 fibroblast lines; I2020T LRRK2 = 1 fibroblast line; N1437S LRRK2 = 2 fibroblast lines; R1441C LRRK2 patients = 1 fibroblast line. **p<0.05, **p<0.01* two-way ANOVA with Tukey's *post hoc* analysis (A-C).

Strikingly, it has been reported a clear inhibitory effect on the LRRK2 kinase activity of WT LRRK2 and G2019S LRRK2 mutant protein after treatment with the specific LRRK2 inhibitor in HEK293 cells (Deng et al., 2011). Following this line, it has also been published that the I2020T LRRK2 protein is approximately 10-fold more resistant to ATP-competitive kinase inhibitors than the LRRK2 WT protein whereas the G2019S is 1.6 more sensitive than the LRRK2 WT protein at cellular concentration levels of ATP (~1mM) (Reichling and Riddle, 2009). Considering that the LRRK2-IN-1 is an ATP-competitive kinase inhibitor, then, these results could be interpreted differently, suggesting that the enhanced cellular adhesion properties observed in I2020T LRRK2 fibroblasts after treatment with the LRRK2-IN-1 inhibitor are not due to inhibition of the LRRK2 kinase activity but instead failure of the LRRK2-IN-1 to inhibit the I2020T LRRK2 kinase activity.

In conclusion, WT LRRK2 (healthy-control subjects) and LRRK2-PD fibroblasts with mutations in the kinase or GTPase domain do not present any difference in cellular adhesion at basal conditions, suggesting that neither LRRK2 WT nor the different pathogenic LRRK2 mutations are involved in the regulation of actin cytoskeleton arrangements and/or dynamics in the process of cell adhesion. Interestingly, after treatment with the LRRK2-IN-1, fibroblasts carrying the I2020T LRRK2 mutation present increased cellular adhesion whereas WT LRRK2 (healthy-control subjects) and G2019S LRRK2 fibroblasts present a slight reduction in cellular adhesion properties These observations could be explained by the fact that inhibition of LRRK2 kinase activity by LRRK2-IN-1 may modulate cellular adhesion only in I2020T-LRRK2 fibroblasts, or alternatively, lack of inhibitory effect in the I2020T LRRK2 fibroblasts and a weak inhibitory effect in WT and G2019S LRRK2 fibroblasts due to different sensitivities towards ATP-competitive kinase inhibitors such as LRRK2-IN-1 (Reichling and Riddle, 2009). Altogether, these results could suggest that the LRRK2 kinase activity, and more specifically mutations in the kinase domain, may be involved in the regulation of actin cytoskeleton arrangements and/or dynamics in the process of cell adhesion.

Based on the results obtained from the cellular adhesion assay, the increased cellular adhesion capability observed in I2020T LRRK2 fibroblasts after LRRK2-IN-1 treatment (Figure 2.11 A, C) was significant. In order to confirm these results, we performed a cell locomotion assay, also known as wound-healing assay. The enhanced cellular adhesion phenotype observed in I2020T LRRK2 fibroblasts, whether it is due to inhibition of the kinase activity by the LRRK2-IN-1 or lack of kinase activity inhibition by the LRRK2-IN-1, should result in an alteration of cell locomotion. The strength of cell adhesion determines the movement velocity of the cell (Vorotnikov, 2011), therefore, the presence of increased adhesions in a cell should results in cell locomotion alterations (Lambrechts et al., 2004). In order to address this question, the process of cell locomotion was studied in healthy-control (WT LRRK2) and LRRK2-PD fibroblasts carrying mutations in the kinase and GTPase domain. Moreover, fibroblasts were treated with DMSO-control and LRRK2-IN-1 in order to understand whether the LRRK2 kinase activity plays a role in the process of cell locomotion. For this, fibroblasts were kept in culture until they reached 90-100% confluence, the moment in which the monolayer of fibroblasts was wounded or scratched, and followed over 48h using a live cell imaging microscope under 0 (DMSO-control), 0.1 and 1μM LRRK2-IN-1 treatment conditions. Analysis performed at 0, 12, 24 and 48h after the wounding did not show any difference in cell locomotion in WT LRRK2 (healthy-control subjects) compared to LRRK2-PD fibroblasts with mutations in the kinase (Figure 2.12 A) or GTPase (Figure 2.12 B) domain in any of the treatment conditions analyzed.

In conclusion, WT LRRK2 (healthy-control subjects) and LRRK2-PD fibroblasts do not present alterations in migration/healing process since the percentage of wounded area not covered for the fibroblasts at 0, 12, 24 and 48h is approximately the same in 0 (DMSO-control), 0.1 and 1μM LRRK2-IN-1 treatment conditions (Figure 2.12 C-E). These results suggest that WT LRRK2, pathogenic LRRK2 mutations or the LRRK2 kinase activity are not involved in the regulation of cytoskeleton arrangements and/or dynamics in the cellular process of cell locomotion.

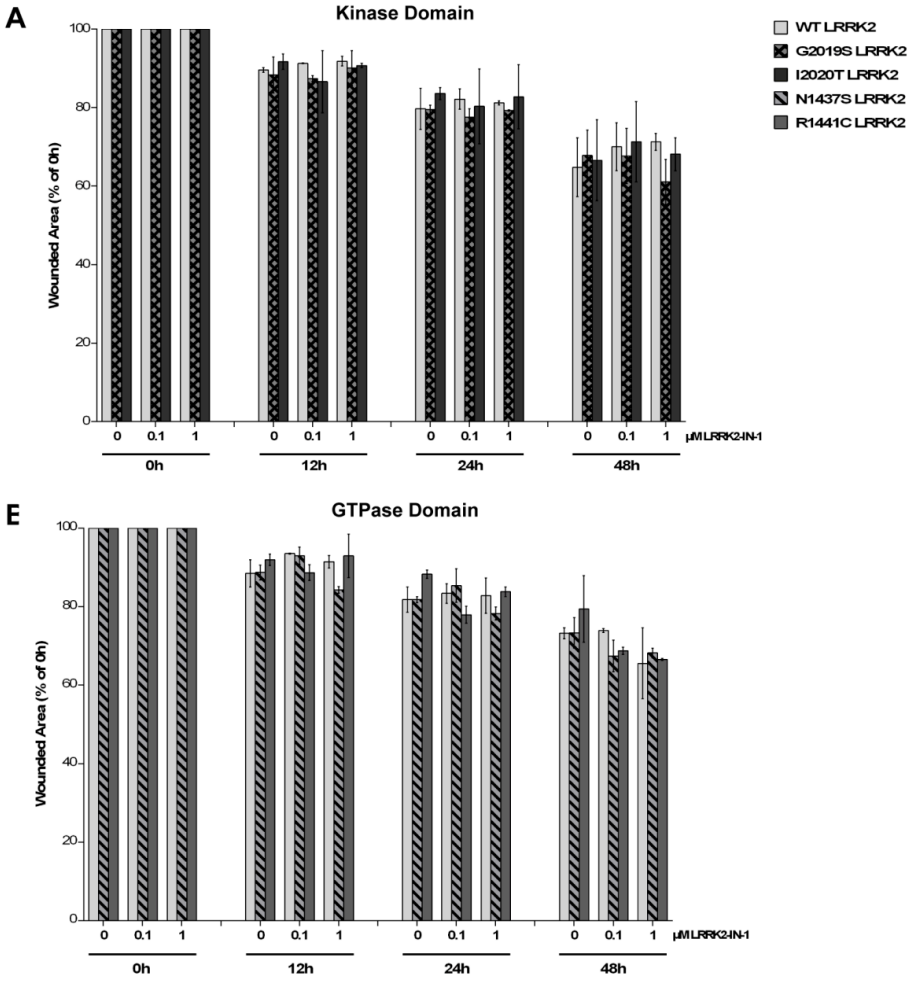
A
Kinase Domain
WT LRRK2
G2019S LRRK2
I2020T LRRK2
N1437S LRRK2
R1441C LRRK2
Wounded Area (% of 0h)
0
20
40
60
80
100
0 0.1 1 0 0.1 1 0 0.1 1 0 0.1 1 µM LRRK2-IN-1
0h
12h
24h
48h
E
GTPase Domain
Wounded Area (% of 0h)
0 0.1 1 0 0.1 1 0 0.1 1 0 0.1 1 µM LRRK2-IN-1
0h
12h
24h
48h

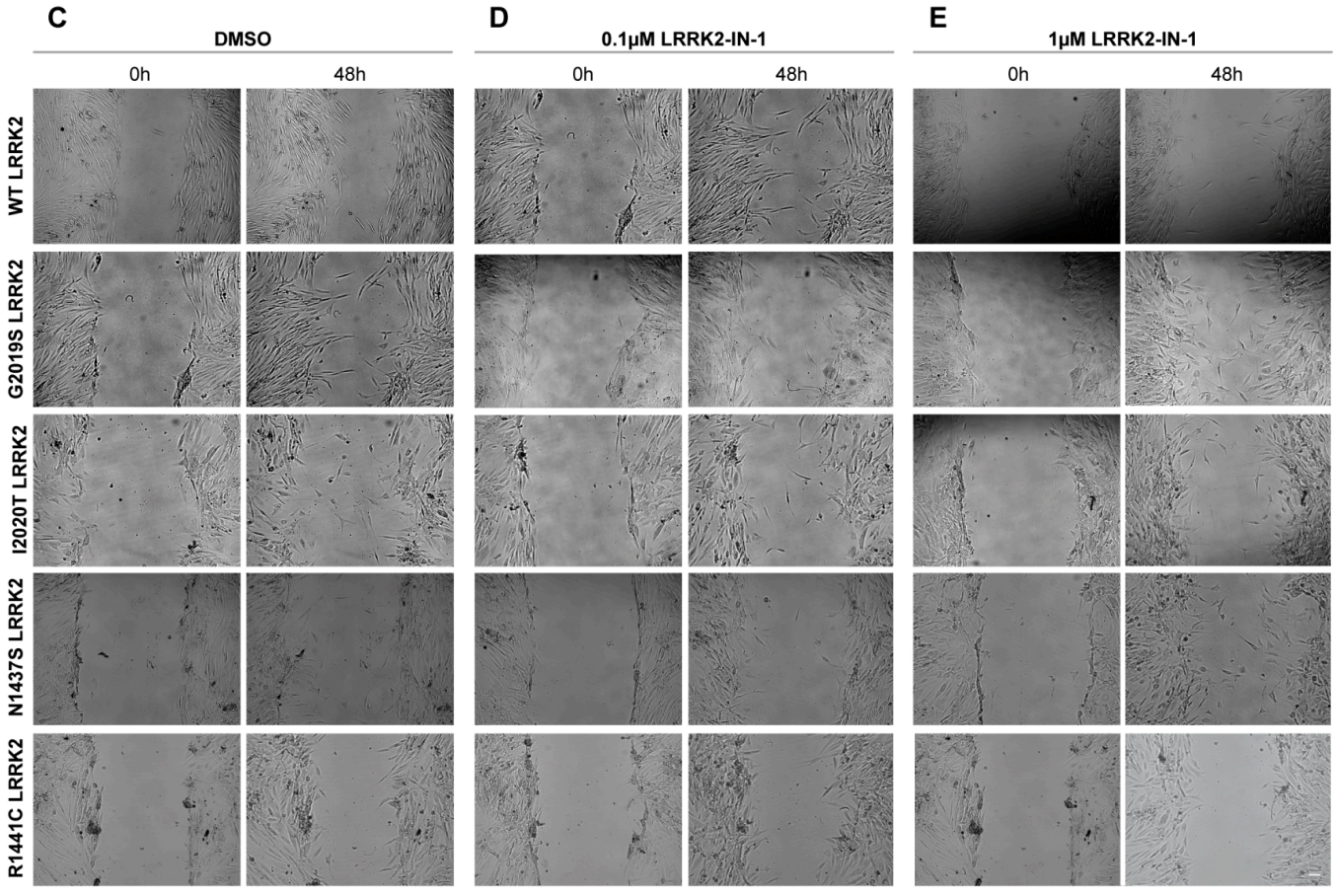
C
DMSO
D
0.1µM LRRK2-IN-1
E
1µM LRRK2-IN-1
0h
48h
WT LRRK2
G2019S LRRK2
I2020T LRRK2
N1437S LRRK2
R1441C LRRK2

Figure 2.12 Cell migration assay in primary human skin fibroblasts from WT LRRK2 (healthy-control subjects) and LRRK2 PD patients. (A-B) Percentage of wounded area covered at 0, 12, 24 and 48h after wounding the monolayer of fibroblasts. No differences in migration/healing were observed in WT LRRK2 fibroblasts compared to LRRK2-PD fibroblast lines with mutations in the LRRK2 kinase domain (A) and LRRK2 GTPase domain (B). **(D-E)** Images obtained at 5X objective from live cell microscopy at 0h and 48h after wounding the monolayer of fibroblasts in 0 (DMSO-control), 0.1 and 1μM LRRK2-IN-1 treatment condition. One representative fibroblast line is showed from healthy-subjects, G2019S LRRK2, I2020T LRRK2, N1437S LRRK2 and R1441C LRRK2 (Table 3) (Scale bar: 100μm). Data represent mean ± SD; n=2 independent experiments. WT LRRK2 (Healthy-control Subjects) = 4 fibroblast lines; G2019S LRRK2 = 3 fibroblast lines; I2020T LRRK2 = 1 fibroblast line; N1437S LRRK2 = 2 fibroblast lines; R1441C LRRK2 patients = 1 fibroblast line:

3 DISCUSSION

Mutations in the *LRRK2* gene have been described to be the most frequent cause of late-onset Parkinson's disease (PD). To date, a total of seven mutations have been demonstrated to be pathogenic including N1437H, R1441C/G/H, Y1699C, G2019S, and I2020T, based upon clear segregation with disease in *LRRK2*-linked families (Bekris et al., 2010; Gasser et al., 2011; Moore, 2008; Ross et al., 2011). Of these, the missense mutation G2019S is the most prevalent contributing to up to 2% of sporadic PD and up to 7% of familial PD cases in Caucasians (Bekris et al., 2010; Farrer, 2006; Gasser et al., 2011), and up to 20% of total PD cases in Ashkenazy Jews, and 40% in North African Berbers (Bekris et al., 2010; Lesage et al., 2006; Ozelius et al., 2006). Despite of these genetic evidences, still the physiopathogenic function of LRRK2 remains largely unknown which is in part due to lack of reliable cellular and animal models able to recapitulate LRRK2-associated PD.(Bekris et al., 2010).

In an attempt to elucidate the pathophysiological function of LRRK2 in the pathogenesis of PD, a novel Thy1.2-LRRK2 transgenic mouse model expressing either hWT or G2019S LRRK2 was generated and characterized in the present work. In addition, cumulative evidence linking the neuropathology of LRRK2-PD with dysfunction in cytoskeleton dynamics prompted to further investigate in detail the implications of physiological expression levels of human LRRK2 protein regulating cytoskeleton arrangements and dynamics in mouse and human cellular systems (Li et al., 2011; Parisiadou and Cai, 2010; Tsika and Moore, 2012) .To this end, primary hippocampal cultures derived from Thy1.2-LRRK2 transgenic mice were analyzed for neurite outgrowth and branching complexity whereas primary human skin fibroblasts derived from PD patients carrying pathogenic LRRK2 mutations in the kinase, i.e.G2019S or I2020T, and the GTPase domain, i.e. R1441C or N1437S were used to explore cellular adhesion and locomotion properties.

3.1 Generation and Characterization of Thy1.2-LRRK2 Transgenic Mice

3.1.1 Generation of Thy1.2-LRRK2 Transgenic Mice

An extensively used strategy to study in vivo gene function as well as to model human diseases such as PD is the generation of genetically modified rodent models (Xu et al., 2012; Yue, 2012). With this purpose, several LRRK2 transgenic mouse models have been developed in the recent years. However, these models present some limitations since they only partially recapitulate clinical and neuropathological features of PD (Yue, 2012). For instance, wild-type, G2019S or R1441C LRRK2 BAC transgenic mice showed abnormalities in striatal DA neurotransmission, but lack selective loss of dopaminergic neurons in SNpc, providing a model for understanding only early PD pathological events (Li et al., 2010; Melrose et al., 2010; Melrose et al., 2007; Xu et al., 2012). The need of a good genetic LRRK2 mouse model able to mirror the clinical and neuropathological features of the human disease, motivated the generation of a novel LRRK2 transgenic mouse model in the present work. To meet this objective, either full-length human WT LRRK2 (hWT) or G2019S LRRK2 protein were expressed under the neuron-specific Thy1.2 promoter obtaining two different lines of the Thy1.2-LRRK2 transgenic mouse model.

To develop the LRRK2 transgenic mouse model, an effective experimental strategy needed to be designed. With this purpose, each step for generating the novel LRRK2 transgenic mouse model was carefully evaluated in order to select the best methodological approach. First, the technology to produce the LRRK2 transgenic mice had to be decided. The most commonly used techniques for producing transgenic mice involve either the pronuclear injection of transgenes into fertilized oocytes, or embryonic stem (ES) cell-mediated gene targeting (Gama Sosa et al., 2010). Whereas pronuclear injection consists of the construction of a plasmid in which the gene/cDNA of interest is placed under the control of a heterologous promoter, gene targeting in ES cells consists of specific genetic modifications to endogenous genomic sequences (Gama Sosa et al., 2010). One disadvantage of pronuclear injection versus ES cell gene targeting is the position site-

dependent effect due to random integration of the transgene which may alter transgene expression, i.e. transgene silencing, disruption of temporal expression, cell and tissue specificity, or alteration of overall expression levels (Gama Sosa et al., 2010; Xu et al., 2012). These challenges can be overcome using ES cell-mediated gene targeting strategy which results in temporal and spatial expression pattern of the targeted gene mirroring that of the endogenous gene due to mouse gene modification in its normal chromosomal location. However, this technique has been more commonly used to produce null mutants or gene "knockouts" (Gama Sosa et al., 2010).

Second, a suitable transgene construct had to be selected in order to express the *LRRK2* gene in the transgenic mice. The most extended choices are cDNA clones under the control of heterologous promoters, whose selection depends on spatial and temporal expression where transgene is desired to be expressed. This technique uses plasmid vectors with a capacity of less than 20kb of DNA insert. Because of the small size; these transgenes are influenced by positional effects (Gama Sosa et al., 2010; Xu et al., 2012). Since PD is a neurodegenerative disorder that affects specific neuronal populations in several areas of the brain such as midbrain and cerebral cortex among others, a promoter able to support neuron-specific expression in the central nervous system was considered the best strategy option. Several promoters are included in this category such as rhomboitin I, enolase (NSE), thymocyte antigen (Thy1), and neurofilament light chain (NF-L), among others (Okabe, 2001). In a previous publication, these four neural-specific promoters were compared in order to study APP expression in transgenic mice, revealing that only the Thy1 promoter resulted in high expression levels of human APP mRNA throughout the brain with human APP levels being similar to endogenous APP levels (Andra et al., 1996). This suggested the thymocyte antigen (Thy1) promoter as the best option to considerate.

Furthermore, detailed studies on the Thy1 promoter have revealed transgene expression in different brain areas such as cortex, cerebellum, hippocampus, olfactory bulb, pontine nuclei, striatum, brain stem, and midbrain in different transgenic mice (Andra et al., 1996; Campsall et al., 2002; Gordon et al., 1987). Thus, these brain areas are consistent with brain areas affected in PD, and correlated with the spatial expression pattern of endogenous LRRK2 (Biskup et al., 2006; Higashi et al., 2007a; Melrose et al., 2007; Westerlund et al., 2008). One limitation is that generally the Thy1 promoter fails to express in dopaminergic neurons of SNpc (van der Putten et al., 2000); however, at the moment there is certain controversy in the LRRK2 field regarding whether endogenous LRRK2 is expressed or not in SNpc (Biskup et al., 2006; Galter et al., 2006; Han et al., 2008; Higashi et al., 2007a; Higashi et al., 2007b; Westerlund et al., 2008).

In addition, the selected promoter not only had to express the transgene in most neurons of the adult brain resembling the spatial expression pattern of PD but also the temporal expression profile had to mirror that of the endogenous gene. It has been described that the expression of endogenous murine *Lrrk2* gene starts at late embryonic stages, i.e. E17, and has an increment at P7 (Biskup et al., 2006; Biskup et al., 2007; Higashi et al., 2007b; Westerlund et al., 2008). Among the different neural-specific promoters previously mentioned, the Thy1 promoter has been reported to be early expressed in the perinatal period, i.e. E15 to P1 (Campsall et al., 2002), and have strong activation in late nervous system development, i.e. P4 to P10 (Aigner et al., 1995; Okabe, 2001), therefore, meeting the temporal expression requirements to mirror endogenous murine *Lrrk2* gene expression in the transgenic mice.

Among all the neural-specific promoters, the Thy1 promoter was considered to best meet all the conditions required for the generation of an effective LRRK2 transgenic mouse model. However, its lack of expression in DA neurons of SNpc results in a known limitation of the model when it comes to study PD. This fact suggests that other neuron-specific promoters that have been shown to express in neurons throughout the brain, but specially in

the midbrain and SN such as the tyrosine hydroxylase (TH) or the platelet-derived growth factor B chain (PDGF-ß) promoter could have been alternatively used for this purpose (Kahle, 2008; Masliah et al., 2000; Okabe, 2001; Ramonet et al., 2011).

The Thy1 promoter is also highly prone to random integration in the genome resulting in position site-dependent effects. An alternative strategy would be to have used a bacterial artificial chromosome (BAC) which can accommodate genomic inserts up to 300kb carrying all sequences needed for autonomous replication and copy-number control, and to optimally regulate transgene expression in time and space recapitulating the pattern of the corresponding endogenous gene (Okabe, 2001; Xu et al., 2012). Still, one disadvantage of this approach is that, due to the big size of the construct they may include other genes that may influence the phenotype independently of the gene of interest (Okabe, 2001). Ultimately, the best strategic option would be to generate a knock-in mouse model in which the native gene, in this case LRRK2, is modified in its normal chromosomal location. Thereby, the targeted gene is expressed mirroring the temporary and spatial pattern of the endogenous gene (Gama Sosa et al., 2010).

Third and last point important to take into account was whether using the human *LRRK2* gene with the human disease mutation or the homologous murine *Lrrk2* gene with the human mutation (Xu et al., 2012). Several studies performed on PD and also Huntingon's disease transgenic mouse models suggested that human genes are more appropriate for modeling human diseases in transgenic mice than the homologous mouse gene which may result in a milder or lack of phenotype (Xu et al., 2012).

In summary, the final strategy was to subclone the cDNA comprising the 51 exons of the human wild-type (hWT) or G2019S *LRRK2* gene into the murine Thy1.2 promoter expression cassette in order to microinject the final constructs into oocytes from the C57BL/6 mouse strain. This approach resulted in the generation of one human WT LRRK2 transgenic mouse line and two human G2019S LRRK2 transgenic mouse lines which were further characterized for transgene expression and PD-associated neuropathology.

3.1.2 Characterization of Thy1.2-LRRK2 Transgenic Mice

The characterization process of the Thy1.2-LRRK2 transgenic mouse model encompassed several steps including assessment of human LRRK2 protein expression levels, investigation of temporal and spatial expression profile of LRRK2 transgene, analysis of PD-associated pathology, and study of clinical features of PD. First, human LRRK2 protein expression levels in brain tissue were assessed in the Thy1.2-LRRK2 transgenic mouse model revealing the interesting finding that human LRRK2 protein was expressed at physiological levels, exceeding only two-fold the levels of endogenous murine Lrrk2 protein. The presence of such moderate protein levels which have not been previously observed in other LRRK2 transgenic mouse models reported until now (Xu et al., 2012), resulted in the generation of the first LRRK2 transgenic mouse model expressing levels of human LRRK2 protein resembling those of the endogenous murine Lrrk2 protein.

These moderate expression levels of transgene have implications to be taken into account compared to other LRRK2 transgenic mouse models (Xu et al., 2012). On one hand, one limitation of this model may reside in the fact that most of LRRK2 transgenic mouse models available until now have been reported to express higher levels of human LRRK2 protein while being partially able to recapitulate the clinical features and neuropathological hallmarks of PD (Xu et al., 2012). Consequently, one challenge is that the effect of physiological two-fold overexpressing systems may be milder than those observed in non-physiological systems overexpressing ~5-15 fold LRRK2 protein (Li et al., 2010; Lin et al., 2009; Melrose et al., 2010; Melrose et al., 2007). On the other hand, the availability of this type of LRRK2 transgenic mouse model can be highly useful for exploring the cellular and molecular physiological function of mutated LRRK2 in early stages of pathogenesis instead of studying its function in standard overexpressed cellular models which usually dramatically alter cellular functions in general. Taking all the points into account, the advantage of having such a model was considered to be greater than its possible limitations, and consequently the Thy1.2-LRRK2 transgenic mouse model was further characterized in detail.

Second, the temporal and spatial expression profile of human LRRK2 transgene was investigated in brain tissue samples of Thy1.2-LRRK2 transgenic mice. Until now, studies on LRRK2 temporal expression profile performed in mouse and rat brain tissue have highlighted consistent views that during early stages of the embryonic development, i.e. <E14, the endogenous expression of LRRK2 is low, starting to increase at the late stages of embryonic development, i.e. E17, and showing a dramatic increment of its activity during postnatal development at P7, finally reaching its mature activity 1 month after birth (Biskup et al., 2006; Biskup et al., 2007; Higashi et al., 2007b; Westerlund et al., 2008). Consistent with these observations, the Thy1.2-LRRK2 transgenic mice showed a low constitutively human *LRRK2* transgene activity at E14, increasing its activity at P2 to reach mature gene activity at P7. This activity was sustained at least until 3 weeks after birth (P21), the last time point of development analyzed. The unchanged LRRK2 expression profile observed from P7 until adulthood in mouse brain suggests that the worsening age-related clinical symptoms observed in PD patients may not be caused by alterations in the *LRRK2* gene expression (Westerlund et al., 2008). Collectively, the human *LRRK2* gene activity profile observed in the Thy1.2-LRRK2 transgenic mice was consistent with the endogenous *Lrrk2* activity observed in other rodent models (Biskup et al., 2006; Biskup et al., 2007; Higashi et al., 2007b; Westerlund et al., 2008).

The spatial expression pattern of endogenous LRRK2 protein in rodent as well as in human PD and control postmortem brains has been extensively analyzed. In mouse and rat models, endogenous LRRK2 has been observed in brain structures important for the pathology of PD mainly involved in the nigrostriatal dopaminergic pathway, i. e. cerebral cortex, striatum, and substantia nigra (Biskup et al., 2006; Braak et al., 2004; Higashi et al., 2007a; Higashi et al., 2007b; Westerlund et al., 2008). Also, endogenous LRRK2 has been detected in other rodent brain structures including olfactory tubercle, brainstem and thalamus (Biskup et al., 2006; Higashi et al., 2007a; Higashi et al., 2007b; Westerlund et al., 2008). Interestingly, LRRK2 is a widespread protein in the brain, and LRRK2 expression has been

detected in other areas of the brain not related to the pathology of PD, like cerebellum and hippocampus, suggesting that LRRK2 may be involved in motor and cognitive aspects of the disease (Biskup et al., 2006; Higashi et al., 2007b; Westerlund et al., 2008). Consistent with these observations, human endogenous LRRK2 expression in postmortem brain tissue from PD patients and controls has been observed in the same brain structures as the murine and rat endogenous LRRK2 (Biskup et al., 2006; Braak et al., 2004; Higashi et al., 2007a; Westerlund et al., 2008).

Accordingly to the spatial expression pattern of endogenous LRRK2 observed in human and rodent brains, human *LRRK2* transgene from the Thy1.2-LRRK2 transgenic mice was also detected in brain structures affected by PD neuropathology including cerebral cortex, brainstem, and at lower levels in midbrain. In addition, strong human *LRRK2* transgene was detected in hippocampus as previously reported in other studies. (Biskup et al., 2006; Galter et al., 2006; Higashi et al., 2007a; Higashi et al., 2007b; Westerlund et al., 2008). Interestingly, human *LRRK2* transgene expression was not detected in SNpc in the Thy1.2-LRRK2 transgenic mice. This finding is consistent with the low levels of LRRK2 protein observed in midbrain tissue in the Thy1.2-LRRK2 transgenic mice. Additionally, human *LRRK2* transgene expression in striatum was also not detectable. It is important to mention that whereas endogenous LRRK2 expression has been consistently reported in human and rodent striatum (Biskup et al., 2006; Galter et al., 2006; Higashi et al., 2007a; Higashi et al., 2007b; Westerlund et al., 2008), there is inconsistent data regarding endogenous LRRK2 protein expression in SN. For example, some studies have reported abundant endogenous LRRK2 expression levels in rodent and human PD brains (Biskup et al., 2006; Han et al., 2008), whereas others have observed low or lack of expression, especially in brains from PD patients (Galter et al., 2006; Higashi et al., 2007a; Higashi et al., 2007b; Westerlund et al., 2008).

Third, one of the main neuropathological hallmarks of PD, the selective loss of DA neurons in SNpc, was analyzed in the Thy1.2-LRRK2 transgenic mouse. For this purpose, analysis of DA neurons was performed in SNpc of hWT and G2019S LRRK2 transgenic mice revealing no differences in total number of nigral and DA neurons compared to non-tg age matched controls at 12-13 month of age. These results suggest that human LRRK2 overexpression in this particular transgenic mouse model is not sufficient to cause neither loss and/or neurodegeneration of nigral nor DA neurons. In addition, three other causes could have contributed to the lack of PD associated neuropathology observed in Thy1.2-LRRK2 transgenic mice including that (i) the Thy1 promoter fails to express in DA neurons of SNpc (van der Putten et al., 2000); (ii) the two-fold overexpression levels of human LRRK2 transgene observed in the mice, and (iii) the low levels of human LRRK2 protein detected in midbrain. Altogether these observations could have participated collectively or independently to the lack of PD-associated neuropathology in the Thy1.2-LRRK2 transgenic mice.

As mention above, the two-fold overexpression levels of human LRRK2 transgene observed in the Thy1.2-LRRK2 transgenic mice could have been one of the reasons for the absence of selective loss of DA neurons in SNpc. Consistent with this results, other recently published LRRK2 transgenic mouse models overexpressing low levels of mutant LRRK2 protein, as well as a LRRK2 R1441C knock-in (KI) mouse model, also failed to reveal loss of DA neurons in SNpc (Maekawa et al., 2012; Ramonet et al., 2011; Tong et al., 2009). In addition, two published LRRK2 BAC transgenic mouse models overexpressing higher levels of hWT (~ 6 fold) or G2019S (~ 15-20 fold) LRRK2 protein did not present differences in number of DA neurons in SNpc (Li et al., 2010; Lin et al., 2009; Melrose et al., 2010; Melrose et al., 2007). Interestingly, loss of LRRK2 protein in knock-out (KO) mouse models also failed to reproduce PD-associated neuropathology (Andres-Mateos et al., 2009; Hinkle et al., 2012; Tong et al., 2010). Altogether, these observations suggest that either overexpression or loss of LRRK2 protein in the aging-brain of mice is not sufficient to cause neurodegeneration of DA neurons in SNpc.

Also, the absence of PD-associated neuropathology observed in the Thy1.2-LRRK2 transgenic mouse model could have been attributed to the low expression of LRRK2 protein observed in the midbrain region in the LRRK2 transgenic mice. Consistent with this finding, other published LRRK2 transgenic mouse models also failed to detect LRRK2 in the SNpc, resulting in the absence of PD-associated neuropathology (Li et al., 2010; Lin et al., 2009; Maekawa et al., 2012; Melrose et al., 2010; Melrose et al., 2007; Ramonet et al., 2011; Tong et al., 2009; Wang et al., 2008). So far, there are only three described G2019S LRRK2 transgenic mouse lines that express LRRK2 in DA neurons in SNpc which revealed DA neuronal loss and/or neurodegeneration in SNpc (Chen et al., 2012; Lee et al., 2010; Ramonet et al., 2011). In conclusion, the Thy1.2-LRRK2 transgenic mouse model lack of PD-associated neuropathology could be attributed to absence of LRRK2 protein expression in DA neurons of SNpc due to failure of Thy1 promoter expression in this region of the brain, or alternatively to the fact that expression of LRRK2 protein together with the process of aging in adult mice is not sufficient to trigger neurodegeneration in the nigrostriatal pathway.

Finally, current reports on mouse models that developed clinical features of PD are conflicting. Two transgenic mouse models expressing either G2019S or R1441G LRRK2 have been able to recapitulate some of the clinical parkinsonism-like phenotypes observed in PD patients such as bradykinesia or akinesia, phenotypes that were also improved after L-dopa treatment (Chen et al., 2012; Li et al., 2009). Other transgenic mice have presented deficits in some locomotor behavioral analysis, deficits in fear/anxiety, or impairment in drug-stimulated locomotor activity, but no clinical parkinsonism-like phenotypes were observed (Maekawa et al., 2012; Melrose et al., 2010; Ramonet et al., 2011; Tong et al., 2009). To investigate whether the Thy1.2-LRRK2 transgenic mice displayed clinical features of PD, mice were followed for approximately 18 months, but no obvious parkinsonism-like or any other abnormal behavioral phenotypes were observed.

In summary, although the Thy1.2-LRRK2 transgenic mouse model did not recapitulate the neuropathological hallmarks of PD, probably due to its almost endogenous levels of human LRRK2 protein, this model could still be a very valuable tool to study in detail the physiological function of human LRRK2 protein and the pathogenic-LRRK2 mutations at the molecular level of different cellular processes. Since different pathogenic-LRRK2 mutations have been suggested to act at the molecular level resulting in long-term yet mild effects requiring decades to be evident in PD patients (Heutink and Verhage, 2012). The reduced mid-life of a mouse might not be sufficiently long for these mild defects to trigger the clinical and neuropathological manifestations of PD pathology.

3.2. Role of LRRK2 Regulating Actin Cytoskeleton Dynamics in Neurite Outgrowth

To date, there is a lack of cellular and molecular evidence about the physiological function of LRRK2 as well as the molecular mechanisms underlying the neuropathology of LRRK2-PD (Bekris et al., 2010). However, in the past years, several studies have linked the neuropathology of PD to dysfunction in cytoskeleton dynamics. One example is the formation of LBs, one of the main hallmarks of PD, as the result of abnormal accumulation of cytoskeletal proteins (Braak et al., 2004; Parisiadou and Cai, 2010; Wakabayashi et al., 2012). In addition, LRRK2 has been related to the maintenance of neuronal processes and neurite outgrowth, both associated with actin dynamics and cytoskeleton remodeling (MacLeod et al., 2006; Parisiadou and Cai, 2010). To date, several studies have shown a reduction in neurite outgrowth and branching complexity in G2019S LRRK2 primary neuronal cultures (Chan et al., 2011; Dachsel et al., 2010; MacLeod et al., 2006; Plowey et al., 2008; Ramonet et al., 2011). However, none of these reports have investigated in detail the physiological function of human LRRK2 protein in this process. Altogether, these data motivated exploring in detail the implication of physiological human LRRK2 protein in the regulation of cytoskeleton dynamics in neurite outgrowth in primary hippocampal cultures

derived from Thy1.2-LRRK2 transgenic mice since the neurons express almost physiological levels of human LRRK2 protein, just exceeding two-fold the murine endogenous Lrrk2.

The decision to select primary hippocampal cultures to perform this study instead of midbrain DA neurons which are the main affected type of neurons in the pathology of PD was based on the higher levels of human LRRK2 mRNA and protein observed in the hippocampus of Thy1.2-LRRK2 transgenic mice in comparison to the low LRRK2 protein levels observed in midbrain. Consistent with this fact, other reported studies have also selected primary hippocampal cultures, as well as primary cortical cultures, as their experimental approach to studying the function of LRRK2 in the pathology of PD due to higher levels of LRRK2 in those two regions of the brain (Cherra et al., 2012; Dachsel et al., 2010; MacLeod et al., 2006; Parisiadou et al., 2009).

In addition, supporting the use of primary hippocampal neuronal cultures in studying LRRK2 pathology in PD, it is worth mentioning that results obtained from studies in primary hippocampal and midbrain cultures derived from a G2019S KI mouse model revealed the same neurite outgrowth and branching complexity phenotype (Dachsel et al., 2010). Also, primary midbrain cultures derived from a CMVE-PDFGβ-G2019S LRRK2 transgenic mouse model (Ramonet et al., 2011) revealed the same G2019S reduced neurite outgrowth and branching complexity phenotype than those observed from hippocampal and cortical cultures expressing G2019S LRRK2 protein (Dachsel et al., 2010; Parisiadou et al., 2009). Along the same line, primary hippocampal and midbrain cultures overexpressed with two other PD genes, *PINK1* and Parkin, resulted in the same fragmented mitochondrial phenotype, and similar trends in mitochondrial changes, i.e. number, size and index (Yu et al., 2011).

Furthermore, the ability to culture and maintain postnatal mouse hippocampal as well as cortical cultures is highly advantageous. In both cases, neurons were shown to be able to survive, develop extensive axonal and dendritic arbors, express neuronal and synaptic markers, and form functional synaptic connections, especially for studies on genetically engineered mouse models (Beaudoin et al., 2012). On the contrary, postnatal DA neurons

are particularly challenging to culture since they do not survive standard fetal cell culture preparation techniques, therefore requiring acute dissociation procedures (Rayport et al., 1992). Moreover, it has been reported that to obtain a culture with a percentage of surviving DA neurons up to a 50%, for a longer period of time, and also with neurons able to establish functional axon terminals and dendrites, DA neurons have to be co-cultured with a monolayer of glial cells, i.e. astrocytes, and quasi free-serum media conditions (Fasano et al., 2008; Rayport et al., 1992). Taken together these findings suggest that primary hippocampal cultures are not only easier to dissociate and maintain in culture but also, findings of G2019S LRRK2 function observed in hippocampal neurons are likely applicable to DA neurons, therefore resulting in a valuable experimental approach to study LRRK2 pathogenicity in PD.

In the present work, implication of physiological levels of human LRRK2 protein in regulating actin cytoskeleton dynamics in neurite outgrowth was studied in primary hippocampal neurons derived from hWT and G2019S Thy1.2-LRRK2 transgenic mice. Previously reported studies performed in overexpressed G2019S LRRK2 cellular and mouse models resulted in a reduction in neurite outgrowth and branching complexity (Chan et al., 2011; Dachsel et al., 2010; MacLeod et al., 2006; Plowey et al., 2008; Ramonet et al., 2011), however, the results obtained from this study revealed that primary hippocampal neurons derived from G2019S Thy1.2-LRRK2 transgenic mice do not recapitulate the reduction in total neurite length and branching complexity. Interestingly, a slightly but significant reduction in total neurite length and branching complexity was observed at DIV7 in hippocampal neurons derived from hWT LRRK2 transgenic mice compared to those derived from non-tg littermate controls. These observations may be explained by the low (endogenous) expression levels of human LRRK2 protein observed in primary hippocampal neurons. Partially in agreement with these results, primary neuronal cultures derived from a G2019S LRRK2 knock-in mouse model expressing endogenous levels of murine Lrrk2 protein did not present reduction in total neurite length and branching complexity, suggesting that

endogenous levels of G2019S LRRK2 protein do not compromise neurite outgrowth and branching complexity (Dachsel et al., 2010). However, this hypothesis does not explain the slight reduction in total neurite length and branching complexity observed in primary hippocampal cultures derived from hWT LRRK2 transgenic mice, suggesting that the hWT LRRK2 protein may act through a different mechanism compared to the G2019S LRRK2 which results in a reduction in neurite outgrowth and branching complexity.

The two different phenotypes observed in hWT and G2019S LRRK2 hippocampal neurons, led to hypothesize the possibility that two different mechanisms may be responsible to explain these two phenotypes. Since the primary hippocampal neurons derived from LRRK2 transgenic mouse model do not only express human LRRK2 protein but also murine Lrrk2, an additive mechanism was thought to explain the phenotype observed in hWT LRRK2 expressing hippocampal neurons, whereas a compensatory mechanism was thought to explain the phenotype observed in G2019S neurons. The presence of both human and murine LRRK2 protein in hWT hippocampal neurons would lead to an increment of LRRK2 kinase activity through an additive effect. Thus, resembling the increased kinase activity that holds the G2019S LRRK2 protein, therefore, resulting in reduction in total neurite length and branching complexity (Dachsel et al., 2010; MacLeod et al., 2006; Plowey et al., 2008; Winner et al., 2011). In contrast, the addition of human G2019S LRRK2 protein which holds already increased kinase activity creates an unbalanced inner environment leading the neurons to start a compensatory mechanism to counteract the effect of the G2019S LRRK2 protein. As a result, G2019S LRRK2 hippocampal neurons would not recapitulate the reduction in neurite outgrowth and branching complexity phenotype observed in other G1029S LRRK2 overexpressed systems (Dachsel et al., 2010; MacLeod et al., 2006; Plowey et al., 2008; Winner et al., 2011).

So far, this compensatory mechanism has not been observed in other neuronal models. One possible explanation could be the difference in LRRK2 protein expression levels observed among the variety of models used until now. Whereas the neurons derived from the Thy1.2-LRRK2 transgenic mice express low (endogenous) G2019S LRRK2 protein levels, other primary neuronal models overexpress G2019S LRRK2 protein at very high levels (Dachsel et al., 2010; MacLeod et al., 2006; Plowey et al., 2008; Winner et al., 2011) which may be high enough for the neuron to compensate pathology. Further evidence could be observed at DIV14 when even high variability does not allow for statistical significance; hippocampal neurons expressing the G2019S LRRK2 protein display a trend towards an increment of neurite outgrowth and branching complexity which may potentially be the result of the compensatory mechanism.

Despite the proposed compensatory mechanism may explain the lack of neurite outgrowth and branching complexity phenotype in hippocampal neurons derived from G2019S Thy1.2-LRRK2 transgenic mice, there is also the possibility that in further days-in-vitro this compensatory mechanism started at DIV7 and continued until DIV14 would no longer be sustained for the neuron. This possibility would lead to observe a reduction in neurite outgrowth and branching complexity resembling the phenotype observed in the previous reported primary neuronal models overexpressing G2019S LRRK2 protein (Dachsel et al., 2010; MacLeod et al., 2006; Plowey et al., 2008; Winner et al., 2011). Taken together, the results observed in hWT hippocampal neurons showing reduction in neurite outgrowth and branching complexity suggests that physiological expression of human LRRK2 protein is indeed involved in the regulation of actin cytoskeleton arrangements and/or dynamics in neurite outgrowth and branching complexity whereas the results obtained in G2019S LRRK2 neurons suggests a potential involvement.

To investigate whether the involvement of human LRRK2 protein in the regulation of neurite outgrowth and branching complexity is kinase activity dependent, a novel specific LRRK2 kinase inhibitor, LRRK2-IN-1, was tested. To date, some studies have observed that abolishment of LRRK2 kinase activity knocking down LRRK2 or expressing the kinase-deficient K1906M LRRK2 protein in primary neuronal cultures and/or SH-SY5Y cells (Chan et al., 2011; MacLeod et al., 2006; Plowey et al., 2008) as well as primary neuronal cultures derived from LRRK2 KO mouse models (Dachsel et al., 2010) result in an increment of neurite outgrowth and branching complexity. Also, primary neuronal cultures treated with the unspecific kinase inhibitor Staurosporine resulted in a partial rescue of the G2019S LRRK2 neurite outgrowth shortening phenotype (Dachsel et al., 2010). In the present work, enhanced neurite outgrowth and branching complexity was observed at DIV7 and DIV14 only in G2019S expressing hippocampal neurons compared to non-tg littermate hippocampal neurons after treatment with the novel specific LRRK2 kinase inhibitor, LRRK2-IN-1. Consistent with previous studies, this results suggest a role of the G2019S LRRK2 kinase domain, but in particular its kinase activity, in the regulation of actin cytoskeleton arrangements and/or dynamics in neurite outgrowth and branching complexity (Chan et al., 2011; Dachsel et al., 2010; MacLeod et al., 2006; Plowey et al., 2008).

In conclusion, in neurite outgrowth and branching complexity was explored in this present study the role of LRRK2 by using a neuronal system that closely resembles the physiological function of LRRK2 protein, primary hippocampal neurons derived from the Thy1.2-LRRK2 transgenic mice expressing physiological levels of human LRRK2 protein (~two-fold). Physiological expression levels of G2019S LRRK2 in primary hippocampal neurons did not compromise neurite outgrowth and branching complexity as previously observed in a G2019S LRRK2 KI mouse model (Dachsel et al., 2010; MacLeod et al., 2006; Plowey et al., 2008; Winner et al., 2011). But, interestingly, a reduction in neurite outgrowth and branching complexity phenotype was recapitulated by primary hippocampal neurons expressing hWT LRRK2 protein. These findings suggest that two different regulatory

mechanisms may be modulated by LRRK2. In addition, the neuronal system used in this study was able to recapitulate the increased neurite outgrowth and branching complexity phenotype already shown by other reports (Chan et al., 2011; Dachsel et al., 2010; MacLeod et al., 2006; Plowey et al., 2008) after abolishing the LRRK2 kinase activity by the specific LRRK2 kinase inhibitor LRRK2-IN-1 (Deng et al., 2011). Taken together, these results suggest that human LRRK2 protein expressed at physiological levels is indeed involved in the regulation of neurite outgrowth and branching complexity, regulation that is dependent on LRRK2 kinase activity.

3.3 Role of LRRK2 Regulating Actin Cytoskeleton Dynamics in Cell Adhesion and Cell Locomotion in Primary Human Skin Fibroblasts.

Analysis of primary hippocampal cultures derived from the Thy1.2-LRRK2 transgenic mouse model pointed towards an involvement of human LRRK2 protein expressed at physiological expression levels regulating actin cytoskeleton arrangements and/or dynamics in neurite outgrowth. These results prompted to further investigate into detail the physiological function of human WT and different pathogenic-LRRK2 mutant proteins at the cytoskeleton. For this purpose, primary human skin fibroblasts derived from LRRK2 PD patients carrying mutations either in the kinase or GTPase domain and healthy-control subjects were studied.

Primary human skin fibroblasts have been shown to be a useful human cell model to investigate several neurodegenerative diseases such as PD or Alzheimer's Disease (AD) since fibroblasts comprise biological aging, genetic background, and environmental etiopathology of the patients (Auburger et al., 2012b). Other advantages include easy availability from patients and age-matched controls, standard culture conditions similar to those used in regular cellular lines, and efficient genetic manipulation (Auburger et al., 2012b; Connolly, 1998). However, there are also several disadvantages that need to be considered before starting to work with primary human skin fibroblasts. Based on our experience and in agreement with previously published reports, the main disadvantage of human skin fibroblasts as a cellular model is the slow growth and expansion ratio that they

present, which depends on the gender and the age of the subject at the time of the biopsy (Auburger et al., 2012b). This variability may represent a difficulty to match cell confluence and seeding densities and may influence findings so it should be taken into account (Auburger et al., 2012b). In order to minimize individual differences between the 11 fibroblast lines used in these experiments (Table 3), the same cellular passage and the same number of seeded cells were used in at least three independent experiments for each type of assay. Still , the use of fibroblasts has been shown to be a very valuable *in vitro* model (i) to study the effect of different drugs, i.e. kinase inhibitors, in order to find new potential therapeutic treatments, (ii) to perform several biological, i.e. cell adhesion or migration assays, and biochemical assays, i.e. co-immunoprecipitation, to bring further insight about the pathology of the disease, and (iii) to find relevant biomarkers for diagnosis in PD and other neurodegenerative diseases (Auburger et al., 2012b; Hoepken et al., 2008).

The main idea behind the use of fibroblasts as a cellular system is model the alterations occuring in the central nervous system (CNS) (Connolly, 1998). Thus, transcriptome analysis of primary skin fibroblasts derived from PINK1-PD patients (PARK6, autosomal-recessive early-onset PD) has shown upregulation of the presynaptic marker SNCA (α-synuclein), deregulation of several synaptic proteins, upregulation of proteins implicated in synaptic remodeling, and proteins associated to α-synuclein and the dopamine transporter (DAT). Upregulation of SNCA and deregulation of proteins involved in synaptic integrity were further observed in primary skin fibroblasts derived from idiopathic sporadic PD patients, and were confirmed in brain tissue from PD patients, therefore, suggesting that changes in fibroblasts can mirror changes within the CNS which potentially can be used as biomarkers for diagnosis (Connolly, 1998; Hoepken et al., 2008). Altogether, these findings support the use of human skin fibroblasts as *in vitro* model to study PD, and also other neurodegenerative diseases (Hoepken et al., 2008).

Previous reports have shown that primary human skin fibroblasts derived from patients with different neurologic disorders including Lesch Nyhan Syndrome, Schizophrenia, and Alzheimer's disease (AD) present dysregulation of cellular adhesion (Mahadik et al., 1994; Stacey et al., 2000; Takeda et al., 1992). In addition, cellular locomotion/migration has been shown to play a key role in morphogenetic changes in normal physiology and also in a wide range of human diseases (Lambrechts et al., 2004; Mitchison and Cramer, 1996; Ulrich and Heisenberg, 2009; Vorotnikov, 2011). Cellular adhesion and locomotion/migration have been shown to be primarily regulated by Rho family small GTPases which control actin polymerization and activation of myosin II (Vorotnikov, 2011). In addition, LRRK2 has been shown to interact with actin and actin-associated proteins (Meixner et al., 2011) as well as proteins involved in actin cytoskeleton regulation, i.e. Rho small family GTPases (Chan et al., 2011; Haebig et al., 2010). Indeed, LRRK2 has been suggested to regulate neurite outgrowth and branching complexity in previous studies (Chan et al., 2011; Dachsel et al., 2010; MacLeod et al., 2006; Plowey et al., 2008; Ramonet et al., 2011; Sanchez-Danes et al., 2012) as also observed in the present work. Collectively, these observations prompted to hypothesize a potential role of LRRK2 in the regulation of cytoskeleton arrangements and/or dynamics during cellular adhesion and cellular locomotion.

In the present study, primary human skin fibroblasts derived from WT LRRK2 (healthy-control subjects) and LRRK2-PD patients carrying mutations in the kinase domain (G2019S and I2020T) or Roc GTPase domain (R1441C and N1437S) were used to test cellular adhesion properties at different time points at basal conditions. No differences in cellular adhesion properties were observed in WT LRRK2 (healthy-control subjects) fibroblasts compared to LRRK2-PD fibroblasts in any of the time points analyzed, suggesting that neither WT LRRK2 protein nor the different pathogenic-LRRK2 mutations play a role in the regulation of actin cytoskeleton arrangements and/or dynamics in the process of cellular adhesion.

The impact of LRRK2 kinase activity regulating neurite outgrowth observed in primary hippocampal cultures suggested to investigate whether in fibroblasts the LRRK2 kinase activity could be also involved in regulating actin cytoskeleton arrangement and/or dynamics in the process of cellular adhesion. To test this hypothesis, the eleven fibroblasts lines were treated with the specific LRRK2 kinase inhibitor, LRRK2-IN-1. Interestingly, inhibition of the kinase activity by the LRRK2-IN-1 led to an increment in the cellular adhesion properties only in fibroblasts carrying the I2020T LRRK2 kinase mutation whereas no significant differences, or even a slight reduction in cellular adhesion properties, were observed in WT LRRK2 (healthy-control) and G2019S LRRK2 fibroblasts. These results suggest that, despite fibroblast lines not showing cellular adhesion differences at basal conditions, LRRK2 kinase activity may have a role in the regulation of actin cytoskeleton arrangements and/or dynamics in fibroblasts carrying the pathogenic I2020T LRRK2 kinase mutation. Strikingly, the effect of this mutation on LRRK2 kinase activity is controversial, being reported to either increase (Gloeckner et al., 2006; West et al., 2007) or decrease (Anand et al., 2009; Jaleel et al., 2007) kinase activity depending on the study. Also, it needs to be mentioned that due to low frequency of the mutation I2020T, only one fibroblast line with this specific LRRK2 mutation was included in the assay. This fibroblast line presented a slow growth ratio compared to other fibroblast lines, resulting in a higher variability among different experiments so more restrictive statistical analysis was undertaken in this case. The results observed in I2020T LRRK2 fibroblasts may suggest that inhibition of LRRK2 kinase activity leads to increased cellular adhesion indicating that the inhibition of mutated I2020T LRRK2 kinase by LRRK2-IN-1 may be different than WT LRRK2, possibly by altering interaction partners, or changing LRRK2 properties.

Although the alterations in cellular adhesion properties observed in WT, G2019S, and I2020T LRRK2 fibroblasts could be explained by the effect of LRRK2-IN-1 inhibiting LRRK2 kinase activity, other observations need to be taken into account before coming to a conclusion. First, it has been reported that there is a clear inhibitory effect of WT LRRK2 and G2019S LRRK2 kinase activity in HEK293 cells by LRRK2-IN-1(Deng et al., 2011). Second, it has been published that G2019S and I2020T LRRK2 protein have distinct sensitivities towards ATP-competitive kinase inhibitors such as LRRK2-IN-1, being the G2019S LRRK2 protein 1.6-fold more sensitive and the I2020T LRRK2 protein 10-fold more resistant than the WT LRRK2 protein to this type of inhibitors in cellular or *in vivo* systems (Reichling and Riddle, 2009). These observations would suggest that the slight non-significant reduction in cellular adhesion properties observed in WT LRRK2 (healthy-control subjects) and G2019S LRRK2 fibroblasts treated with LRRK2-IN-1 compared to DMSO-control could be attributed to a weaker effect of the LRRK2-IN-1 in fibroblasts than its effect on other cellular models (Deng et al., 2011). In addition and taking into account that LRRK2-IN-1 is an ATP-competitive kinase inhibitor (Deng et al., 2011), the increased cellular adhesion properties observed in I2020T LRRK2 fibroblasts could be explained as a lack of inhibitory effect on I2020T LRRK2 kinase activity due its increased resistance to this type of inhibitors. To validate whether this thought is true, a larger number of experiments and I2020T LRRK2 fibroblast lines should be included in the study. Taken together, these observations suggest that human LRRK2 protein expressed at physiological levels is not involved in the regulation of actin cytoskeleton dynamics in cell adhesion, whereas the LRRK2 kinase activity may be weakly involved. Furthermore, the different sensitivities observed towards ATP-competitive kinase inhibitors in WT, G2019S and I2020T LRRK2 proteins supports the use of human skin fibroblasts as a possible tool for testing different drugs, and finding new potential therapeutic treatment for PD. In addition, these results bring further insight about the fact that different pathogenic LRRK2 mutations may respond differently to the same drug, proposing the use of mutant specific and/or personalized drugs as the future therapeutic approach for the treatment of PD, and other neurodegenerative diseases.

Possible effects of LRRK2 in cellular locomotion were also studied in the present work. The process of cellular adhesion is involved in the cellular process of cell locomotion, being responsible for determining the movement velocity of the cell (Lambrechts et al., 2004). Therefore, any alteration in the process of cell adhesion, i.e., increased or decreased cellular adhesion to a substrate, would result in cell locomotion alterations (Lambrechts et al., 2004). In this study, human fibroblast lines treated with the specific LRRK2 kinase inhibitor LRRK2-IN-1 showed differences in cellular adhesion properties, pointing to putative alterations in cellular locomotion in those fibroblast lines. These results brought to hypothesize a potential involvement of physiological expression levels of human LRRK2 protein in the regulation of cytoskeleton dynamics during the process of cellular locomotion. To test this hypothesis, the process of cellular locomotion was studied using a wound-healing assay in WT LRRK2 (healthy-control subject) and LRRK2-PD fibroblasts. The role of LRRK2 kinase activity in the process of cellular locomotion was also investigated by using the specific LRRK2 kinase inhibitor, LRRK2-IN-1. No differences in cellular locomotion were observed in any of the conditions analyzed in WT LRRK2 (healthy-control subjects) and LRRK2-PD fibroblasts carrying mutations either in the LRRK2 kinase or GTPase domain. These results suggest that the altered cellular adhesion properties observed in I2020T LRRK2 fibroblasts, and the slight alteration observed in WT LRRK2 and G2019S LRRK2 fibroblasts may not be strong enough to cause changes in the process of cellular locomotion in fibroblast either with or without LRRK2-IN-1 treatment at any of the different time points analyzed. Hence, WT LRRK2, pathogenic-LRRK2 proteins, and LRRK2 kinase activity do not seem to be involved in regulating of cytoskeleton organization or dynamics in the process of cellular locomotion.

In conclusion, the role of physiological expression levels of human LRRK2 protein regulating actin cytoskeleton was explored in the processes of cellular adhesion and cellular locomotion using primary skin fibroblasts derived from LRRK2-PD patients. At basal condition, LRRK2-PD fibroblasts did not show any difference in cellular adhesion properties compared to WT LRRK2 from healthy-control subject fibroblasts. Interestingly, the treatment of primary skin fibroblasts with the specific LRRK2 kinase inhibitor LRRK2-IN-1 resulted in a slight reduction in cellular adhesion properties in both G2019S LRRK2 and WT LRRK2 fibroblasts, whereas an increment in cellular adhesion properties was observed only in fibroblasts with the I2020T LRRK2 mutation. The different effect of the LRRK2-IN-1 observed in WT, G2019S and I2020T LRRK2 protein is most likely attributed to different sensitivities to the inhibitor LRRK2-IN-1 (Deng et al., 2011; Reichling and Riddle, 2009). The specific inhibition of LRRK2 kinase activity affects the modulation of actin cytoskeleton arrangements and/or dynamics in cellular adhesion, especially in LRRK2 proteins with mutations in the kinase domain, suggesting a potential role of LRRK2 kinase activity in this particular process.

In summary, the present study supports the involvement of physiological expression levels of human LRRK2 in the regulation of actin cytoskeleton arrangements and dynamics in neurite outgrowth but not in cellular adhesion and locomotion. This work also shows that the inhibition of LRRK2 kinase activity modulates actin cytoskeleton in neurite outgrowth and cellular adhesion only in cells carrying the G2019S and I2020T in the regulation of actin cytoskeleton arrangements and/or dynamics that depends on LRRK2 kinase activity.

4 OUTLOOK

Idiopathic PD is currently considered the result of a complex interplay of cumulative genetic, environmental, and age-related factors (Gao and Hong, 2011; Varcin et al., 2012). Because mutations in the *LRRK2* gene are the most frequent cause of PD, and LRRK2-associated PD is clinical and neuropathological indistinguishable from idiopathic PD (Berwick and Harvey, 2011; Wider et al., 2010), intensive research efforts have been dedicated to elucidate the pathophysiological function of the *LRRK2* gene. Despite of continued progresses in this line, still the main function of the gene remains unknown as well as true substrates and interactor partners of LRRK2 *in vivo*. In addition, the availability of reliable rodent models able to recapitulate clinical and neuropathological features of PD is scarce; therefore, major efforts in this field are still needed (Daniels et al., 2011a; Li et al., 2011; Xu et al., 2012; Yue, 2009).

In this work, a novel Thy1.2-LRRK2 transgenic mouse model was generated and characterized aiming to reproduce clinical and neuropathological features observed in LRRK2-associated PD (Berwick and Harvey, 2011; Wider et al., 2010). Although the mice showed expression of LRRK2 protein in PD-affected brain areas (Biskup et al., 2006; Braak et al., 2004; Higashi et al., 2007a; Higashi et al., 2007b; Westerlund et al., 2008), no degeneration of DA neurons in the SNpc was observed, suggesting that LRRK2 expression alone does not trigger LRRK2-associated neuropathological phenotypes, at least when over-expressed LRRK2 at physiological levels. These findings could be explained by the reduced penetrance reported in the G2019S LRRK2 mutation, suggesting the participation of additional unknown modifying factors (Bekris et al., 2010; Farrer, 2006; Gasser et al., 2011; Ross et al., 2011), together with the low/physiological expression levels of human LRRK2 protein induced in the LRRK2 transgenic mouse model. Despite the lack of phenotype in the Thy1.2-LRRK2 transgenic mice, this model could still be a useful tool to study the physiological function of LRRK2 or the effect of modeled environmental stressors i.e. exposure to neurotoxins such as paraquat or rotenone (Varcin et al., 2012).

Several studies have shown that LRRK2 regulates neurite outgrowth and branching complexity (Dachsel et al., 2010; MacLeod et al., 2006; Parisiadou et al., 2009; Plowey et al., 2008), and also interacts with proteins related to cytoskeleton regulation and/or dynamics (Chan et al., 2011; Haebig et al., 2010; Meixner et al., 2011). Thus, the implications of physiological levels of human LRRK2 protein in the regulation of actin cytoskeleton dynamics were explored in detail in the novel Thy1.2-LRRK2 transgenic mouse model. To meet this objective, primary hippocampal neurons derived from Thy1.2-LRRK2 transgenic mice and primary human skin fibroblast derived from LRRK2-PD patients were used to study whether WT LRRK2 and different pathogenic-LRRK2 mutations modulate actin cytoskeleton dynamics in neurite outgrowth, and cellular adhesion and locomotion. The results obtained from this study suggested that LRRK2 is involved in the regulation of actin cytoskeleton dynamics in neurite outgrowth and branching complexity in neurons however, LRRK2 did not modulate actin cytoskeleton dynamics in cellular adhesion and cellular locomotion in fibroblasts.

To further investigate the possible mechanisms by which LRRK2 might modulate neurite outgrowth and branching complexity, neuronal cultures could be treated with pharmacologic compounds with known effects on neurite outgrowth reduction associated to G2019S-LRRK2 expression. The purpose of treating neurons with those compounds would be ultimately to attenuate or exacerbate the alterations in neurite outgrowth and branching complexity phenotype observed in primary hippocampal cultures derived from the Thy1.-LRRK2 transgenic mice. Thus, providing a hint towards the potential cellular pathway involved in the regulation of this process. Among others, treatments could include (i) disruption of actin filaments by Cytochalasin D or partial depolymerization of actin cytoskeleton with Foskolin (Parisiadou et al., 2009), (ii) induction or blockage of autophagy with rapamycin or knocking down LC3 protein, respectively (Plowey et al., 2008), and (iii) regulation of mitochondrial and calcium homeostasis with the calcium chelator BAPTA-AM or inhibition of voltage-gated calcium channels with nitrenpidine (Cherra et al., 2012).

In parallel, cytoskeleton dynamics were studied in primary human skin fibroblasts derived from LRRK2-PD patients to extend our findings obtained from primary hippocampal neurons to a human cellular model. No differences in cellular adhesion and cellular locomotion properties were observed in WT LRRK2 (healthy-control subjects) fibroblasts compared to LRRK2-PD fibroblasts lines, suggesting that LRRK2 is not involved in the regulation of actin cytoskeleton dynamics in these two particular processes, at least in fibroblasts.

Fibroblasts are considered a valuable cellular system to study neurodegenerative disorders, since the cells are easy to obtain, propagate, and present the genetic background of a disease patient (Auburger et al., 2012a). As a result of all these properties, a wide range of experiments and biochemical tests can be performed using very small samples of fibroblasts (Auburger et al., 2012b; Connolly, 1998). However, it may be possible that cytoskeleton defects associated to LRRK2 observed in CNS primary neurons from mouse cannot be further detected in human fibroblasts derived from LRRK2-PD patients, since those defects might be possibly related only to specific neuronal functions. Nevertheless, our results do not invalidate the use of primary human skin fibroblasts as a cellular model to study the physiological function of LRRK2 in other cellular and molecular pathways such as autophagy, and mitochondria and calcium homeostasis. Indeed, human fibroblasts have been successfully used to investigate the regulation of calcium (Ca^{2+}) levels in several neurodegenerative diseases including Alzheimer's disease and amyotrophic lateral sclerosis (ALS) as well as to study lysosomal and mitochondrial disorders which can also be present in some neurological diseases (Connolly, 1998). These studies have proposed the use of fluorescent dyes to measure several physiological parameters such as concentration of free Ca^{2+} in the cytoplasm or mitochondrial and cell potentials (Connolly, 1998).

A possible alternative approach to investigate the physiological function of LRRK2 using primary human skin fibroblast could be to study calcium homeostasis. Recently, LRRK2 has been involved in the homeostasis of lysosomal Ca^{2+} with a downstream effect on autophagy regulated through a calcium-dependent pathway. In this study, increased autophagy induced by LRRK2 overexpression could be reverted by calcium chelation (Gomez-Suaga et al., 2012a; Gomez-Suaga et al., 2012b). In addition, pathogenic LRRK2 mutations have been shown to cause alterations in calcium homeostasis leading to dendrite mitophagy in neurons, effect that was reverted by calcium chelation or inhibition of voltage-gated Ca^{2+} channels (Cherra et al., 2012). A putative future line of research could focus on exploring whether calcium homeostasis is altered in primary human skin fibroblast derived from LRRK2-PD patients, which molecular pathways are involved in calcium homeostasis dysregulation and what is the effect of different pathogenic-LRRK2 mutations on these pathways (Cherra et al., 2012; Gomez-Suaga et al., 2012a; Gomez-Suaga et al., 2012b). Extending the study adding more human fibroblast lines derived from familial LRRK2-PD and sporadic PD patients, and healthy-control subjects as well as from fibroblasts derived from patients with other neurodegenerative disorders would allow to determine whether calcium homeostasis alterations could be used as specific biomarker for PD. Because of PD is characterized by the selective loss of DA neurons in SNpc, further corroborative studies on calcium homeostasis alterations should be performed in neuronal cellular systems.

The identification of physiological changes in LRRK2-PD fibroblasts would allow formulating new hypothesis and testing new potential drugs for future PD treatments. In this line, the different sensitivities towards ATP-competitive kinase inhibitors such as LRRK2-IN-1 observed in WT, G2019S and I2020T LRRK2 fibroblasts suggests the study of personalized therapeutic approaches for the treatment of PD.

To further investigate the role of LRRK2 regulating actin cytoskeleton dynamics in mouse and human cells, and to understand whether this putative function is kinase activity dependent, we tested the novel ATP-competitive kinase inhibitor LRRK2-IN-1 in both cellular models. Inhibition of LRRK2 kinase activity resulted in increased neurite outgrowth and branching complexity in primary hippocampal cultures, and alterations in cellular adhesion properties in WT, G2019S and I2020T LRRK2 fibroblasts. These effects might be due to different sensitivities towards the specific LRRK2 kinase inhibitors LRRK2-IN-1, suggesting differential interaction between LRRK2-IN-1 and mutated LRRK2 kinase, mutation-specific changes in other LRRK2 properties, i.e protein stability, or modification of interactor partners compared to the WT LRRK2 kinase. Therefore, a possible line of investigation could focused on using the novel LRRK2-IN-1 kinase inhibitor to identify potential mutant specific LRRK2 interactors by co-immunoprecipitation, mass spectrometry, and crystal structure analysis. The access to different cellular models such as primary hippocampal neurons and primary human fibroblasts, as well as tissue lysates from our Thy1.2-LRRK2 transgenic mouse model would allow further validation of the results. Also, the use of fibroblasts carrying different pathogenic LRRK2 mutations would help to understand how the disease-associated LRRK2 mutations modify the interaction between LRRK2 protein and the LRRK2-IN-1 kinase inhibitor bringing further insight about the mechanism underlying the different phenotypes observed.

Recently, two publications have shed light on the physiological function of LRRK2 proposing two possible mechanisms underlying LRRK2-related PD pathology. The first study addresses the biological function of LRRK2 identifying a new presynaptic substrate and suggesting loss of synapse function as an early aspect of PD neurodegeneration (Heutink and Verhage, 2012; Matta et al., 2012). The second study has pointed to changes in gene expression through aberrant activation of ERK as the mechanism underlying G2019S LRRK2-PD pathogenesis (Reinhardt et al., 2013).

In the first publication, Mata et al. identified EndoA, a protein involved in synaptic vesicle endocytosis, as a new substrate of LRRK2. Using loss-of-function and G2019S LRRK2 mutants in genetic models of Drosophila and biochemical studies, they observed that LRRK2 affected synaptic vesicle endocytosis by phosphorylating EndoA at serine 75. The study also suggested a regulatory mechanism in which reduced LRRK2 kinase activity facilitates EndoA membrane association whereas increased kinase activity would lead to the opposite effect. Thereby, both mechanisms would result in a mild and chronic dysfunction of synaptic endocytosis underlying the slow progressing and age-dependent course of PD. Consequently, they proposed a model in which LRRK2 kinase activity is part of an EndoA phosphorylation cycle that facilitates efficient vesicle formation at synapses (Matta et al., 2012).

The identification of EndoA as a novel LRRK2 substrate in genetic LRRK2 models of Drosophila has opened new lines of investigation regarding the pathogenic mechanisms of LRRK2 that need to be further explored. Considering that PD is a progressive and age-dependent disease, the results obtained in *Drosophila* suggesting EndoA as a LRRK2 substrate should be further confirmed in LRRK2 transgenic mouse models, that have longer life span, and therefore can recapitulate better the age-dependent and progressive pathology of the human disease. A possible approach to assess the effect of LRRK2 on EndoA would be to first characterize the phosphorylation state of EndoA in different brain regions of LRRK2 transgenic mice and second, to investigate whether phosphorylation of EndoA is age-dependent. Increased levels of phospho-EndoA should be evident in G2019S LRRK2 transgenic mice, since G2019S mutation has been consistently shown to augment LRRK2 kinase activity. However, not only increased but also reduced EndoA phosphorylation can result in vesicle recycling effects. Therefore, to prove whether LRRK2 regulates EndoA phosphorylation and synaptic vesicle trafficking, it would be highly valuable to perform the same study using KO or KD LRRK2 mouse models. Primary neuronal cultures derived from LRRK2 transgenic mice expressing either WT or G2019S LRRK2 protein would also be a

useful cellular model to study LRRK2 and EndoA subcellular co-localization. Furthermore, track alterations in synaptic vesicle formation can be studied by confocal microscopy and/or live-cell imaging using FM dyes which fluorescence increases when they are partitioned in the membrane (Cheung and Cousin, 2011). Along this line, knocking down LRRK2 or EndoA in neuronal cultures would help to decipher the physiological role of both proteins on synaptic vesicle formation.

In the second publication, Reinhardt et al. reported the generation of midbrain dopaminergic (mDA) neurons differentiated from human induced pluripotent stem cells (iPSCs) harboring the G2019S LRRK2 mutation. These cells showed a number of features commonly associated to neurodegeneration, such as reduced neurite outgrowth, aberrant autophagy, and increased sensitivity to oxidative stress which could be rescued by genetic correction of the G2019S mutation. Additionally, four new genes (*CPNE8, CADPS2, MAP7, and UHRF2)* were identified to be dysregulated in mutant lines contributing to the observed phenotypes via activation of extracellular-signal-regulated kinase 1/2 (ERK). Selective inhibition of ERK1/2 protein in G2019S LRRK2 lines returned the expression of *UHRF2*, *CADPS2* and *CPNE8* to normal levels and ameliorated neurodegeneration (Reinhardt et al., 2013). In this line, other publications have previously reported a link between LRRK2 and ERK activation that would lead to increased autophagy (Bravo-San Pedro et al., 2013; Plowey et al., 2008) and induction of α-synuclein expression (Carballo-Carbajal et al., 2010), providing mechanistic insights into the pathogenesis induced by G2019S LRRK2 mutant protein. To verify the results obtained in mDA neurons differentiated from iPSCs, changes in UHRF2, CADPS2 and CPNE8 mRNA expression and protein levels dependent on ERK activation could be further confirmed in different regions of the brain in LRRK2 transgenic mouse models. Analysis of these changes at different stages of the development would bring further information about the role of these genes in the progression of PD. Moreover, specific analysis of UHRF2, CADPS2 and CPNE8 protein function in LRRK2 transgenic mouse models and primary neuronal cultures could be performed.

The first gene, UHRF2, encodes a E3 ubiquitin ligase protein known to enhance clearance of polyglutamine aggregates in several neurodegenerative diseases that would point to a similar function for α-synuclein aggregates formation (Reinhardt et al., 2013). Thereby, decreased levels of UHRF2 protein observed in G2019S LRRK2 mDA neurons would lead to an enhanced α-synuclein protein aggregate formation particularly in early stages of PD (Reinhardt et al., 2013). On the contrary, knocking down UHRF2 protein would lead to a reduction in α-synuclein protein aggregate formation which could contribute to ameliorate PD pathology.

The second gene, CADPS2, is known to regulate neurotransmission of monoamines such as DA (Reinhardt et al., 2013). The formation of reactive metabolites by DA causes an increase in oxidative stress which might result in degeneration of DA neurons (Napolitano et al., 2011). In this line, altered formation of DA reactive metabolites could be explored in WT LRRK2 transgenic mice brain compared to G2019S LRRK2. Further experiments could involve siRNA molecules targeting *CADPS2* gene in order to assess whether the formation of DA reactive metabolites is modified by changes in *CAPS2* gene expression (Reinhardt et al., 2013).

The third gene, CPNE8, encodes a Ca^{2+}-dependent, phospholipid-binding protein with intrinsic kinase activity known as Copine 8 that belongs to the family of Copine proteins (Maitra et al., 2003; Tomsig and Creutz, 2002). Despite their functions has not been studied in depth, Copines are thought to be involved in membrane trafficking because of their properties in phospholipid-binding as well as in signal transduction related to Ca^{2+} (Maitra et al., 2003; Tomsig and Creutz, 2002). The role of CPNE8 protein in membrane trafficking could be further investigated by determining the levels of CPNE protein associated to different membranous structures in the brain of LRRK2 transgenic mice and primary neuronal cultures as well as the different cellular processes that involve membrane trafficking such as endocytosis, secretion, lysosomal pathway, and autophagy. Several publications have already linked LRRK2 function to membrane trafficking processes. For example,

LRRK2 has been reported to regulate EndoA phosphorylation cycle in synaptic endocytosis (Matta et al., 2012), and lysosomal Ca^{2+} homeostasis with a downstream effect on autophagy regulated through a calcium-dependent pathway (Gomez-Suaga et al., 2012a; Gomez-Suaga et al., 2012b). In fact, pathogenic LRRK2 mutations have been shown to cause alterations in calcium homeostasis leading to dendrite mitophagy in neurons (Cherra et al., 2012). Taken together, all these data merit a closer look into the effect of Ca^{2+} chelation on the interplay between membrane trafficking processes, CPNE8 protein levels and LRRK2. Extended experiments could be focused on the effect of CPNE8 knockdown on membrane trafficking and Ca^{2+} homeostasis.

Finally, regulation of changes in UHRF2, CADPS2 and CPNE8 expression by LRRK2 through aberrant activation of ERK, might be investigated by specific knockdown of LRRK2 or ERK in the LRRK2 transgenic mice brain by intracranial lentiviral injections. This approach would allow examining the effect of LRRK2 or ERK on UHRF2, CADPS2 and CPNE8 protein levels in different regions of the brain as well as on the different processes in which UHRF2, CADPS2 and CPNE8 are involved.

In conclusion, further investigation of the pathophysiological function of LRRK2 could be addressed by studying in detail cellular processes at the molecular level in primary neuronal cultures, primary human skin fibroblasts, and LRRK2 transgenic mice. In the past years, LRRK2 has been suggested to regulate Ca^{2+} homeostasis, ERK activation, and EndoA proteins with a downstream effect on cellular processes related to membrane trafficking such as autophagy, lysosomes, and synaptic endocytosis (Carballo-Carbajal et al., 2010; Cherra et al., 2012; Gomez-Suaga et al., 2012a; Gomez-Suaga et al., 2012b; Matta et al., 2012; Reinhardt et al., 2013; Shin et al., 2008). In this work, primary hippocampal neurons derived from a Thy1.2-LRRK2 transgenic mouse model exhibited alterations in neurite outgrowth and branching complexity, suggesting a physiological function of LRRK2 in this process. Treatment of these neurons with pharmacologic compounds with known effect on neurite outgrowth is proposed to further decipher the mechanism underlying the observed

phenotype. Also, primary human skin fibroblasts were used to study LRRK2 function regulating cytoskeleton dynamics in cellular adhesion and locomotion, although, no alterations in any of those processes were observed. The analysis of other physiological changes in fibroblasts such as Ca^{2+} homeostasis, recently linked to LRRK2, would allow the formulation of further hypothesis regarding LRRK2 function as well as assessing whether these alterations could be used as a potential specific biomarker for PD. Validation of these changes in neuronal cultures could focus on Ca^{2+}-related cellular processes such as autophagy or regulation of lysosomal Ca^{2+} levels. The effect of the specific LRRK2 kinase inhibitor LRRK2-IN-1 used in primary hippocampal neurons and human skin fibroblasts suggested a function of LRRK2 regulating cytoskeleton arrangements and/or dynamics in a kinase-dependent manner in both cellular models. Detailed studies on LRRK2 interaction with the specific LRRK2 kinase inhibitor LRRK2-IN-1 in primary neuronal cultures, fibroblasts, and tissue lysates obtained from the Thy1.2-LRRK2 transgenic mice could be used to identify new substrates and interactor partners of LRRK2. Finally, other lines of investigation should be focused on two mechanisms recently described to underlie LRRK2 pathogenicity, (i) synaptic endocytosis and (ii) the interplay between LRRK2 and 3 genes (UHRF2, CADPS2 and CPNE8) recently identified to contribute to LRRK2 pathogenicity via activation of the ERK1/2 pathway (Reinhardt et al., 2013).

In this work, not only the recent progress made in the past years in the LRRK2 research field has been discussed in depth but also new insights into the physiological function of LRRK2 regulating cytoskeleton dynamics have been described and proposed in the present study. Still, many questions regarding the pathophysiological function of LRRK2 and the mechanisms underlying LRRK2-PD neuropathology remain unanswered. Therefore, current and future studies on LRRK2 function would be crucial to shed some light into the role of LRRK2 in the neuropathology of PD as well as for developing new therapeutic compounds for the treatment of the disease.

5 MATERIALS AND METHODS

5.1 Materials, Chemicals and Reagents

ABC Antibody-Kit (Rabbit)	Vectastain
Accumax	Millipore
Accustain	Accustain
Acetic acid (glacial) 100%	Merck
Acrylamide/Bis solution 40% (19:1)	Biorad
Agarose	Invitrogen
Ammonium persulfate (APS)	Sigma
BCA Protein Assay Kit	Pierce
Bovine Serum Albumin (BSA)	Roth
Bromphenol blue sodium salt (BPB)	Merck
B27-supplement	Gibco
Complete protease inhibitor cocktail	Roche
Coverslip, SuperFrost Plus	Fisher Scientific
DAB Substrate Kit	Vectorlabs
DABCO	Roth
Dimethylsulfoxide (DMSO)	Sigma
DNA 1kb ladder	NEB/Fermentas
Ethanol	Merck
Ethidium bromide (1% in water)	Merck
Fetal bovine serum gold (FBS)	PAA laboratories

Fluorescence mounting medium	Dako
Glycerol	AppliChem
GlutaMAX-1-supplement (100X)	Gibco
Hank's Balanced Salt Solution (HBSS)	Invitrogen
Hydrochloric acid (HCl)	Merck
Hybond-P polyvinyllidene difluoride (PVDF) membrane	Millipore
Hyperfilm ECL high performance chemiluminiscence	GE Healthcare
H2O2 30%	Roth
Immobilion Western HRP Substrate	Millipore
Ketamin	WDT
LightCycler I (32 samples)	Roche
Magnesium Chloride (MgCl)	Roth
Methanol	Merck
Natriumpyruvat	Sigma
Neurobasal-A medium	Gibco
N,N,N',N'-Tetramethylethylendiamine (TEMED)	Merck
Non fat milk powder Sucofin	(Edeka)
Normal Goat Serum (NGS)	Sigma
NuPAGE Novex Tris-Ace 3-8%	Invitrogen
Paraformaldehyde	Roth
PBS	PAA
PCR lysis buffer	Viagen

Penicilin/Streptomycin	Biochrom AG
Pertex	Merck
Phosphatase inhibitor cocktail	Roche
Poly-DL-Ornithine hydrobromide (PORN)	Sigma
Ponceau S Staining Solution	Sigma
Precision Plus Protein Standard, prestained	Biorad/Fermentas
Proteinase K	Roche
RNase Free DNase Set	Qiagen
RNeasy Lipid Tissue Mini Kit	Qiagen
RPMI-1640 medium	Biochrom
RPMI-1640 with HEPES medium	ATCC
Sedaxylen	WDT
Sodium chloride (NaCl)	Merck
Sodium dodecyl sulfate (SDS)	Sigma
Sodium hydroxide (NaOH)	Merck
Sucrose	Roth
Super pap pen	Daido Sangyo
SYBR Green	Invitrogen
Taq PCR Master Mix Kit	Qiagen
TritonX-100	AppliChem
TRIZMA® Base (Tris base)	Roth
Trypsin-EDTA 0.25%	Gibco

Tween-20	Merck
Vectastain Elite ABC Kit	Vectorlabs
Xylol	Roth
ß-FGF	Sigma
ß-Mercaptoethanol	Roth

5.2 Solutions, Buffers and Media

5.2.1 Molecular Biology

10X Loading Buffer

250mg bromphenol blue, 33mL 150mM Tris-base (pH 7.6), 60mL glycerol and 7mL ddH_2O.

Storage at 4°C.

10X TBE - Tris-Borat-EDTA Buffer

Dissolve 108mg Tris, 55g boric acid in 900mL ddH_2O. Add 40mL 0.5M Na2EDTA (pH 8.0) and bring total volume to 1L with ddH_2O.

1.5% Agarose

Dissolve 1.5g agarose in 100mL 1X TBE by microwave heating. After stirring and cooling down, add 2µL ethidium bromide.

5.2.2 Cell Biology

Cell Lysis Buffer

1% TritonX-100, 1X complete protease inhibitor complex, 1x phosphatase inhibitor cocktail in PBS.

Cell Freezing Media for Primary Skin Fibroblasts

10% DMSO, 90% Fetal bovine serum (FBS)

PORN - Poly-DL-Ornithine Hydrobromide

Dissolve 500mg PORN in 10mL PBS.

Culture Medium for Primary Hippocampal Neurons

1X GlutaMAX-I supplement (Gibco), 1X B27 supplement (Gibco), 5 ng/ml ßFGF (Sigma-Aldrich) and dimethyl-sulfoxide (Sigma-Aldrich) or 0.1µM LRRK2-IN-1 in Neurobasal-A medium (Gibco).

Culture Medium for Primary Skin Fibroblasts

- Cell Culture: 15% FBS (PAA), 1% penicillin/streptomycin (Biochrom AG) and 1.1% natriumpyruvat in RPMI-1640 media w/o Glutamine (Biochrom AG).

- Adhesion Assay Timeline: 1% FBS (PAA) or serum free, 1% penicillin/streptomycin (Biochrom AG) and 1.1% natriumpyruvat in RPMI-1640 media w/o Glutamine (Biochrom AG) and serum-free

- Adhesion Assay with specific LRRK2 inhibitor: 1% FBS (PAA), 1% penicillin/streptomycin (Biochrom AG) and 1.1% natriumpyruvat in RPMI-1640 media (Biochrom AG) or serum-free, 1% penicillin/streptomycin (Biochrom AG), 1.1% natriumpyruvat and DMSO or 0.1µM LRRK2-IN-1 in RPMI-1640 media w/o Glutamine (Biochrom AG).

- Migration Assay: containing 15% FBS, 1% penicillin/streptomycin, 1.1% natriumpyruvat and DMSO or 0.1µM LRRK2-IN-1 or 1µM LRRK2-IN-1 in RPMI-1640 medium with HEPES buffer (ATCC)

DMSO – Dimethyl Sulfoxide (vehicle)

2µL of media diluted into 198µL of DMSO

1 mM Specific LRRK2 Inhibitor (LRRK2-IN-1) Stock Solution

2µL of 100mM LRRK2-IN-1 stock solution diluted in 198µL DMSO

5.2.3 Protein Biochemistry

0.5M Tris Stacking Gel

Dissolve 30.3g Tris in 500mL ddH_2O (pH 6.8).

1.5M Tris Resolving Gel

Dissolve 90.85g Tris in 500mL ddH_2O (pH 8.8).

10% APS - Ammonium Persulfat

Dissolve 1g APS in 10mL ddH_2O. Use freshly made or store in aliquots at -20°C.

10% SDS - Sodium Dodecyl Sulfat

Dissolve 50g SDS in 500mL ddH_2O.

10X SDS-PAGE Running Buffer

Dissolve 30.2g Tris-base, 144g Glycine in 800mL ddH_2O. Add 100mL 10% SDS and bring total volume to 1L with ddH_2O. Store at 4°C.

10X Transfer Buffer

Dissolve 29g Tris-base, 144g Glycine in 1L ddH_2O.

4X SDS-PAGE Sample Buffer (4X Lämmli buffer)

2.5mL 1M Tris-Cl (pH 6.8), 4mL glycerol, 2mL 20% SDS, 250mg Bromphenol blue, 1mL ß-Mercaptoethanol adjusted to 10mL ddH_2O.

10X TBST - Tris Buffered Saline/0.1% Tween-20

Dissolve 12.11g Tris, 87.66g NaCl in 800mL ddH_2O. Add 1mL Tween-20 and bring total volume up to 1L with ddH_2O. Store at 4°C.

Western Blot Stripping Solution

Dissolve 7.57g Tris-base (pH 7.6), 20g SDS, 6.98mL ß-Mercaptoethanol in 1L ddH_2O.

5% Blocking Solution

5g non-fat milk powder in 100mL 1X TBST.

Primary Antibody Solution

Dilution of 1st Antibody in 5% (w/v) Non-Fat Milk Powder in 1X TBST.

Secondary Antibody Solution

Dilution of 2nd Antibody in 5% (w/v) Non-Fat Milk Powder in 1X TBST.

5.2.4 Histology

4% PFA – Paraformaldehyde

Dissolve 40g PFA in 800mL PBS on a stir plate under a ventilated hood. Heat while stirring to 60°C. Slowly raise the pH by adding NaOH until the PFA is dissolved and cool down on ice. Adjust the pH to 7.4 with HCl and bring volume to 1L with 1xPBS. Filter, aliquot and freeze at -80°C.

25% Sucrose

25g sucrose in 100mL PBS

Endogenous Peroxidase Blocking Solution

0.3% (v/v) H_2O_2 in PBS

PBST - Phosphate Buffered Saline/0.1% Tween-20 (washing solution)

0.5mL Tween-20 in 500mL 1xPBS

Blocking Solution

4% (v/v) normal goat serum (NGS), 0.4% (v/v) TritonX-100 in 1xPBS

Primary Antibody Solution

Dilute primary antibody in 2% (v/v) normal goat serum (NGS), 0.2% (v/v) TritonX-100 in 1xPBS

Secondary Antibody Solution

Dilute secondary antibody in 2% (v/v) normal goat serum (NGS), 0.2% (v/v) TritonX-100 in 1xPBS

Nissl Counterstain

0.1% (v/v) cresyl violet in ddH_2O. Add 1-2 drops of acetic acid/glacial.

Dehydration Solutions

95% ethanol: 95mL ethanol adjusted to 100mL ddH_2O.

100% ethanol: 100mL ethanol

100% xylol: 100mL xylol

5.3 Methods

5.3.1 Molecular Biology

I.Genotyping PCR (Polymerase Chain Reaction)

DNA Extraction

Mix ear punch with 7µL proteinase K (Roche) and 180µL PCR lysis buffer (Viagen) and incubate overnight at 56°C and 650rpm. Deactivation for 45 min at 85°C on water bath.

PCR Reaction

Taq PCR Master Mix Kit from Qiagen was used.

- 12.5µL Master Mix
- 5mL Q-solution
- 0.4µL primer Fwd (10 pmol/µL)
- 0.4µL primer Rev (10 pmol/µL)
- 2µL DNA
- 10.2µL ddH_2O

PCR Program

- 94°C for 2 min
- 94°C fro 30 sec
- 58°C for 1 min
- 72°C for 45 sec

} 35x times

- 72°C fro 5 min
- 12°C forever

Primer Sequences

Human LRRK2

- Fwd: 5'-GCC CTC AAG GTA AAT GGG GAC CCA C-3'

- Rev: 5'-CAT TGG CTG GAA ATG AGT GCA TGG C-3'

II. Light Cycler Semi-quantitative RT-PCR (Reverse Transcriptase Polymerase Chain Reaction)

RNA Extraction

Total RNA was extracted from hemi-brains of LRRK2 transgenic mice at embryonic day 14 and postnatal day 2, 7, 10, 15 and 21 using RNAeasy Lipid Tissue Mini Kit (Qiagen) and posterior treatment with RNase-free DNase Set (Qiagen) following manufacturer's recommendations.

Semi-quantitative RT-PCR

Semi-quantitative RT-PCR was performed in LightCycler (Roche) with QuantiTect SYBR Green RT-PCR (Qiagen). Briefly, 1µl of total RNA was reverse transcribed and amplified using QuantiTect SYBR Green RT-PCR Master mix (Qiagen).

RT-PCR Reaction

- 8.3µL ddH_2O
- 0.25µL primer Fwd
- 0.25µL primer Rev
- 1µL RNA
- 0.2µL Reverse Transcriptase
- 10µL CyBR

Semi-quantitative RT-PCR Program:

Reverse transcription: 25 min at 50°C,

PCR initial activation step: 15 min at 95°C,

Amplification for 45 cycles:

- Denaturation: 15 sec at 94°C,
- Annealing: 30 sec at 55°C and
- Extension: 30 sec at 72°C),

Melting Curve analysis: 60 sec at 95°C and 30 sec at 55°C

Cooling 30 sec at 40°C.

Semi-quantitative RT-PCR Primer Sequences:

Human LRRK2:

- Fwd:5'-TCC CTG CCA TAC GAG ATT ACC-3'

- Rev:5'-GCA CAT TTT TAC GCT CCG ATA-3'

Mouse LRRK2:

- Fwd:5'-CCA AGC AGA GCA AGC AAA GT-3'

- Rev:5'-GGC GTA CTG ACA TCG CCT AT-3'

Mouse HMBS (housekeeping gene):

- Fwd:5'-TCG GGG AAA CCT CAA CAC C-3'

- Rev:5'-CCT GGC CCA CAG CAT ACA T-3'

5.3.2 Cell Biology

5.3.2.1 Primary Hippocampal Culture

96-well Microplate Coating with Poly-DL-Ornithine Hydrobromide

100X Poly-DL-Ornithine hydrobromide (PORN) stock solution was diluted to 1X in PBS and 60µL/well was added and incubated for 1h at RT. PORN was removed and then washed 3 times with HBSS.

Dissection

Hippocampus from P0 mice was isolated and dissociated with 0.25% Trypsin/EDTA (Gibco) for 14 min at 37°C (waterbath). To stop Trypsin/EDTA reaction, 1mL of Neurobasal-A/GlutaMAX-I was added. Tissue fragments were washed 3 times with Neurobasal-A/GlutaMAX-I and after last wash step 500µL of Neurobasal-A/GlutaMAX-I were added. Tissue fragments were triturated pipetting up and down 10 times with a 200µL yellow tip. 5µL of cell suspension in a total volume of 100µL of medium was seeded into each well of a 96-well microplate (BD Falcon™).

Culture

Primary hippocampal neurons were grown on 96-well microplate (BD Falcon™) pre-coated with 0.5 mg/ml poly-DL-ornithine hydrobromide (Sigma, 500 mg) in media for primary hippocampal neurons. Media was changed every 2 days until cultures were fixed with PFA.

5.3.2.2 Neurite Outgrowth Assay

Immunocytochemistry,

Hippocampal neurons were fixed at DIV3, DIV7 or DIV14 with 3.7% PFA for 10 min at RT, washed twice with 1xPBS and permeabilized with 0.1% TritonX-100 in PBS for 5min at RT. Then, fixed neurons were washed twice with 1xPBS and blocked with 3% NGS in 1xPBS for 30 min at RT. Blocking solution was removed and 1st antibody Alexa Fluor 488 mouse anti-ß-Tubulin, Class III (1:50; BD Pharmingen™) diluted in 1xPBS was incubated for 1h at RT. Fixed neurons were washed 3 times with PBS, incubated with the nuclear marker Hoechst33342 diluted in 1xPBS (1:2000) for 1min at RT and washed twice with 1xPBS.

Image Acquisition and Neurite Outgrowth Analysis

Fluorescent images were captured using the BD Pathway™ 855 High-Content Bioimager (BD Bioscience) at 20X magnification and a montage of 25 adjoining images (5x5) per each well was obtained. Following image acquisition and using the BD AttoVision™ V1.6 Software (BD Bioscience) images were processed by setting up the segmentation parameters option of the software and then analyzed for neurite outgrowth (Figure 5.1) (Table 4).

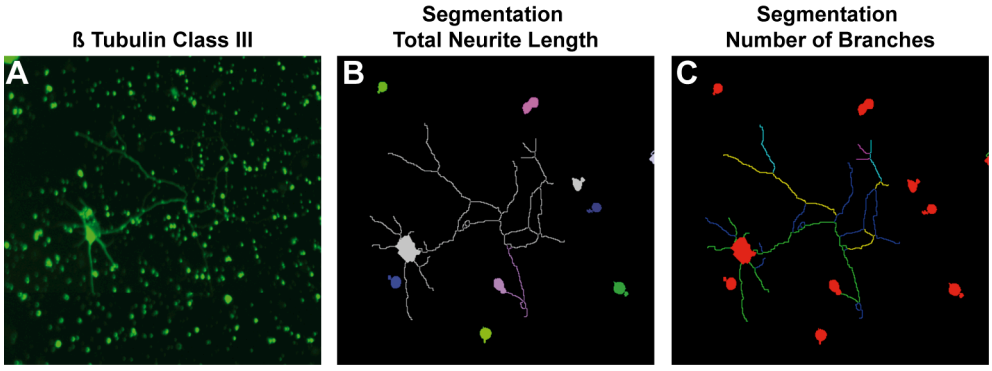

Figure 5.1 Image acquisition of primary hippocampal neurons derived from Thy1.2-LRRK2 transgenic mice with the BD Pathway 855 high content bioimager and segmentation analysis with the Attovision Software V1.6. **(A)** Image of ß-Tubulin Class III staining of primary hippocampal neurons derived from the Thy1.2-LRRK2 transgenic mice at DIV7 obtained with the BD Pathway 855 high content Bioimager. (**B)** Segmentation image obtained from Attovision Software showing total neurite length from LRRK2 hippocampal neurons corresponding to ß-tubulin III staining (A). (**A2-G2)** Segmentation image obtained from Attovision Software showing number of branches from LRRK2 hippocampal neurons corresponding to ß-tubulin III staining (A).

Neurite Outgrowth Parameters	Description
Neurite Maximum Length	Maximum length (pixels) of the longest neurite segment for each cell body.
Neurite Total Length	Total length (pixels) of all segments for each cell body.
Neurite Average Length	Average length (pixels) of all segments for each cell body. (Total length/segment count)
Neurite Tree Count	Number of neurite trees from cell body.
Neurite Branches Count	Total number of primary, secondary, tertiary, etc., branches per cell body.

Table 4 Neurite outgrowth parameters analyzed with the Attovision Software V1.6

5.3.2.3 Primary Human Skin Fibroblasts Culture

Human skin fibroblasts were obtained from the Biobank of the Hertie Institute for Clinical Brain Research. Fibroblasts were obtained with written informed consent from all subjects and the study was approved by the local medical ethics committee.

Human skin fibroblasts were obtained by biopsies from healthy subjects and LRRK2 Parkinson's Disease patients (Table 4) and cultured in RPMI-1640 media (Biochrom AG) containing 15% fetal bovine serum (PAA), 1% penicillin/streptomycin (Biochrom AG) and 1.1% natriumpyruvat (Sigma-Aldrich) at 37°C in 5% CO2. Culture media was changed every three or four days with passaging at 85-95% confluency.

5.3.2.4 Cellular Migration Assay

Cell Migration Cycle

Cell locomotion or migration of fibroblasts is an important event in wound healing and tissue repair which requires coordinated activity of actin-cytoskeletal, membrane, and adhesion systems (Vorotnikov, 2011). Cell migration is a complex and cyclic process which uses dynamic rearrangements of cytoskeleton and it is subdivided in four steps. The first step, ***protrusion***, starts with the polarization of the cell and the formation of cell membrane extensions, known as protrusions, driven by the polymerization of actin filaments (Figure 5.2

A). In the second step, ***adhesion***, protrusions are stabilized to the substrate by adhesions that link actin-cytoskeleton to the underlying extracellular matrix providing advance of the leading edge (Figure 5.2 B). The third step, ***traction***, is the contractile force generated by actomyosin to lead forward movement of the cell body and nucleus (Figure 5.2 C). The fourth and last step, ***retraction***, involves two distinct processes, rear detachment and retraction of the tail edge allowing the cell to move forward (Figure 5.2 D)(Vorotnikov, 2011).

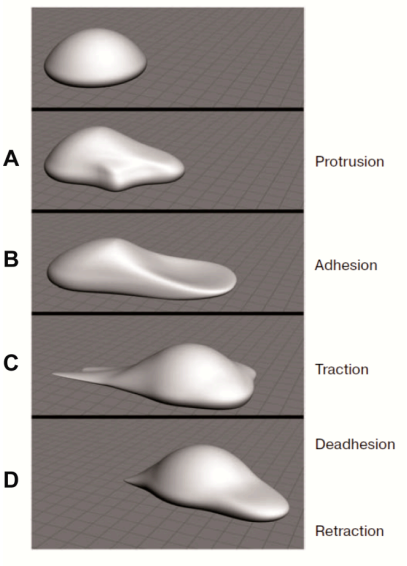

Figure 5.2 The cell cycle of migration in fibroblasts (modified from (Vorotnikov, 2011). Schematically shown the complex and cyclic process of cell migration which requires dynamic rearrangements of cytoskeleton: The cell cycle migration is initially started from unpolarized cells (top) that move following 4 cyclic steps: protrusion (A), adhesion (B), traction (C), and retraction (D).

Migration Assay Preparation

Human skin fibroblasts were plated on 48-well plate (Greiner bio-one) at the density of 50.000 cells/well, cultured with RPMI-1640 media containing 15% fetal bovine serum, 1% penicillin/streptomycin and 1.1% natriumpyruvat until they reached 95-100% confluency (approximately 1 week later). Then, the monolayer of fibroblasts was wounded with a linear scratch by a sterile 10-µl pipette tip. Fibroblasts were washed twice with RPMI-1640 medium with HEPES buffer (ATCC) containing 15% FBS, 1% penicillin/streptomycin and 1.1% natriumpyruvat and 500µL of the same medium containing DMSO (vehicle control), 0.1 and 1 µM LRRK2-IN-1 in DMSO was added.

Live Cell Imaging

The 48-well plate containing live fibroblasts were placed at the live cell Imager mircroscope (Zeiss) stage located inside a chamber maintaining the cells at 37°C and 5% CO_2 atmosphere Two different positions along the scratch/wound were monitored during 48h for each fibroblast line and condition, acquiring images every 30 min at 5X magnification with the brightfield lamp.

Migration Assay Analysis

The wounded area at 0, 12, 24 and 48 h was measured from each fibroblast line and condition with the free software ImageJ (National Institute of Health, USA). Briefly, stack images per each position were separated and single images corresponding to 0, 12, 24 and 48 h were stored as *.tif files (Figure 5.3 A). Each image was processed (Find Edge, Sharpen and Threshold) (Figure 5.3 B) and then the option analyze particle (Size pixel:100.000; Show: Outline) was chosen to calculate the area of the scratch/wound (Figure 5.3 C).

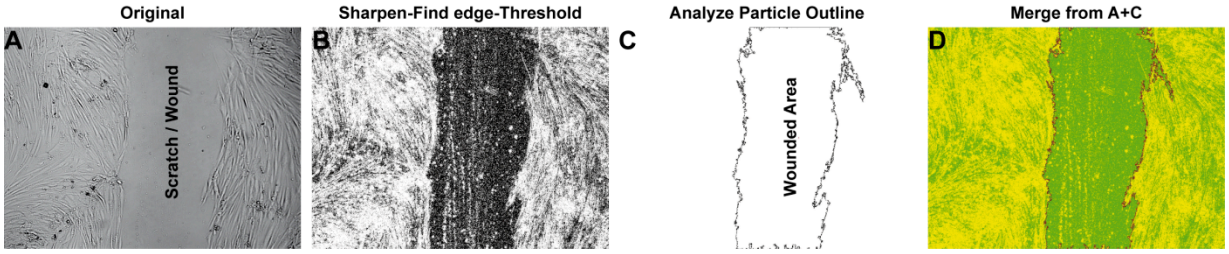

Figure 5.3 Migration assay analysis by ImageJ. (A) Original single image file showing the scratch/wound of the monolayer of fibroblasts. **(B)** Image after sharpening, find edge and threshold processing of the image in A. **(C)** Image corresponding to the outline of the scratch/wound from image A obtained after analysis. The outline of the scratch is used to measure the area of the scratch/wound (wounded area) by the ImageJ. **(D)** Merge image from A and C.

5.3.2.5 Cellular Adhesion Assay

Cellular Adhesion Process

Cellular adhesion is the second step of the cell locomotion cycle (Figure 5.2 B) and consists of the stabilization of membrane protrusion to the substrate linking the actin cytoskeleton to the underlying extracellular matrix. The strength of adhesions is spatially regulated inside moving cells, maintaining stronger attachments at the front and weaker toward the rear where they disengage, allowing forward movement of the cell (Vorotnikov, 2011). The strength of these adhesions determines the movement velocity of the cell where too weak or too strong adhesions result in slower migration being the optimal velocity reached at intermediate adhesion strength as a result of a proper balance ratio between protrusion and retraction at the rear (Lambrechts et al., 2004). The adhesion dynamics are primarily regulated through the Rho family small GTPases. Rac1 and Cdc42 control actin polymerization at the front and Rho regulates adhesion assembly by activation of myosin-II at the front and rear of the cells (Vorotnikov, 2011).

Primary Skin Fibroblasts Preparation

Human skin fibroblasts were cultured in RPMI-1640 media containing 1% fetal bovine serum, 1% penicillin/streptomycin and 1.1% natriumpyruvat at 37°C in 5% CO_2 for 3 hours. Afterwards, cells were washed twice with serum-free RPMI-1640 media containing 1% penicillin/streptomycin and 1.1% natriumpyruvat, followed by addition of Accumax (Millipore) for 10 min at 37°C to detached cells. Reaction was stopped by adding 3-4ml medium and cells were pelleted by centrifugation at 1500 rpm for 7 min and resuspended in 1ml serum-free medium for cell counting.

Adhesion AssayTimeline (Basal conditions)

For each fibroblast line, 2000 cells/well were plated on 96-well microplate (BD Falcon™) and incubated in a tissue culture incubator at 37°C and 5% CO_2. After 10 min, 30 min, 1h, 2h and 3h of incubation, cells were washed twice with 1xPBS (PAA), fixed with Accustain for 1 min (Sigma) and whased twice with 1xPBS.A seeding control was established at 3h of incubation where the cells were directly fixed with Accustain without prior washing with 1xPBS. For each time point, duplicates were used.

Adhesion Assay with Specific LRR2 Inhibitor

For each fibroblast line, 2000 cells/well were plated on 96-well microplate (BD Falcon™) with media containing DMSO (vehicle control), 0.1μM and 1μM LRRK2-IN-1 in DMSO, fixed 1 min with Accustain (Sigma) after 30 min and 2h of incubation at 37°C and washed twice with 1xPBS. For each time point, duplicates were used.

Immunocytochemistry, Image Acquisition and Adhesion Assay Analysis

Fixed fibroblasts were incubated with the nuclear marker Hoechst33342 diluted in 1xPBS (1:5000) for 10 min at RT and then washed twice with 1xPBS. Fluorescent images were captured using the BD Pathway™ 855 High-Content Bioimager (BD Bioscience) at 20X magnification and a montage of 25 not adjoining images (5x5 with 1000 μm gap) per each well was obtained (Figure 5.4 A). Following image acquisition and using the BD AttoVision™ V1.6 Software (BD Bioscience), images were first processed by setting up the segmentation parameters option of the software and then intensity of Hoechst33342 staining was measured and used as parameter to count number of adhered fibroblasts to the surface (Figure 5.4 B).

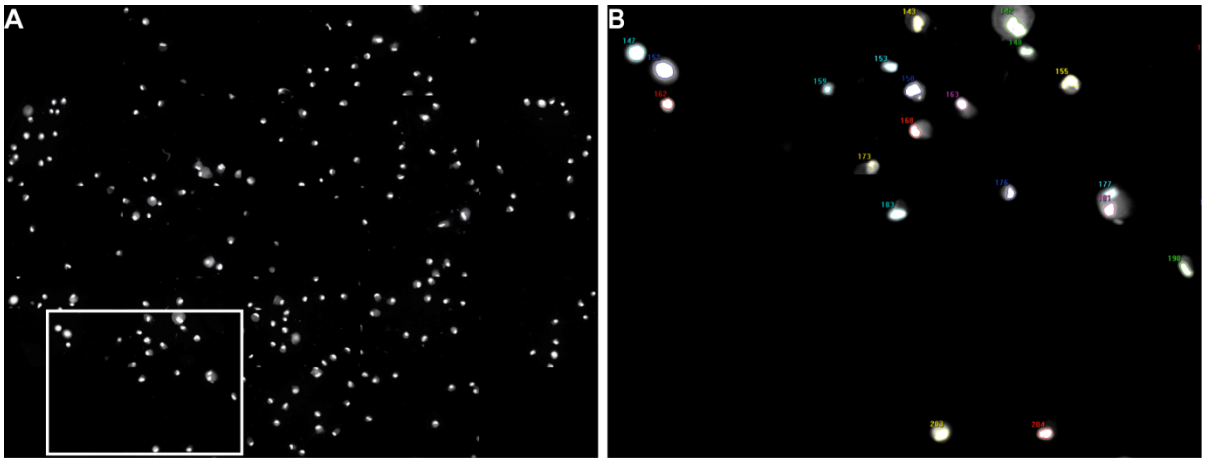

Figure 5.4 Adhesion assay analysis. (A) Image montage of 25 not adjoining images (5x5 with 1000 µm gap) from fibroblasts stained with Hoechst33342 obtained with the BD Pathway™ 855 High-Content Bioimager (BD Bioscience) at 20X. **(B)** Enlarged image of area selected in A and segmentation analysis from obtained from BD AttoVision™ V1.6 Software. The intensity of Hoechst33342 staining was used as a parameter to count the number of fibroblasts adhered to the surface.

5.3.3 Protein Biochemistry

5.3.3.1 Cell Lysis

Primary skin fibroblasts were incubated 3h in RPMI-1640 medium containing 1% FBS gold, 1% penicillin/streptomycin and 1.1% natriumpyruvat, washed twice with medium and incubated 2h with DMSO or 0.1µM LRRK2-IN1 in DMSO. Then, fibroblasts were incubated with Accumax for 10 min at RT to detached cells, reaction was stop with 3-4mL of medium, cells were collected and centrifuged at 1500 rpm for 7 min. Pelleted cells were resuspended in freshly made lysis buffer and rotated in a wheel for 1h at 12 rpm and 4°C. Then, samples were centrifuged for 15 min at 14.000 rpm and 4°C and protein concentration was measured using the BCA protein Assay Kit (Pierce Thermo Scientific) following manufacturer's instructions.

5.3.3.2 Brain Tissue Lysis

Whole brain and different brain regions from mice were homogenized with freshly made lysis buffer and kept on ice for 1h with shaking every 15 min. Then, samples were centrifuged for 15 min at 14.000 rpm and 4°C and protein concentration was measured using the BCA protein Assay Kit (Pierce Thermo Scientific) following manufacturer's instructions.

5.3.3.3 Western Blotting

SDS-Polyacrylamide-Gel Electrophoresis (SDS-PAGE)

Cell, whole brain and different brain regions lysate samples were mixed in 4X Lämmli sample buffer and load onto SDS-polyacrylamide gels. Gels consist of two parts, a 4% acrylamide stacking gel on top of a separating gel with range between 5 to 7% of acrylamide content (Table 5). To separate proteins accordingly to molecular weight, proteins were run through the gel at a constant voltage of 80 until proteins reached the bottom of the stacking gel and then, at a constant voltage of 100-120 thorough the separating gel.

Stacking Gel (for 2 gels)	**4%**
ddH_2O	2.3mL
40% Acrylamide	0.666mL
0.5M Tris (pH 6.8)	1mL
10% SDS	40µL
10% APS	40µL
TEMED	4µL

Separating Gel (for 1 gel)	**5%**	**6%**	**7%**
ddH_2O	2.79mL	2.7mL	2.54
40% Acrylamide	0.81ml	1mL	1.16mL
1.5M Tris (pH 8.8)	1.3mL	1.3mL	1.3mL
10% SDS	50µL	50µL	50µL
10% APS	50µL	50µL	50µL
TEMED	2µL	2µL	2µL

Table 5. Composition of SDS-polyacrylamide gels

Transfer and Immunoblotting

After SDS-PAGE electrophoresis, separated proteins were transfer onto polyvinylidenfluorid (PDVF) membranes previously activated with methanol and equilibrated with transfer buffer using a wet transfer. Transfer was performed over night at 4°C and at a constant voltage of 25. Then, membranes were blocked with blocking solution for 1h at RT and shaking, washed briefly with 1XTBST and incubated with primary antibody diluted in blocking solution over night at 4°C. Next day, membrane was washed 3 times (5 min each wash) with 1XTBST, incubated with secondary antibody diluted with blocking solution for 1h at RT and washed 3 times (5 min each wash) with 1XTBST. Immunoreactive signals were detected by chemiluminiscence HRP substrate (Immobilion Western HRP substrate) and images were acquired using development techniques in dark room using ECL high performance chemiluminiscenct hyperfilm (Amersham).

Stripping PDVF Membranes

To further re-probing the membrane with other antibodies, the membrane was stripped by incubation with stripping solution in water bath at 56°C and shaking for 20 min. Then, membranes were washed 3 times (10 min each wash) with 1xTBST and blocked 1h at RT with blocking solution. Then, immunoblotting was proceeded as above.

5.3.4 Histology

Intracardiacal Perfusion

LRRK2 transgenic mice and age-matched non-tg controls were anesthetized with Ketamin (120 mg/Kg) and Sedoxylen (10 mg/Kg) before intracardial perfusion with cold PBS and 4% paraformaldehyde (PFA).

Postfixation and Cryopreservation

Brains were post-fixed with 4% PFA overnight at 4°C, cryopreserved in 25% sucrose in PBS at 4°C until complete dehydration and stored at -80°C until use.

Cryosectioning

Coronal cryosections (20 µm width) in series of 6 were thawed onto glass slides (SuperFrost; VWR, Stockholm, Sweden) and stored at -20°C until use.

DAB-Staining

- Sections were washed 10 min in PBS to remove OCT embedding

- Endogenous peroxidases were blocked with 0.3% H_2O_2 in PBS for 20 minutes and then sections were washed 3 times in 0.1% tween-20 in 1xPBS (PBST) (5 min each wash).

- Blocking was done in 4% normal goat serum (NGS) and 0.4% Triton X-100 (Carl Roth) in PBS for 1h at RT.

- 1st Antibody: tyrosine hydroxylase antibody (1:1000; Pel-Freez Biologicals) was incubated with 2% NGS and 0.2% Triton X-100 in 1xPBS overnight at 4°C. Next day, sections were washed 3 times with PBST (5 min each wash)

- 2nd Antibody: biotinylated goat anti-rabbit (1:200, Vector Labs) was incubated with 2% NGS and 0.2% Triton X-100 in 1xPBS for 1h at RT .Then, sections were washed 3 times with PBST (5 min each wash).

- AB complex (Vectastain Elite ABC kit, Vector Labs) was prepared 30 min before use as follow: for 1mL of 1xPBS, 10µL Avidin and 10µL Biotin were mixed, incubated for 90 min on sections and then washed 3 times with PBST (5 min each wash).

- Substrate incubation in DAB (DAB substrate kit for peroxidases, Vector Labs): 5mL ddH_2O were mixed with 2 drops of buffer stock solution. Then, 4 drops of DAB and 2 drops of H_2O_2 were added and mixed. Solution was incubated 2 min on sections and then washed 5 min with 1xPBS.

- Nissl counterstain: 2 drops of acetic acid/glacial were added into 10mL of 0.1% Cresyl-violet and the mixed solution was incubated on the sections for 30 minute at RT. Then sections were washed 5 min in ddH_2O.

- Sections were dehydrated 5 min in 95% ethanol, 5 min in 100% ethanol, and 5 min in 100% xylol.

- Sections were mounted with Pertex mounting medium (Medite Gmbh).

Stereology

Unbiased stereology and genotype blinded system was used to count TH+ and Nissl+ neurons in SNpc from both hemispheres of every sixth section, counting a total number of 8 sections per brain. Quantification was performed with the Stereo Investigator Software (MBF Bioscience, Williston, VT, USA) with optical fractionator probe connected to an Axioplan2 microscope (Carl Zeiss) and Axiocam MRm Camera (Carl Zeiss). A 40 x 40 µm counting frame size, a 100 x100 µm grid size, a 16 µm dissector height and 2 µm guard was used.

5.4 Antibodies

Antibody	Target	Source	Dilution	Manufacturer	Catalogue No.
Primary	LRRK2 (H)	Rb	WB: 1/1000	Novus Biologicals	NB300-267
	LRRK2 (H, M)	Rb	WB:1/1000	Home made	
	LRRK2 (H, M, R)	Rb	WB: 1/1000	Epitomics (clone C41-2)	3514-1
	LRRK2 (H)	Rb	WB: 1/500	Epitomics (clone c68-7)	
	ß-Tubulin-III	M	WB: 1/5000	Sigma	T2200
	Tyrosine Hydroxilase (TH)	Rb	IHC: 1/1000	Pel-Freez Biologicals	P40101-0
	Vinculin	M	WB: 1/100000	Sigma-Aldrich	V9131
	Hoechst33342		IF: 1/2000 1/5000	Molecular Probes	H1399
Secondary	anti-mouse-HRP	G	WB: 1/5000	Jackson ImmunoResearch	70380
	anti-rabbit-HRP	G	WB: 1/5000	Dako	P0448
	Biotynilated anti-rabbit	G	IHC:1/200	VectorLabs	115-035-003
Conjugated	Alexa Fluor 488 mouse ß-tubulin Class III	mouse	IF: 1/50	BD Pharmingen	560338

H, human; M, mouse; Rb, rabbit; G, goat; WB, western blot; IHC, immunohistochemistry;IF, Immunofluorescence

Table 6. List of antibodies used.

5.5 Thy1.2-LRRK2 Transgenic Mice

The local animal welfare and ethics committee of the country commission Tübingen approved all experiments and procedures. To perform the experiments heterozygote mice from the WT04 line (LRRK2 WT) and Mut01 and Mut18 lines (LRRK2 G2019S) from Thy1.2-LRRK2 transgenic mice of C57BL/6 background and aged matched wild-type controls were used. The transgenic mice expressed the human full-length LRRK2 wild-type or G2019S under control of the CNS neuron specific Thy1.2 promotor expression cassette and were generated in the Department of Cellular Neurology, Llaboratory of Prof. Dr. Jucker at the Hertie Institute for Clinical Brain Research, Tübingen, Germany.

5.6 Statistical Analysis

5.6.1 Neurite Outgrowth Statistical Analysis

Several parameters for neurite outgrowth analysis (see Table X) were measured by the BD AttoVision™ V1.6 Software (BD Bioscience) and then statistically analyzed with SPSS (independent *t*- test) and GraphPad Prism V5 (two-way ANOVA with Tukey's *post hoc* test).

5.6.2 Adhesion Assay Statistical Analysis

Per each time point and/or condition the number of fibroblasts adhered to the surface was expressed as percentage of total number of fibroblasts seeded per well and the results obtained from duplicate wells were averaged. Then, per each independent experiment, all fibroblast lines from healthy-control subjects and all fibroblast lines from each LRRK2-PD mutations were averaged. Final data represent mean ± SEM; n=3-4 independent experiments. WT LRRK2 (Healthy-control Subjects) = 4 fibroblast lines; G2019S LRRK2 = 3 fibroblast lines; I2020T LRRK2 = 1 fibroblast line; N1437S LRRK2 = 2 fibroblast lines; R1441C LRRK2 patients = 1 fibroblast line. Results were statistically analyzed with GraphPad Prism V5 (two-way ANOVA with repeated measures and two-way ANOVA with Tukey's *post hoc* test).

5.6.3 Migration Assay Statistical Analysis

Two positions over the scratch were monitored over 48 h per each fibroblast line and condition, then the measurements from the wounded area obtained from each fibroblast line and time point were averaged and data was expressed as percentage of wounded area relative to the wounded area at 0h in the same fibroblast line and condition. Then, per each independent experiment, the results obtained from all fibroblast lines from healthy-control subjects and all fibroblast lines from each LRRK2-PD mutation were averaged. Final data represent mean ± SEM; n=2 independent experiments. WT LRRK2 (Healthy-control Subjects) = 4 fibroblast lines; G2019S LRRK2 = 3 fibroblast lines; I2020T LRRK2 = 1 fibroblast line; N1437S LRRK2 = 2 fibroblast lines; R1441C LRRK2 patients = 1 fibroblast line.

5.6.4 Stereology Statistical Analysis

Results obtained from stereologic TH+ and Nissl+ counting were statistical analyzed with GraphPad Prims V5 (one-way ANOVA with Tukey's *post hoc* test).

6 REFERENCES

Aigner, L., et al., 1995. Overexpression of the neural growth-associated protein GAP-43 induces nerve sprouting in the adult nervous system of transgenic mice. Cell. 83, 269-78.

Alves, G., et al., 2008. Epidemiology of Parkinson's disease. Journal of neurology. 255 Suppl 5, 18-32.

Anand, V. S., Braithwaite, S. P., 2009. LRRK2 in Parkinson's disease: biochemical functions. The FEBS journal. 276, 6428-35.

Anand, V. S., et al., 2009. Investigation of leucine-rich repeat kinase 2 : enzymological properties and novel assays. The FEBS journal. 276, 466-78.

Andra, K., et al., 1996. Expression of APP in transgenic mice: a comparison of neuron-specific promoters. Neurobiol Aging. 17, 183-90.

Andres-Mateos, E., et al., 2009. Unexpected lack of hypersensitivity in LRRK2 knock-out mice to MPTP (1-methyl-4-phenyl-1,2,3,6-tetrahydropyridine). The Journal of neuroscience : the official journal of the Society for Neuroscience. 29, 15846-50.

Auburger, G., et al., 2012a. Primary skin fibroblasts as a model of Parkinson's disease. Mol Neurobiol. 46, 20-7.

Auburger, G., et al., 2012b. Primary Skin Fibroblasts as a Model of Parkinson's Disease. Molecular neurobiology.

Beaudoin, G. M., 3rd, et al., 2012. Culturing pyramidal neurons from the early postnatal mouse hippocampus and cortex. Nat Protoc. 7, 1741-54.

Bekris, L. M., et al., 2010. The genetics of Parkinson disease. Journal of geriatric psychiatry and neurology. 23, 228-42.

Berger, Z., et al., 2010. Membrane localization of LRRK2 is associated with increased formation of the highly active LRRK2 dimer and changes in its phosphorylation. Biochemistry. 49, 5511-23.

Berwick, D. C., Harvey, K., 2011. LRRK2 signaling pathways: the key to unlocking neurodegeneration? Trends Cell Biol. 21, 257-65.

Berwick, D. C., Harvey, K., 2012. LRRK2 functions as a Wnt signaling scaffold, bridging cytosolic proteins and membrane-localized LRP6. Hum Mol Genet. 21, 4966-79.

Biskup, S., et al., 2006. Localization of LRRK2 to membranous and vesicular structures in mammalian brain. Annals of neurology. 60, 557-69.

Biskup, S., et al., 2007. Dynamic and redundant regulation of LRRK2 and LRRK1 expression. BMC neuroscience. 8, 102.

Bohlhalter, S., Kaegi, G., 2011. Parkinsonism: heterogeneity of a common neurological syndrome. Swiss medical weekly. 141, w13293.

Braak, H., et al., 2004. Stages in the development of Parkinson's disease-related pathology. Cell and tissue research. 318, 121-34.

Bravo-San Pedro, J. M., et al., 2013. The LRRK2 G2019S mutant exacerbates basal autophagy through activation of the MEK/ERK pathway. Cell Mol Life Sci. 70, 121-36.

Campsall, K. D., et al., 2002. Characterization of transgene expression and Cre recombinase activity in a panel of Thy-1 promoter-Cre transgenic mice. Dev Dyn. 224, 135-43.

Carballo-Carbajal, I., et al., 2010. Leucine-rich repeat kinase 2 induces alpha-synuclein expression via the extracellular signal-regulated kinase pathway. Cell Signal. 22, 821-7.

Chan, D., et al., 2011. Rac1 protein rescues neurite retraction caused by G2019S leucine-rich repeat kinase 2 (LRRK2). The Journal of biological chemistry. 286, 16140-9.

Chen, C. Y., et al., 2012. (G2019S) LRRK2 activates MKK4-JNK pathway and causes degeneration of SN dopaminergic neurons in a transgenic mouse model of PD. Cell death and differentiation. 19, 1623-33.

Cherra, S. J., 3rd, et al., 2012. Mutant LRRK2 Elicits Calcium Imbalance and Depletion of Dendritic Mitochondria in Neurons. Am J Pathol.

Cheung, G., Cousin, M. A., 2011. Quantitative analysis of synaptic vesicle pool replenishment in cultured cerebellar granule neurons using FM dyes. J Vis Exp.

Connolly, G. P., 1998. Fibroblast models of neurological disorders: fluorescence measurement studies. Trends Pharmacol Sci. 19, 171-7.

Cookson, M. R., 2010. The role of leucine-rich repeat kinase 2 (LRRK2) in Parkinson's disease. Nat Rev Neurosci. 11, 791-7.

Dachsel, J. C., et al., 2010. A comparative study of Lrrk2 function in primary neuronal cultures. Parkinsonism & related disorders. 16, 650-5.

Daniels, V., et al., 2011a. On the road to leucine-rich repeat kinase 2 signalling: evidence from cellular and in vivo studies. Neurosignals. 19, 1-15.

Daniels, V., et al., 2011b. Insight into the mode of action of the LRRK2 Y1699C pathogenic mutant. J Neurochem. 116, 304-15.

Dauer, W., Przedborski, S., 2003. Parkinson's disease: mechanisms and models. Neuron. 39, 889-909.

Deng, J., et al., 2008. Structure of the ROC domain from the Parkinson's disease-associated leucine-rich repeat kinase 2 reveals a dimeric GTPase. Proceedings of the National Academy of Sciences of the United States of America. 105, 1499-504.

Deng, X., et al., 2011. Characterization of a selective inhibitor of the Parkinson's disease kinase LRRK2. Nature chemical biology. 7, 203-5.

Ding, X., Goldberg, M. S., 2009. Regulation of LRRK2 stability by the E3 ubiquitin ligase CHIP. PLoS One. 4, e5949.

Dzamko, N., et al., 2010. Inhibition of LRRK2 kinase activity leads to dephosphorylation of Ser(910)/Ser(935), disruption of 14-3-3 binding and altered cytoplasmic localization. Biochem J. 430, 405-13.

Fahn, S., 2003. Description of Parkinson's disease as a clinical syndrome. Annals of the New York Academy of Sciences. 991, 1-14.

Fahn, S., 2008a. The history of dopamine and levodopa in the treatment of Parkinson's disease. Movement disorders : official journal of the Movement Disorder Society. 23 Suppl 3, S497-508.

Fahn, S., 2008b. How do you treat motor complications in Parkinson's disease: Medicine, surgery, or both? Annals of neurology. 64 Suppl 2, S56-64.

Farrer, M. J., 2006. Genetics of Parkinson disease: paradigm shifts and future prospects. Nat Rev Genet. 7, 306-18.

Fasano, A., et al., 2012. Treatment of motor and non-motor features of Parkinson's disease with deep brain stimulation. Lancet neurology. 11, 429-42.

Fasano, C., et al., 2008. Culture of postnatal mesencephalic dopamine neurons on an astrocyte monolayer. Curr Protoc Neurosci. Chapter 3, Unit 3 21.

Funayama, M., et al., 2002. A new locus for Parkinson's disease (PARK8) maps to chromosome 12p11.2-q13.1. Annals of neurology. 51, 296-301.

Galter, D., et al., 2006. LRRK2 expression linked to dopamine-innervated areas. Ann Neurol. 59, 714-9.

Gama Sosa, M. A., et al., 2010. Animal transgenesis: an overview. Brain Struct Funct. 214, 91-109.

Gandhi, P. N., et al., 2008. The Roc domain of leucine-rich repeat kinase 2 is sufficient for interaction with microtubules. J Neurosci Res. 86, 1711-20.

Gandhi, S., Wood, N. W., 2005. Molecular pathogenesis of Parkinson's disease. Human molecular genetics. 14, 2749-55.

Gao, H. M., Hong, J. S., 2011. Gene-environment interactions: key to unraveling the mystery of Parkinson's disease. Progress in neurobiology. 94, 1-19.

Gasser, T., et al., 2011. Milestones in PD genetics. Movement disorders : official journal of the Movement Disorder Society. 26, 1042-8.

Giguere, V., et al., 1985. Structure of the murine Thy-1 gene. EMBO J. 4, 2017-24.

Gillardon, F., 2009. Leucine-rich repeat kinase 2 phosphorylates brain tubulin-beta isoforms and modulates microtubule stability--a point of convergence in parkinsonian neurodegeneration? J Neurochem. 110, 1514-22.

Gloeckner, C. J., et al., 2010. Phosphopeptide analysis reveals two discrete clusters of phosphorylation in the N-terminus and the Roc domain of the Parkinson-disease associated protein kinase LRRK2. J Proteome Res. 9, 1738-45.

Gloeckner, C. J., et al., 2006. The Parkinson disease causing LRRK2 mutation I2020T is associated with increased kinase activity. Human molecular genetics. 15, 223-32.

Gloeckner, C. J., et al., 2009. The Parkinson disease-associated protein kinase LRRK2 exhibits MAPKKK activity and phosphorylates MKK3/6 and MKK4/7, in vitro. J Neurochem. 109, 959-68.

Gomez-Suaga, P., et al., 2012a. A link between LRRK2, autophagy and NAADP-mediated endolysosomal calcium signalling. Biochem Soc Trans. 40, 1140-6.

Gomez-Suaga, P., et al., 2012b. Leucine-rich repeat kinase 2 regulates autophagy through a calcium-dependent pathway involving NAADP. Hum Mol Genet. 21, 511-25.

Gordon, J. W., et al., 1987. Regulation of Thy-1 gene expression in transgenic mice. Cell. 50, 445-52.

Greggio, E., et al., 2006. Kinase activity is required for the toxic effects of mutant LRRK2/dardarin. Neurobiol Dis. 23, 329-41.

Greggio, E., et al., 2009. The Parkinson's disease kinase LRRK2 autophosphorylates its GTPase domain at multiple sites. Biochem Biophys Res Commun. 389, 449-54.

Greggio, E., et al., 2008. The Parkinson disease-associated leucine-rich repeat kinase 2 (LRRK2) is a dimer that undergoes intramolecular autophosphorylation. The Journal of biological chemistry. 283, 16906-14.

Guo, L., et al., 2007. The Parkinson's disease-associated protein, leucine-rich repeat kinase 2 (LRRK2), is an authentic GTPase that stimulates kinase activity. Experimental cell research. 313, 3658-70.

Habig, K., et al., 2008. RNA interference of LRRK2-microarray expression analysis of a Parkinson's disease key player. Neurogenetics. 9, 83-94.

Haebig, K., et al., 2010. ARHGEF7 (Beta-PIX) acts as guanine nucleotide exchange factor for leucine-rich repeat kinase 2. PloS one. 5, e13762.

Han, B. S., et al., 2008. Expression of the LRRK2 gene in the midbrain dopaminergic neurons of the substantia nigra. Neurosci Lett. 442, 190-4.

Heasman, S. J., Ridley, A. J., 2008. Mammalian Rho GTPases: new insights into their functions from in vivo studies. Nature reviews. Molecular cell biology. 9, 690-701.

Heutink, P., Verhage, M., 2012. Neurodegeneration: new road leads back to the synapse. Neuron. 75, 935-8.

Higashi, S., et al., 2007a. Localization of Parkinson's disease-associated LRRK2 in normal and pathological human brain. Brain Res. 1155, 208-19.

Higashi, S., et al., 2007b. Expression and localization of Parkinson's disease-associated leucine-rich repeat kinase 2 in the mouse brain. Journal of neurochemistry. 100, 368-81.

Hinkle, K. M., et al., 2012. LRRK2 knockout mice have an intact dopaminergic system but display alterations in exploratory and motor co-ordination behaviors. Molecular neurodegeneration. 7, 25.

Ho, C. C., et al., 2009. The Parkinson disease protein leucine-rich repeat kinase 2 transduces death signals via Fas-associated protein with death domain and caspase-8 in a cellular model of neurodegeneration. J Neurosci. 29, 1011-6.

Hoepken, H. H., et al., 2008. Parkinson patient fibroblasts show increased alpha-synuclein expression. Experimental neurology. 212, 307-13.

Hsu, C. H., et al., 2010. MKK6 binds and regulates expression of Parkinson's disease-related protein LRRK2. J Neurochem. 112, 1593-604.

Hubbard, S. R., Till, J. H., 2000. Protein tyrosine kinase structure and function. Annu Rev Biochem. 69, 373-98.

Imai, Y., et al., 2008. Phosphorylation of 4E-BP by LRRK2 affects the maintenance of dopaminergic neurons in Drosophila. EMBO J. 27, 2432-43.

Ito, G., et al., 2007. GTP binding is essential to the protein kinase activity of LRRK2, a causative gene product for familial Parkinson's disease. Biochemistry. 46, 1380-8.

Jaleel, M., et al., 2007. LRRK2 phosphorylates moesin at threonine-558: characterization of how Parkinson's disease mutants affect kinase activity. The Biochemical journal. 405, 307-17.

Kahle, P. J., 2008. alpha-Synucleinopathy models and human neuropathology: similarities and differences. Acta Neuropathol. 115, 87-95.

Kett, L. R., Dauer, W. T., 2012. Leucine-rich repeat kinase 2 for beginners: six key questions. Cold Spring Harbor perspectives in medicine. 2, a009407.

Klein, C., Westenberger, A., 2012. Genetics of Parkinson's disease. Cold Spring Harbor perspectives in medicine. 2, a008888.

Klein, C. L., et al., 2009. Homo- and heterodimerization of ROCO kinases: LRRK2 kinase inhibition by the LRRK2 ROCO fragment. J Neurochem. 111, 703-15.

Ko, H. S., et al., 2009. CHIP regulates leucine-rich repeat kinase-2 ubiquitination, degradation, and toxicity. Proc Natl Acad Sci U S A. 106, 2897-902.

Kumar, A., Cookson, M. R., 2011. Role of LRRK2 kinase dysfunction in Parkinson disease. Expert reviews in molecular medicine. 13, e20.

Lambrechts, A., et al., 2004. The actin cytoskeleton in normal and pathological cell motility. The international journal of biochemistry & cell biology. 36, 1890-909.

Lang, A. E., Lozano, A. M., 1998. Parkinson's disease. Second of two parts. The New England journal of medicine. 339, 1130-43.

Langston, J. W., et al., 1983. Chronic Parkinsonism in humans due to a product of meperidine-analog synthesis. Science. 219, 979-80.

Lee, B. D., et al., 2010. Inhibitors of leucine-rich repeat kinase-2 protect against models of Parkinson's disease. Nature medicine. 16, 998-1000.

Lees, A. J., et al., 2009. Parkinson's disease. Lancet. 373, 2055-66.

Lesage, S., et al., 2006. LRRK2 G2019S as a cause of Parkinson's disease in North African Arabs. N Engl J Med. 354, 422-3.

Lewis, P. A., et al., 2007. The R1441C mutation of LRRK2 disrupts GTP hydrolysis. Biochem Biophys Res Commun. 357, 668-71.

Li, T., et al., 2011. Models for LRRK2-Linked Parkinsonism. Parkinsons Dis. 2011, 942412.

Li, X., et al., 2010. Enhanced striatal dopamine transmission and motor performance with LRRK2 overexpression in mice is eliminated by familial Parkinson's disease mutation G2019S. The Journal of neuroscience : the official journal of the Society for Neuroscience. 30, 1788-97.

Li, X., et al., 2007. Leucine-rich repeat kinase 2 (LRRK2)/PARK8 possesses GTPase activity that is altered in familial Parkinson's disease R1441C/G mutants. J Neurochem. 103, 238-47.

Li, Y., et al., 2009. Mutant LRRK2(R1441G) BAC transgenic mice recapitulate cardinal features of Parkinson's disease. Nature neuroscience. 12, 826-8.

Lin, C. H., et al., 2010. LRRK2 G2019S mutation induces dendrite degeneration through mislocalization and phosphorylation of tau by recruiting autoactivated GSK3ss. J Neurosci. 30, 13138-49.

Lin, X., et al., 2009. Leucine-rich repeat kinase 2 regulates the progression of neuropathology induced by Parkinson's-disease-related mutant alpha-synuclein. Neuron. 64, 807-27.

Luzon-Toro, B., et al., 2007. Mechanistic insight into the dominant mode of the Parkinson's disease-associated G2019S LRRK2 mutation. Hum Mol Genet. 16, 2031-9.

Mackay, D. J., Hall, A., 1998. Rho GTPases. The Journal of biological chemistry. 273, 20685-8.

MacLeod, D., et al., 2006. The familial Parkinsonism gene LRRK2 regulates neurite process morphology. Neuron. 52, 587-93.

Maekawa, T., et al., 2012. The I2020T Leucine-rich repeat kinase 2 transgenic mouse exhibits impaired locomotive ability accompanied by dopaminergic neuron abnormalities. Molecular neurodegeneration. 7, 15.

Mahadik, S. P., et al., 1994. Decreased adhesiveness and altered cellular distribution of fibronectin in fibroblasts from schizophrenic patients. Psychiatry research. 53, 87-97.

Maitra, R., et al., 2003. Cloning, molecular characterization, and expression analysis of Copine 8. Biochem Biophys Res Commun. 303, 842-7.

Marin, I., et al., 2008. The Roco protein family: a functional perspective. FASEB journal : official publication of the Federation of American Societies for Experimental Biology. 22, 3103-10.

Masliah, E., et al., 2000. Dopaminergic loss and inclusion body formation in alpha-synuclein mice: implications for neurodegenerative disorders. Science. 287, 1265-9.

Mata, I. F., et al., 2006. LRRK2 in Parkinson's disease: protein domains and functional insights. Trends in neurosciences. 29, 286-93.

Matta, S., et al., 2012. LRRK2 controls an EndoA phosphorylation cycle in synaptic endocytosis. Neuron. 75, 1008-21.

Meixner, A., et al., 2011. A QUICK screen for Lrrk2 interaction partners--leucine-rich repeat kinase 2 is involved in actin cytoskeleton dynamics. Molecular & cellular proteomics : MCP. 10, M110 001172.

Melrose, H. L., et al., 2010. Impaired dopaminergic neurotransmission and microtubule-associated protein tau alterations in human LRRK2 transgenic mice. Neurobiology of disease. 40, 503-17.

Melrose, H. L., et al., 2007. A comparative analysis of leucine-rich repeat kinase 2 (Lrrk2) expression in mouse brain and Lewy body disease. Neuroscience. 147, 1047-58.

Mitchison, T. J., Cramer, L. P., 1996. Actin-based cell motility and cell locomotion. Cell. 84, 371-9.

Moore, D. J., 2008. The biology and pathobiology of LRRK2: implications for Parkinson's disease. Parkinsonism Relat Disord. 14 Suppl 2, S92-8.

Napolitano, A., et al., 2011. Oxidation chemistry of catecholamines and neuronal degeneration: an update. Curr Med Chem. 18, 1832-45.

Nichols, R. J., et al., 2009. Substrate specificity and inhibitors of LRRK2, a protein kinase mutated in Parkinson's disease. Biochem J. 424, 47-60.

Nichols, R. J., et al., 2010. 14-3-3 binding to LRRK2 is disrupted by multiple Parkinson's disease-associated mutations and regulates cytoplasmic localization. Biochem J. 430, 393-404.

Obeso, J. A., et al., 2010. Missing pieces in the Parkinson's disease puzzle. Nature medicine. 16, 653-61.

Okabe, S., 2001. Gene expression in transgenic mice using neural promoters. Curr Protoc Neurosci. Chapter 3, Unit 3 16.

Ozelius, L. J., et al., 2006. LRRK2 G2019S as a cause of Parkinson's disease in Ashkenazi Jews. N Engl J Med. 354, 424-5.

Paisan-Ruiz, C., et al., 2004. Cloning of the gene containing mutations that cause PARK8-linked Parkinson's disease. Neuron. 44, 595-600.

Parent, M., Parent, A., 2010. Substantia nigra and Parkinson's disease: a brief history of their long and intimate relationship. The Canadian journal of neurological sciences. Le journal canadien des sciences neurologiques. 37, 313-9.

Parisiadou, L., Cai, H., 2010. LRRK2 function on actin and microtubule dynamics in Parkinson disease. Communicative & integrative biology. 3, 396-400.

Parisiadou, L., et al., 2009. Phosphorylation of ezrin/radixin/moesin proteins by LRRK2 promotes the rearrangement of actin cytoskeleton in neuronal morphogenesis. The Journal of neuroscience : the official journal of the Society for Neuroscience. 29, 13971-80.

Parkinson, J., 2002. An essay on the shaking palsy. 1817. The Journal of neuropsychiatry and clinical neurosciences. 14, 223-36; discussion 222.

Plowey, E. D., et al., 2008. Role of autophagy in G2019S-LRRK2-associated neurite shortening in differentiated SH-SY5Y cells. Journal of neurochemistry. 105, 1048-56.

Ramonet, D., et al., 2011. Dopaminergic neuronal loss, reduced neurite complexity and autophagic abnormalities in transgenic mice expressing G2019S mutant LRRK2. PloS one. 6, e18568.

Rayport, S., et al., 1992. Identified postnatal mesolimbic dopamine neurons in culture: morphology and electrophysiology. J Neurosci. 12, 4264-80.

Reichling, L. J., Riddle, S. M., 2009. Leucine-rich repeat kinase 2 mutants I2020T and G2019S exhibit altered kinase inhibitor sensitivity. Biochemical and biophysical research communications. 384, 255-8.

Reinhardt, P., et al., 2013. Genetic correction of a LRRK2 mutation in human iPSCs links parkinsonian neurodegeneration to ERK-dependent changes in gene expression. Cell Stem Cell. 12, 354-67.

Ross, O. A., et al., 2011. Association of LRRK2 exonic variants with susceptibility to Parkinson's disease: a case-control study. Lancet Neurol. 10, 898-908.

Rudenko, I. N., et al., 2012. Is inhibition of kinase activity the only therapeutic strategy for LRRK2-associated Parkinson's disease? BMC Med. 10, 20.

Samii, A., et al., 2004. Parkinson's disease. Lancet. 363, 1783-93.

Sanchez-Danes, A., et al., 2012. Disease-specific phenotypes in dopamine neurons from human iPS-based models of genetic and sporadic Parkinson's disease. EMBO molecular medicine. 4, 380-95.

Sancho, R. M., et al., 2009. Mutations in the LRRK2 Roc-COR tandem domain link Parkinson's disease to Wnt signalling pathways. Hum Mol Genet. 18, 3955-68.

Satake, W., et al., 2009. Genome-wide association study identifies common variants at four loci as genetic risk factors for Parkinson's disease. Nat Genet. 41, 1303-7.

Savitt, J. M., et al., 2006. Diagnosis and treatment of Parkinson disease: molecules to medicine. The Journal of clinical investigation. 116, 1744-54.

Schapira, A. H., Jenner, P., 2011. Etiology and pathogenesis of Parkinson's disease. Mov Disord. 26, 1049-55.

Sen, S., et al., 2009. Dependence of leucine-rich repeat kinase 2 (LRRK2) kinase activity on dimerization. The Journal of biological chemistry. 284, 36346-56.

Shin, N., et al., 2008. LRRK2 regulates synaptic vesicle endocytosis. Exp Cell Res. 314, 2055-65.

Simon-Sanchez, J., et al., 2009. Genome-wide association study reveals genetic risk underlying Parkinson's disease. Nat Genet. 41, 1308-12.

Smith, W. W., et al., 2006. Kinase activity of mutant LRRK2 mediates neuronal toxicity. Nat Neurosci. 9, 1231-3.

Stacey, N. C., et al., 2000. Abnormalities in cellular adhesion of neuroblastoma and fibroblast models of Lesch Nyhan syndrome. Neuroscience. 98, 397-401.

Stafa, K., et al., 2012. GTPase activity and neuronal toxicity of Parkinson's disease-associated LRRK2 is regulated by ArfGAP1. PLoS genetics. 8, e1002526.

Takeda, M., et al., 1992. Change in the cytoskeletal system in fibroblasts from patients with familial Alzheimer's disease. Progress in neuro-psychopharmacology & biological psychiatry. 16, 317-28.

Taymans, J. M., et al., 2011. LRRK2 kinase activity is dependent on LRRK2 GTP binding capacity but independent of LRRK2 GTP binding. PLoS One. 6, e23207.

Thomas, B., Beal, M. F., 2007. Parkinson's disease. Human molecular genetics. 16 Spec No. 2, R183-94.

Tomsig, J. L., Creutz, C. E., 2002. Copines: a ubiquitous family of Ca(2+)-dependent phospholipid-binding proteins. Cell Mol Life Sci. 59, 1467-77.

Tong, Y., et al., 2009. R1441C mutation in LRRK2 impairs dopaminergic neurotransmission in mice. Proceedings of the National Academy of Sciences of the United States of America. 106, 14622-7.

Tong, Y., et al., 2010. Loss of leucine-rich repeat kinase 2 causes impairment of protein degradation pathways, accumulation of alpha-synuclein, and apoptotic cell death in aged mice. Proceedings of the National Academy of Sciences of the United States of America. 107, 9879-84.

Tsika, E., Moore, D. J., 2012. Mechanisms of LRRK2-Mediated Neurodegeneration. Current neurology and neuroscience reports. 12, 251-60.

Ulrich, F., Heisenberg, C. P., 2009. Trafficking and cell migration. Traffic. 10, 811-8.

van der Putten, H., et al., 2000. Neuropathology in mice expressing human alpha-synuclein. J Neurosci. 20, 6021-9.

Varcin, M., et al., 2012. Oxidative stress in genetic mouse models of Parkinson's disease. Oxid Med Cell Longev. 2012, 624925.

Vidal, M., et al., 1990. Tissue-specific control elements of the Thy-1 gene. EMBO J. 9, 833-40.

Vorotnikov, A. V., 2011. Chemotaxis: movement, direction, control. Biochemistry. Biokhimiia. 76, 1528-55.

Wakabayashi, K., et al., 2012. The Lewy Body in Parkinson's Disease and Related Neurodegenerative Disorders. Molecular neurobiology.

Wang, L., et al., 2008. The chaperone activity of heat shock protein 90 is critical for maintaining the stability of leucine-rich repeat kinase 2. The Journal of neuroscience : the official journal of the Society for Neuroscience. 28, 3384-91.

Webber, P. J., et al., 2011. Autophosphorylation in the leucine-rich repeat kinase 2 (LRRK2) GTPase domain modifies kinase and GTP-binding activities. J Mol Biol. 412, 94-110.

Wennerberg, K., et al., 2005. The Ras superfamily at a glance. J Cell Sci. 118, 843-6.

West, A. B., et al., 2007. Parkinson's disease-associated mutations in LRRK2 link enhanced GTP-binding and kinase activities to neuronal toxicity. Human molecular genetics. 16, 223-32.

Westerlund, M., et al., 2008. Developmental regulation of leucine-rich repeat kinase 1 and 2 expression in the brain and other rodent and human organs: Implications for Parkinson's disease. Neuroscience. 152, 429-36.

Wider, C., et al., 2010. Leucine-rich repeat kinase 2 gene-associated disease: redefining genotype-phenotype correlation. Neurodegener Dis. 7, 175-9.

Winner, B., et al., 2011. Adult neurogenesis and neurite outgrowth are impaired in LRRK2 G2019S mice. Neurobiology of disease. 41, 706-16.

Xu, Q., et al., 2012. Mouse models for LRRK2 Parkinson's disease. Parkinsonism & related disorders. 18 Suppl 1, S186-9.

Yu, W., et al., 2011. The PINK1/Parkin pathway regulates mitochondrial dynamics and function in mammalian hippocampal and dopaminergic neurons. Hum Mol Genet. 20, 3227-40.

Yue, Z., 2009. LRRK2 in Parkinson's disease: in vivo models and approaches for understanding pathogenic roles. FEBS J. 276, 6445-54.

Yue, Z., 2012. Genetic mouse models for understanding LRRK2 biology, pathology and pre-clinical application. Parkinsonism & related disorders. 18 Suppl 1, S180-2.

Yue, Z., Lachenmayer, M. L., 2011. Genetic LRRK2 models of Parkinson's disease: Dissecting the pathogenic pathway and exploring clinical applications. Movement disorders : official journal of the Movement Disorder Society. 26, 1386-97.

Zimprich, A., et al., 2004. Mutations in LRRK2 cause autosomal-dominant parkinsonism with pleomorphic pathology. Neuron. 44, 601-7.